Using Surface Winds to Improve the Accuracy of Fire Spread Modeling for Hazard Assessment: A Case Study in Santa Monica Mountains National Recreation Area, California

A Group Project submitted in partial satisfaction of the requirements for the degree of Master's in Environmental Science and Management

Researched and Produced by:
Adam Anderson
Kyung Koh
Danica Schaffer-Smith
Erin Shapiro
Wendy Su

Faculty Advisors:
Bruce Kendall

March 16, 2010

THIS PAGE INTENTIONALLY LEFT BLANK

Using Surface Winds to Improve the Accuracy of Fire Spread Modeling for Hazard Assessment: A Case Study in Santa Monica Mountains National Recreation Area

As authors of this Group Project report, we are proud to archive this report on the Bren School's website such that the results of our research are available for all to read. Our signatures on the document signify our joint responsibility to fulfill the archiving standards set by the Bren School of Environmental Science & Management.

Adam Anderson

Kyung Koh

Danica Schaffer-Smith

Erin Shapiro

Wendy Su

The mission of the Bren School of Environmental Science & Management is to produce professionals with unrivaled training in environmental science and management who will devote their unique skills to the diagnosis, assessment, mitigation, prevention, and remedy of the environmental problems of today and the future. A guiding principal of the School is that the analysis of environmental problems requires quantitative training in more than one discipline and an awareness of the physical, biological, social, political, and economic consequences that arise from scientific or technological decisions.

The Group Project is required of all students in the Master's of Environmental Science and Management (MESM) Program. It is a three-quarter activity in which small groups of students conduct focused, interdisciplinary research on the scientific, management, and policy dimensions of a specific environmental issue. This Final Group Project Report is authored by MESM students and has been reviewed and approved by:

Bruce Kendall, Advisor

Steve Gaines, Dean

March 2010

THIS PAGE INTENTIONALLY LEFT BLANK

ABSTRACT

Santa Monica Mountains National Recreation Area (SMMNRA), in southern California, is subject to Santa Ana wind events which can lead to destructive fires. Population growth within the wildland-urban interface has been accompanied by dramatic increases in fire loss and associated cost. SMMNRA uses fire spread modeling to inform fire management and outreach programs. Existing models use prevailing wind inputs, but recent advancements have enabled fine-scale landscape modeling of surface wind, without the need for supercomputers. This project investigates whether these surface, or gridded, wind inputs can improve the accuracy of fire spread predictions. In recreating a historic fire, gridded wind inputs showed superior performance to prevailing wind inputs. A fire hazard index map was created for all of SMMNRA, incorporating 1) how rapidly and 2) how frequently different areas in the landscape burned in fire simulations using historic ignition locations and gridded wind inputs. According to our model, the highest hazard is located between Simi Valley, Thousand Oaks and Calabasas. The most influential factors in determining hazard were wind speed and the distance from ignition location. The method developed by this project could be used to focus and efficiently allocate resources for education strategies, mitigation measures and land preservation.

THIS PAGE INTENTIONALLY LEFT BLANK

ACKNOWLEDGEMENTS

We would like to extend sincere thanks to the people who helped make this project possible. In particular, we thank our advisor, Bruce Kendall, whose expertise and guidance was invaluable to the development of the project.

We would also like to thank our external advisors for their guidance and feedback during the course of project development and execution:

Frank Davis – Bren School of Environmental Science and Management
James Frew – Bren School of Environmental Science and Management
Christina Tague – Bren School of Environmental Science and Management

In addition, thanks to those organizations and individuals who provided data and support during project development and analysis:

Darren Hardy – Bren School of Environmental Science and Management
Charles Jones – UCSB Institute for Computational Earth System Science
Max Moritz – UCB Department of Environmental Science, Policy, and Management
Seth Peterson – UCSB Geography Department
Dar Roberts – UCSB Geography Department
Catherine Shields – Bren School of Environmental Science and Management
Robert Taylor – Santa Monica Mountains National Recreation Area
Marti Witter – Santa Monica Mountains National Recreation Area

Missoula Fire Sciences Laboratory, United States Forest Service

THIS PAGE INTENTIONALLY LEFT BLANK

TABLE OF CONTENTS

List of Figures

LIST OF TABLES

APPENDICES

ACRONYMS & DEFINITIONS

CDF – California Department of Forestry and Fire Protection

CWPP – Community Wildlife Protection Plan is a plan by federal, state and local agencies designed to identify priority actions for wildlife prevention and overall fire safety on both private and public lands

Defensible space – area around structures where vegetation modification is maintained in order to slow the rate and intensity of advancing wildfires, prevent the spread of fire from structure to the surrounding environment and provide room for firefighters to work

DEM – digital elevation model; a model that represents topography or terrain; also known as a digital terrain model (DTM)

FARSITE - Fire Area Simulator, a fire spread and growth simulator model

Fire hazard – based on factors such as fuel, slope and fire weather

Fire risk – considers the potential for damage based on factors such as the ability of a fire to ignite the structure, the flammability of the construction material, and mitigation measures such as defensible space, building design, ignition resistant building materials and ignition resistant construction techniques that reduce risk

GIS – geographic information system; integrates and displays geographic information with spatial data

HIZ – home ignition zone; usually defined as the area within 100 feet of a structure

Indefensible locations – areas that firefighters will most likely not be able to defend without loss of life

LFM – live fuel moisture

MRT – Mountains Restoration Trust

NPS – National Park Service; SMMNRA is a part of this agency which cares for natural, cultural and recreational sites across the U.S.; overseen by US Department of the Interior

NWS – National Weather Service, formerly known as the Weather Bureau and is a part of NOAA

RAM – random-access memory; a form of computer data storage

RAWS – Remote Automated Weather Stations

SAW – Santa Ana wind

SMM – Santa Monica Mountains

SMMC – Santa Monica Mountains Conservancy

SMMNRA – Santa Monica Mountains National Recreation Area, part of the National Park Service; our client

USFS – U.S. Forest Service, an agency under the USDA that administers that nation’s forests and grasslands

WindWizard – a gridded wind model that provides information on the effect that topography has on local wind flow at the 100- to 300-meter scale

WUI – wildland-urban interface

I. EXECUTIVE SUMMARY

Wildfires in southern California threaten millions of homes, and suppression costs in the western United States have risen to more than $1 billion annually (Joint Fire Science Program, 2007). Wildfires spread under a specific set of conditions dictated by three major factors: vegetation, weather and topography. The largest and most costly wildfires in southern California are driven by high winds (Keeley & Zedler, 2009). Santa Monica Mountains National Recreation Area (SMMNRA) is dominated by chaparral and coastal sage scrub vegetation types, which provide an abundance of highly ignitable fuels (Witter et al., 2007). The area's steep terrain, with major canyons running northeast to southwest, is conducive to rapid fire spread. Additionally, seasonal patterns of high temperatures, low relative humidity and high-speed off-shore SAWs increase fire hazard. The determination of fire hazard is associated with factors such as fuel, slope and fire weather.

SAWs occur seasonally when a cool, dry air mass from the interior western United States flows towards the Pacific Coast. The air mass sinks, compresses, strengthens and warms, desiccating vegetation and increasing fire hazard (Westerling, et al., 2004). Multi-day SAW events, occurring mostly between late September and December, are the primary drivers of fire behavior in southern California (Dennison et al., 2008). However, most conceptual models of fire hazard (developed for other ecosystems) do not place emphasis on extreme wind conditions. In some portions of SMMNRA, canyons with high fuel loads line up with the prevailing north to northeasterly SAWs (Radtke et al., 1982). In such areas, it will be particularly important to identify the spatial distribution of high intensity surface winds in order to fully understand the fire hazard.

There are two major objectives of this study: 1) to determine whether incorporating surface wind increases the accuracy of fire spread model predictions, and 2) to identify the spatial pattern of relative fire hazard in SMMNRA based on fire spread modeling that incorporates surface winds, also known as gridded winds. Gridded wind takes topography into account so that wind speed and direction values vary across the landscape. This is different from currently used prevailing wind inputs, which assume a uniform wind direction and speed across the landscape. Hazard index maps based on fire spread modeling have been previously prepared, such as those the state of California adopted in 2008 (FRAP-CDF, 2009). However, none of the methods previously used have incorporated gridded wind. A more accurate model of the spatial pattern of fire spread under strong wind conditions could help managers in multiple jurisdictions improve fire management practices, long-term land use planning in the region, education and outreach programs. To date, geographic variability in wind intensity in SMMNRA has been incorporated into post-fire analysis, but not in large-scale planning due to the expense and computational intensity of gridded wind modeling. Combined with other factors, such as topography, vegetation and weather, information on wind intensity can be used to identify areas which face higher fire hazard, in order to facilitate a more effective allocation of fire management and educational resources. Due to future land development potential, knowledge of areas with higher fire hazard will be important to determine where development should be avoided within SMMNRA.

Prior to conducting simulations, we analyzed trends in hourly wind direction and speed during SAW events within the past four years, as recorded by nearby weather stations. We also collected fuel moisture data from the same set of weather stations. The Missoula Fire Sciences Laboratory ran WindWizard, a gridded wind-modeling program, for SMMNRA. The Missoula Fire Sciences Laboratory ran the wind model based on four wind directions (0°, 45°, 90°, 337.5°) at two different speeds (15 miles per hour (mph) and 25 mph). Information from the National Weather Service (NWS) currently serves as the baseline for wind data. WindWizard provides finer-scale results than the NWS without requiring high intensity computing power, and its validity can be checked against historical wind data. The WindWizard simulations were used to create a map of gridded winds during Santa Ana conditions in SMMNRA. Additional data for the study area, including slope, aspect, elevation and a vegetation map, were provided by SMMNRA.

To evaluate the effectiveness of gridded wind, as compared to prevailing wind, we used HFire, a fire spread model, to recreate the 2007 Corral Fire. Gridded wind showed promise in recreating a historic fire more accurately than can be accomplished using prevailing wind inputs; however, results were limited by only having eight wind grids to work with.

Additional fire simulations were conducted throughout the study area to construct an overall hazard index map. Fire hazard index values were based on how frequently, and how quickly, a given location burned in simulated fires from many different ignition points using the four directional wind grids. Only one grid was used for a 24-hour period in each simulation. Based on the fire hazard index maps produced using gridded wind, the area between Simi Valley, Thousand Oaks and Calabasas has the highest relative fire hazard within SMMNRA. Changes in wind speed had the largest effect on the magnitude and spatial arrangement of modeled fire hazard. A sensitivity analysis revealed that spatial distribution of modeled fire hazard was most sensitive to distance from the nearest ignition point, which accounted for approximately 20 percent of the variation in hazard ($p<0.0001$). Fixed inputs, including topography and the fuel model map, were also found to be significant predictors of fire hazard, according to a multiple regression analysis. Furthermore, a low R-squared value (0.2417) showed that the model results have a low probability of being replicated by simply summing the inputs.

We have also identified several improvements that could be made to our model. To further validate the use of wind grids, the WindWizard outputs could be compared with field measurements (i.e., measuring wind direction and speed on ridgetops and in canyons). A longer period of SAW data would increase confidence that the model is capturing climate variations such as the El Niño-Southern Oscillation, which is a climate pattern that manifests as weather disturbances in the Pacific Ocean roughly every five years. Finally, an analysis of ignition points, with respect to time of day and association with particular landscape features, could also refine the probability space used for randomizing ignition conditions. Further refinement of the model and confirmation of its accuracy will allow land managers to assess the physical and economic effects of specific scenarios and management strategies. These studies could assist in selecting and implementing management strategies which would facilitate coordination between stakeholders concerned with human community and natural resource protection in the vicinity of SMMNRA.

THIS PAGE INTENTIONALLY LEFT BLANK

II. PROBLEM STATEMENT

The Santa Monica Mountains National Recreation Area (SMMNRA), part of the U.S. National Park Service (NPS), is a unique location because of its rich biodiversity and proximity to one of the fastest growing regions in the country. SMMNRA spans a highly urbanized area from Los Angeles to Ventura County, characterized by an extensive wildland-urban interface (WUI). This complex mosaic of public land, residential neighborhoods and private in-holdings within multiple jurisdictions, complicates fire management coordination in the region

SMMNRA's current fire management plan incorporates years of observation and data on the relationship between topography, fuel loads and weather. These three "fire hazard elements" influence fire behavior and are used to determine the fire hazard level in a given area. However, current weather inputs do not address the fine-scale geographic variability of wind events, such as the Santa Ana winds (SAWs), but rather assume similar conditions across a large area. While long-term residents and local fire personnel may be aware of the variation of SAW patterns and the location of major wind corridors, this information has not been formally documented. Geographic wind variability has not been incorporated into models because of the difficulty and expense of accurate modeling of such locally variable winds. Previously, SMMNRA lacked the resources to incorporate both the spatial variability of wind intensity and the portion of the WUI most vulnerable to structure loss and other damage into its models. However, a recently developed wind model, WindWizard, has provided an inexpensive alternative to other gridded wind models and can be used to model conditions in SMMNRA.

Wildfire hazard in SMMNRA is highest during late summer to early winter, and this risk increases during SAW events. When widespread, high intensity SAWs occur in conjunction with antecedent drought and vegetation dieback, the potential for multiple wildfires across southern California increases.

THIS PAGE INTENTIONALLY LEFT BLANK

III. Significance

Southern California's shrublands can collectively be considered a high fire hazard area. The costs of fire damage continue to outpace fire prevention and suppression resources because of the increasing WUI. Faced with these resource constraints, land managers are looking for more appropriate offensive strategies. Knowledge about which parts of the WUI routinely experience the most extreme fire weather conditions could yield important information about the locations of the greatest potential for structure loss. SMMNRA is an ideal case study for this analysis, and the methods and information produced by this project could be transferable to other high fire hazard areas.

SMMNRA has experienced some of the most damaging fires in the state. The SAWs interacting with mountainous topography create complex surface wind patterns that have driven many large, uncontrollable fires. This combined with an increasing population living within the WUI has complicated fire management issues. Gridded wind inputs have been used in conjunction with fire spread modeling as a method for analyzing the likelihood of an area burning and the rate at which it will burn (FRAP-CDF, 2007). The pioneering aspects of the project include the use of gridded wind in the HFire program to produce fire hazard index maps, which have traditionally considered only prevailing wind. Additional uses for the model include the analysis of alternative management scenarios. This could be useful for SMMNRA, as well as other jurisdictions in efficiently allocating limited funding for fire management programs.

IV. Objectives

The purpose of this project is to recommend how SMMNRA can use gridded wind modeling in conjunction with fire spread modeling for fire management, outreach and resource allocation in high fire hazard areas. The principle objectives of this study are to:

1. incorporate WindWizard output into the fire spread model, HFire;
2. attempt to validate the model based on a historic fire event at a local scale;
3. produce a fire hazard index map for SMMNRA managers and
4. assess the sensitivities of HFire / WindWizard by randomizing ignition points and varying wind grids.

THIS PAGE INTENTIONALLY LEFT BLANK

V. Literature Review

Wildfire History in California and the Western U.S.

In the past, wildfire suppression was the primary fire policy in the United States. Numerous devastating fires around the 1900s led to the public perception that all fires were deleterious (Dombeck et al., 2004). However, research has shown that fire suppression can lead to far more damaging fires. Therefore, in recent years, prescribed burning has become one popular method of fire management. Prescribed burns apply fire under specific weather conditions to a predetermined area to reduce fire hazard (Wade & Lunford, 1988). This method has proven effective in coniferous forests, but is not as successful in chaparral and coastal scrub ecosystems (Keeley & Fotheringham, 2001), particularly under high wind conditions (Wardell-Johnson, 2009). In spite of these two policies, wildfires in southern California have continued to become more frequent and destructive.

Wildfires occur naturally throughout the western United States, but can be particularly devastating when combined with dense fuels, drought conditions and urban development. The intensity, severity and cost of fires have increased exponentially as the population density within the wildland-urban interface (WUI) has increased. Table 1 demonstrates this trend in the Santa Monica Mountains between 1977 and 2007, during which population steadily increased.

Table 1: Large fires in the Santa Monica Mountains, 1977-2007.

Fire	Date	Cost of Fighting ($)/ Hectare
Topanga Canyon	11/14/1977	493.84
Carlisle (near Encinal Canyon)	11/15/1977	494.43
Kanan (from Agoura Hills to Pacific Ocean)	10/23/1978	543.64
Dayton Canyon (N of LA County to Pacific Ocean)	10/9/1982	555.98
Sherwood (in/around Westlake Village)	6/30/1985	568.49
Green Meadow (largely to west in Ventura County)	10/23/1993	597.25
Old Topanga (S of Calabasas to Pacific Ocean)	11/2/1993	597.28
Calabasas (Calabasas to Pacific Ocean)	10/21/1996	791.86
Topanga (118 Freeway to Calabasas)	9/28/2005	1,737.71
Pacific (Trancas Canyon near Pacific Coast Hwy.)	1/6/2006	7,417.58
Canyon Fire	10/21/2007	503.44
Corral Canyon	11/24/2007	1,563.29

Source: CDF (2007), Los Angeles County Burn Area Recovery Task Force Report (2007); CAL FIRE (2007)

The Fire Regime in Southern California

Fire intensity and severity are based on three major factors (known as the fire triangle): vegetation (fuel loads, live fuel moisture levels), weather and topography (Figure 1).

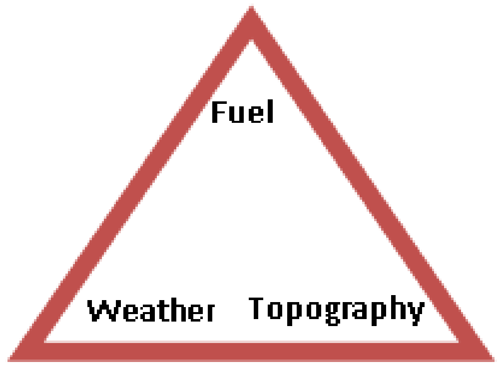

Figure 1: The fire triangle. Three factors that drive fire.

The Santa Monica Mountains (SMMs), about 90,000 hectares (222,395 acres) in size, is dominated by dense chaparral and coastal sage scrub vegetation that burns in intense, stand-replacing fires (Witter et al., 2007). There has been extensive debate over what constitutes a 'natural' fire regime in southern California. Historical fire regimes in chaparral ecosystems such as the SMMs are not well documented because these fires generally burn or destroy all biomass above the ground, and the fire return interval is estimated to be about 50 to more than 100 years (Conard & Weise, 1998).

Nevertheless, there is some information about the factors that influenced fire history in the Santa Monica Mountains (i.e., land use, vegetation, topography and climate) to make inferences about the past fire regime (Conard & Weise, 1998). Early work in the 1980's argued that the pre-suppression historic fire regime in the southern California chaparral ecosystem differed substantially from the modern fire regime. Some researchers hypothesized that fire suppression policies altered the historic regime of frequent, small fires that fragmented the chaparral landscape into a patchwork of young and old fuels (i.e., fine-grain age patch mosaic model), which used to prevent the occurrence of large-scale fires (Radtke et al., 1982, Minnich 1983). However, more recently, fire ecologists have argued that the southern California fire regime has remained largely unchanged, and that large landscape-scale fires were, and are, driven by SAWs (Keeley & Zedler, 2009).

Unique Conditions that Contribute to Fire in Southern California

Wind and Weather

Southern California has a Mediterranean climate characterized by variable winter and spring precipitation and a dry summer and fall. Most experts agree that the fire season in southern California tends to occur in the fall, coinciding with SAW events and low fuel moisture levels, which follow the hot summer season. SAWs are a seasonal event, resulting when a cool, dry air mass flows from the interior western United States towards the Pacific Coast (Figure 2). A previous study indicated that an average of 20 SAW events occur each season, with each lasting roughly 1.5 days (Raphael, 2003).

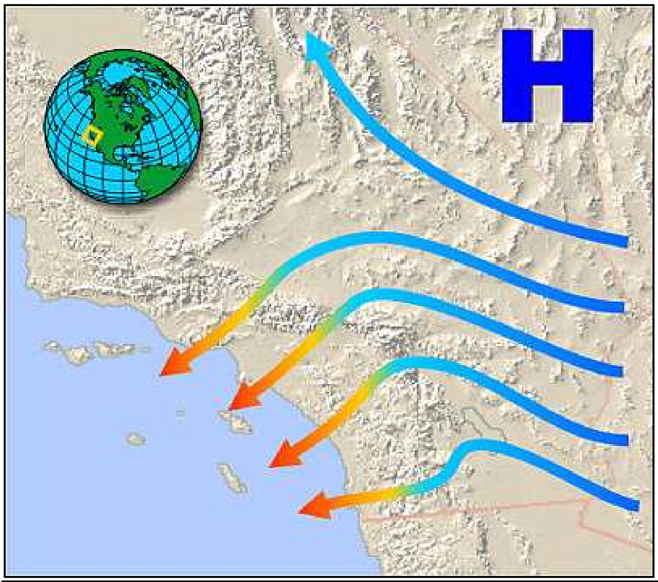

Figure 2: Santa Ana winds in southern California. Source: NOAA (2008).

The sinking air compresses and warms, producing a strong, dry, warm, foehn-like wind that can decrease fuel moisture levels and increase the chance of fires (Westerling et al., 2004). From late September through December and sometimes even into February, SAWs are the primary drivers of the fire regime in southern California, outweighing all other factors (Dennison et al., 2008). Clarke et al. (2008) found that wind speed was more than three times more influential in predicting fire size than fine dead fuel moisture and wind direction.

While most ignitions result in manageable fires, a small percentage of fires that coincide with the SAWs become large, uncontrollable, regional threats (Keeley & Fotheringham, 2001). The month of October alone accounts for 25 percent of the total area burned in southern California from 1950 through 2007 (Moritz el al., 2010). Large wildfires during SAW events have consistently occurred in areas experiencing high fire weather severity (Moritz el al., 2010). In a fire-prone region under high winds, an ignition is likely to result in a large, unstoppable wildfire. Additionally, both the unique topography and vegetation of the Santa Monica Mountains are conducive to fire spread (Keeley & Zedler, 2009).

Topography

The SMMs are a part of the Transverse Ranges (i.e., mountain ranges running east to west). This geographic configuration is particularly important in the eastern part of the SMMs, where the canyons are parallel to the north to northeasterly direction of the SAWs (Radtke et al., 1982). As a result of this topography, winds tend to channel up and down the canyons, creating conditions conducive to rapid fire spread (Radtke et al., 1982).

Vegetation

The SMMs are dominated by fire-prone vegetation; 50 percent of SMMNRA consists of chaparral and 20 percent is composed of coastal sage scrub community types. Both of these communities burn readily because of the high-density and continuity of vegetation, small twig and stem size and a high proportion of dead biomass (Witter et al., 2007). Furthermore, many of the common shrubs in these systems, such as chamise (*Adenostoma fasciculatum*), contain volatile oils which, when combined with low fuel moisture, make for extremely flammable fuels (Rundel & Parson, 1979).

Living and dead vegetation will both burn in warm, dry conditions, but how quickly they ignite, in addition to how long and how hot they burn, depends on plant size as well as horizontal and vertical structure (Randall, 2003). Live fuel moisture (LFM) is the water content of live vegetation as a percentage of the dry biomass (Dennison et al., 2008). Many fire managers use LFM as a measure of fire hazard because the moisture of both live and dead fuels must be exhausted before actual combustion occurs (Dennison et al., 2008). Given the climatic patterns in southern California, LFM normally begins to decline following the spring rains, becoming increasingly lower through the dry summer and fall. The LFM may eventually reach a critical level that increases the risk of large wildfires. Most importantly, the timing of the lowest LFM occurs during the same time of year that SAWs occur most frequently in the SMMs. Under these conditions of high winds and extremely dry fuels, rates of fire spread can increase significantly (Beer, 1991).

Concerns with Increasing Fire Frequency

Given the short fire return interval in SMMNRA, managers face the daunting task of protecting natural resources, as well as life and property. The number of anthropogenic ignitions in the vicinity of SMMNRA is considerably higher than the number of natural ignitions (Figure 3). Previous studies have shown that more fires occur along the WUI than in remote areas because anthropogenic ignitions are concentrated near human infrastructure (Pyne, 2001; and Keeley et al., 2004; Syphard, Clarke et al., 2007; Syphard, Radeloff et al., 2007)

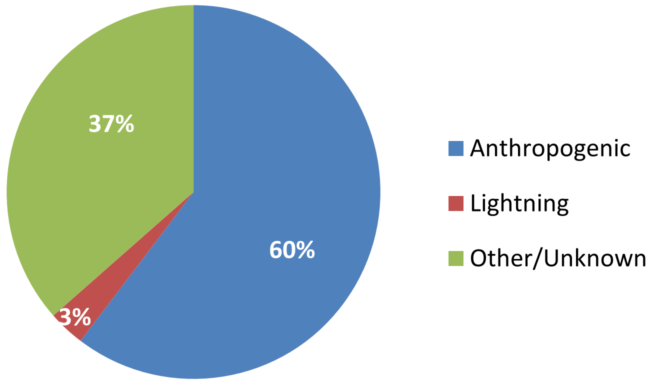

Figure 3: Percentage of wildfire ignitions for the Santa Monica Mountains by source, 1982-2008. Source: SMMNRA

There are many natural resource impacts associated with wildfires. As fire frequency increases, the persistence of native ecosystems (e.g., chaparral) is put at risk. For example, fires in the same area over short time intervals can result in significant decreases in biodiversity and increases in non-native species composition (Keeley, 2005). Post-fire intrusion of herbaceous non-native species in SMMNRA, which provide more fine surface fuels earlier in the year, further contributes to increased fire frequency and a longer fire season, as previously documented (Witter et al., 2007). An increase in herbaceous non-native species can create a positive feedback loop, which in turn alters the plant community and leads to type conversion of native shrubland to non-native grassland (Syphard et al., 2007).

Wildland-Urban Interface & Fire Hazard

SMMNRA, the study site, has a large, sprawling WUI. The population of Los Angeles County, where most of SMMNRA is located, increased 18.5 percent from 1980 to 1990, 7.4 percent from 1990 to 2000, and 3.6 percent from 2000 to 2008 (United States Census Bureau, 2010). This resulted in an increased number of people living within the WUI. Similarly, nearby Ventura County grew 13 percent from 1990 to 2000 and 6 percent from 2000 to 2008 (United States Census Bureau, 2010). The natural scenic beauty of the area and its proximity to metropolitan Los Angeles and Ventura has resulted in SMMNRA having some of the highest land and home values in the nation (Los Angeles Almanac, 2008).

Structures close to dense vegetation are likely to be lost in fires driven by high winds (Troy & Romm, 2007). According to the Natural Hazard Disclosure Law (Assembly Bill (AB) 1195), passed in 1998, all home sellers are required to fill out a form disclosing to potential buyers whether their residence is in a statutory wildfire zone (Troy & Romm, 2007). Despite this information, current WUI homeowners may remain ignorant of, or may not acknowledge that they are likely to be personally affected by, the risks inherent in living in these high fire hazard areas (Huggett Jr., 2003).

The Grass Valley Fire in October of 2007 in the San Bernardino Mountains is one example of a fire that occurred in close proximity to a dense residential area. Dry SAWs blowing over rugged terrain of chaparral and conifer forests provided perfect conditions for the Grass Valley Fire (Cohen & Stratton, 2008). Sparks from the fire moved south, igniting residential vegetation and several homes. The post-fire evaluation concluded that the destruction of almost 200 homes resulted from fire spreading structure to structure. Given that only six homes showed signs consistent with being engulfed by a high intensity wildfire, the Grass Valley Fire illustrates that homes within the WUI may be threatened more by indirect ignition from embers than by direct ignition from fire (Cohen & Stratton, 2008). Thus, it is important to note that residences not immediately adjacent to chaparral or coastal sage scrub also experience a high risk of wildfire. Greater distance from chaparral and coastal sage scrub does not necessarily mean a residence is at a lower risk when fires occur.

The Role of Education and Fire Policy in the Wildland-Urban Interface

The Grass Valley Fire also demonstrates the need for improved fire education and policy. When destructive fires occur, such as those in 2003 and 2007, the usual response is to spend more state and federal money on fire resources and fuel treatment projects. However, the increased budget for firefighting and fuels treatments has not decreased the number of damaging fires in California. Similarly, current policy is focused on fighting fire, instead of learning to live with it (Stephens et al., 2009). In contrast, the recently endorsed Australian policy of ‘Stay or Go’ (or ‘Prepare, stay and defend, or leave early’) has resulted in reductions of loss and life and property, until the devastating fires that occurred in February 2009 (Table 2).

Table 2: Life and property losses in major Victorian bushfires, Australia.

Types of Losses	1939	1983	2003	2009
Fatalities	71	47	1	210
Houses destroyed	650	2000+	41	2029
Area burnt (hectares)	1.5 million	200,000	1.12 million	400,000

Source: Tibbits & Whittaker (2007); Esplin (2009)

Australia Comparison

At the beginning of each fire season, fire authorities in Australia encourage residents to decide whether they will prepare, stay and defend their property, or leave before the fire threatens their area (Tibbits & Whittaker, 2007). If residents decide to stay, they need to adequately prepare their property through fuel management, appropriate home protection measures, and ensuring they have both the physical and psychological resources to actively defend their property from embers throughout the fire event (Stephens et al., 2009). The Australian policy is based on several assumptions: 1) the fire front will pass quickly; 2) houses can survive and protect the occupants; 3) well-prepared houses can be successfully defended from bushfires and;

4) wind-blown embers are the most common source of home ignition (Stephens et al., 2009; Tibbits & Whittaker, 2007). Additionally, fire authorities must emphasize that ‘stay and defend’ means staying and defending the property until the fire passes. Residents should not keep late evacuation as an option because studies have shown that twice as many deaths occurred in vehicles or out in the open than inside houses (Handmer & Tibbits, 2005). Lastly, it is important to recognize that the Australian policy of ‘Stay or Go’ is not the same as ‘shelter in place’ (Stephens et al., 2009). The ‘Stay or Go’ policy emphasizes active homeowner involvement, as opposed to the much more passive and consequently dangerous ‘shelter in place’ idea.

The ‘Stay or Go’ policy has worked in Australia, but the success of the policy is contingent on proper education about the policy, thorough preparation before a fire and an effective early warning system (Stephens et al., 2009). The Australian policy could be effective in certain areas of California, but only with revision of the current system. There is a need for stronger partnership between communities and fire authorities, agency and community support of the policy, substantial education and outreach about the policy and the risks and choices involved, and communities willing to accept responsibility for their own safety (McCaffrey & Rhodes, 2008). However, as the statistics from the 2009 Australian bushfires show (Table 2), when extreme fire conditions exist (i.e., low fuel moisture levels, high winds, hot temperatures) (Victorian Bushfires Royal Commission, 2009), fires can and will devastate the landscape and destroy property and lives despite successful implementation of fire policies.

Options for Mitigating Fire Damage in the WUI

Many WUI residents do not understand the ecosystem in which they have chosen to live, nor do they believe they will be affected, especially if a fire has already occurred relatively recently (Gardner et al., 1987). Many residents incorrectly assume that wildfires only affect residences along the edges of the WUI; however, many destroyed homes are a result of ignition from smaller flames or from wind-blown embers (Cohen & Stratton, 2008). Structure design can play an integral part in structure ignition and fire spread, as observed in the 2007 Grass Valley Fire. Additionally, maintenance of defensible space is very important in the WUI. The area within 100 feet of the home is considered the “home ignition zone” (HIZ), the most important area to manage (Sutherland, 2004). The HIZ usually falls within private property, and management is therefore the responsibility of the homeowner. However, there are numerous resources that educate homeowners on how to create a perimeter around infrastructure in order to provide a defensible space from which fire fighters can safely protect structures and minimize wildfire spread (State Board of Forestry and Fire Protection, 2006).

There are also guidelines available for construction and landscaping, such as the Firewise Construction Checklist (National Fire Protection Association, 2009). These may include choosing a fire safe location for new construction, or using non-combustible materials, such as slate, clay tile or metal roofing, in place of traditional materials. Retrofits on existing homes are also possible, such as installing wire screens with mesh one-eighth of an inch or less on vents in order to exclude sparks (National Fire Protection Association, 2009). Choosing appropriate plantings and regularly maintaining vegetation in the HIZ can also greatly reduce fire hazard (Sutherland, 2004). However, under extreme fire conditions, and especially during SAW events, these guidelines do not guarantee that residences will remain undamaged. Without strict requirements, an actual fire may be needed to make residents fully recognize the danger. For instance, one study found that willingness to pay for fire-resistant roofing was highest in the two years following a fire (Huggett Jr., 2003).

The Existing Planning Framework in SMMNRA

There are three major planning documents that have jurisdiction over land use within SMMNRA: the Los Angeles County General Plan, the Ventura County General Plan and the Los Angeles County Coastal Area Plan. There are many smaller planning units covered in each of these major units often with their own planning documents. Land use policy maps set the total number of units that can be placed on a parcel of land governed by a planning document. Zoning standards affect how the land can be used, and other regulatory agency policies may also impact the number of structures that can be placed on a property.

There is potential for additional development within SMMNRA in both Los Angeles and Ventura Counties. Although the Los Angeles County General Plan states that new development is most acceptable in “areas free from natural hazards” (County of Los Angeles VI-49), this excludes fire hazard. Only sites with a high hazard of flooding or unstable soils are not considered developable according to the Los Angeles County General Plan (County of Los Angeles VI-49). The Ventura County Fire Protection District also discourages development in High Fire Hazard Areas (Ventura County Planning Division, 2005); however, construction may still proceed.

In communities in the vicinity of SMMNRA, there are varying requirements for fire protection, creating inconsistent policies across the landscape. Ventura County’s Area Plans contain policies for residences in High Fire Hazard Areas, such as requirements for non-combustible roofs, landscape plans that use fire retardant plant material, ensuring adequate access for water and other firefighting purposes, and clearing brush within 100 feet of a structure, and in some cases, 200 feet. Even within the same county, local jurisdictions use inconsistent fire management policies. For example, within Ventura County, the Area Plans for Lake Sherwood, Oak Park, Thousand Oaks and Piru are consistent with the Ventura County General Plan’s fire policies, while Lake Sherwood/Hidden Valley Area Plans are consistent with the Santa Monica Mountains Comprehensive Plan (Ventura County Planning Division, 2005). Within Los Angeles County, many communities adhere to the County fire requirements, including a brush clearance requirement of 100 feet from structures and 200 feet in High Fire Hazard Areas. However, some cities have adopted much more stringent ordinances, such as the City of Agoura Hills, which has provisions for new construction, as well as required retrofits concurrent with alterations of existing structures (City of Agoura Hills, 2009).

Fire Management and Coordination in SMMNRA

Fire management is the range of human activities, such as suppression of ignitions or modification of fire behavior, that are implemented to protect human life or property or to modify ecosystem properties (Santa Monica Mountains National Recreation Area, 2005). SMMNRA has a large, sprawling WUI, in which the primary concern is development on private in-holdings within the park. Another issue is the build-up of brush which provides fuel loads for fire. The objectives of a fire management plan in a chaparral ecosystem such as SMMNRA are: 1) to contain wildfires strategically within easily defended boundaries; 2) to maintain a chaparral fire regime that fosters healthy, sustainable ecosystems in wildland areas; and 3) to prevent anthropogenic ignitions and to prevent wildfire spread into urban areas (Conard & Weise, 1998).

The year 2005 marked the publication of the Final Environmental Impact Statement for a Fire Management Plan for SMMNRA. With the adoption of the new plan, SMMNRA has moved toward implementing a new fire management policy. The plan attempted to meet the three objectives delineated by Conard and Weise (1998) listed above. The SMMNRA Fire Management Plan advocates moving away from prescribed burning to create an age-class mosaic, and toward the development of strategically placed fuel management zones. In addition, fuel management in and around the WUI is also emphasized (Santa Monica Mountains National Recreation Area, 2005).

Prescribed burning is the application of a controlled fire to a predetermined area (Natural Resources Conservation Science, 2002). In relation to fire management, the purpose of prescribed burns is to control undesirable vegetation, remove debris and to reduce wildfire hazards. Limits of prescribed burning include: the risk of a prescribed burn spreading to adjoining lands; the fact that prescribed burns often take place near potential hazards such as roads, residences, windbreaks, flammable conduits, electrical power poles and transmission lines; the compounded respiratory problems due to the smoke from a prescribed burn; and unplanned intrusion of wind potentially leading to a large unplanned fire. Under extreme conditions, such as that of SAWs, even young fuels will support an intense fire, which is a problem that prescribed burning cannot remedy (Keeley & Zedler, 2009). As a result of these limitations and research that has shown fuel modification does not decrease fire hazard (Keeley, 2002), especially during SAW events, SMMNRA has eliminated their prescribed burning program.

Currently, as part of the development of a new regional Santa Monica Mountains Community Wildlife Protection Plan (CWPP) by federal, state and local agencies, public meetings have been occurring in SMMNRA to help homeowners identify how to better protect their homes. The first series of thirteen public meetings took place in October 2009. The second series of public meetings took place in January 2010. The CWPP is designed to identify priority actions for wildfire prevention and overall fire safety on both private and public lands. The plan will include approximately 52,609 hectares (130,000 acres) of land. Homeowners, landowners, agencies and service providers that reside or conduct business in the area are included in the process. Ultimately, the goal is to provide a blueprint for fire hazard reduction projects to increase community safety. This could include fuel reduction, or non-fuels related projects such as upgrading homes to be more fire-resistant (McGrath, 2009).

Fire Spread Modeling as a Tool

Rothermel's Equation

The Rothermel fire spread equation (Rothermel, 1972) is a mathematical model for predicting the direction and rate of fire spread in models of wildland fuels. It is used for hypothetical fires and forecasting the behavior of active wildfires. Rothermel's model is composed of a nonlinear set of equations that relate environmental input parameters such as fuel type, fuel moisture, terrain and wind to describe the fire environment.

The heat from a fire dehydrates potential nearby fuel through internal radiation and convection. Continual heating raises temperatures until the fuel starts to burn and release combustible gases. When there is sufficient gas to support combustion, the gas is ignited by flames and the fire spreads to a new position. In no-wind fires the surrounding fuel temperature rises slowly and ignites when the fire approaches within one or two inches of the fuel. The fuel temperature is higher than the surrounding air temperature, so convective heating or direct flame contact occurs only when the fire reaches the fuel.

In a wind-driven fire, the temperature of the surrounding fuel rises faster even when the fire is farther away. Wind accelerates the flame in the prevailing direction, causing the flame to make contact with more potential fuel at further distances. Additionally, wind can transport flames into surrounding areas. The air temperature in this case is higher than the fuel temperature. This indicates the presence of convective heating and radiation from the flame in addition to internal radiation and convection. Conversely, in a wind-driven fire on a sloped terrain, these same factors come into play. The wind as well as convection, radiation and internal radiation all work to spread the fire uphill.

Rothermel's model reduces fire behavior into several components: the heat required for ignition, propagating flux, reaction intensity, the effect of wind and slope, approximate rate of spread, heat sink heat of pre-ignition, heat sink effective bulk density, heat source reaction intensity, heat source reaction velocity, heat source moisture damping coefficient, mineral damping coefficient, physical fuel parameters, wind coefficient and slope coefficient. Rothermel's fire spread equation defines rate of spread as the heat received by fuels ahead of the fire divided by the heat required to ignite the fuels. Shown below is the equation for rate of spread of the flaming front of a fire, which is based on multiple other equations:

$$R = \frac{I_R \, \xi \, (1 + \Phi_W + \Phi_S)}{\rho_\eta \, \varepsilon \, Q_{ig}}$$

Where:

- R = rate of spread of the flaming front
- I_R = reaction intensity
- ξ = proportion of the reaction intensity that heats adjacent fuel particles to ignition
- Φ_W = dimensionless multiplier accounting for the effect of wind in increasing the proportion of heat that reaches adjacent fuels
- Φ_S = dimensionless multiplier accounting for the effect of slope in increasing the proportion of heat that reaches adjacent fuels
- ρ_η = oven dry fuel per cubic foot of fuel bed (lb/ft)
- ε = dimensionless number accounting for the proportion of a fuel particle that is heated to ignition temperature at the time flaming combustion starts (near unity for fine fuels and decreases toward zero as fuel size increases)
- Q_{ig} = heat of pre-ignition, or the amount of heat required to ignite one pound of fuel (Btu/lb)

Rothermel's fire spread equation is the basis for most computerized fire spread models used in the United States today.

How Fire Spread Models are Used

Fire spread models are commonly used to determine how to protect communities within the WUI. Fire spread models can be used to determine where the landscape should be altered (i.e., prescribed burns) to decrease fire hazard, how much defensible space is required to protect a structure, or to guide real-time decision-making. One such model, known as the Wildland-Urban Interface Evacuation (WUIVAC) model, is used to determine an evacuation trigger or a point on the landscape, that when crossed by a wildfire, signals that the threatened community needs to begin evacuation (Dennison et al., 2006). Information from fire spread models can also be used for educational purposes, and have been used to aid in the development of the Fire Information Engine Toolkit developed by the Center for Fire Research and Outreach at the University of California, Berkley. This web-based toolkit is intended for a wide variety of users including homeowners, decision makers, fire operations and researchers, and can be used at the local, community and regional scale (Kearns et al., 2007). More recently, changes in fire behavior and severity due to climate change are also being evaluated using fire spread modeling. However, it is important to keep in mind that while models can be useful, they are an oversimplification or approximation of reality and cannot reflect all reality (Burnham & Anderson, 2002).

Currently, fire ecologists and researchers at SMMNRA use fire spread models in the following ways (Taylor, 2009):

- to calculate expected fire behavior adjacent to structures to determine how much defensible space is necessary to protect them;
- to identify locations where fire behavior is expected to be especially severe;

- to illustrate expected conditions for future wildfires (i.e., for future planning purposes);
- to assess the potential value of proposed fuel modification projects; and
- to develop educational materials for public fire education programs.

This project specifically focuses on identifying locations where fire behavior is expected to be especially severe.

Many experts have modeled and studied fuels and the effect of fuel moisture on fire spread (Dennison et al., 2008). Although it is well known that wind significantly contributes to fire spread (Beer, 1991), little has been done to identify areas of high fire hazard during high winds. Since winds, particularly SAWs, can become the primary drivers of fire spread, the areas with the highest intensity winds are of particular interest. Knowing the areas in which the winds blow the strongest, synthesized with other fire factors, can define spatial areas of highest fire hazard within SMMNRA. Wind modeling can assist fire managers in better approximating local wind patterns and the potential for wind-based increases in fire spread rate and intensity (Butler, et al., 2006). Outputs from wind modeling programs such as WindWizard are beginning to be incorporated into fire spread models.

Two Fire Spread Models

Both HFire and FARSITE are based on Rothermel's equations. FARSITE, a fire spread modeling program that contains modules for predicting fire spread in grassland, shrubland and forested landscapes, is the program most widely used by federal and state land management agencies for predicting fire spread and behavior (FireModels.org, 2009). FARSITE is used to determine where a fire will go, how large a fire can become and the rate at which the fire will move through an area. Unfortunately, FARSITE is also highly sensitive to the spatial resolution of input fuels, ignition locations and perimeter resolution. Peterson et al. (2009) observed that the calculation time for FARSITE increases exponentially as the fire perimeter increases.

Another fire spread modeling program, HFire (Highly Optimized Tolerance Fire Spread Model), which was created in the Geography Department at the University of California, Santa Barbara, uses a raster-based fire spread model based on the empirical double ellipse formula used by Anderson (1983), as opposed to the elliptical-based spread model of FARSITE (Morais, 2001). HFire is a model of surface fire spread through shrubland fuels (Peterson, et al., 2009), although HFire can be used in any ecosystem that FARSITE is used in. Lastly, HFire does not model spotting which FARSITE does.

A study of FARSITE and HFire modeling results for a major southern California fire found that the two fire spread simulation models produced similar results (Peterson et al., 2009). Although FARSITE has a graphic user interface, making it more user-friendly than HFire, more fire simulations can be completed in HFire in a shorter period of time. HFire fire spread simulations can be completed much more quickly on desktop computers than FARSITE fire spread simulations. So while both HFire and FARSITE fire spread modeling programs allow land managers to determine the locations most susceptible to wildfires, HFire seemed most appropriate for the project because of the finer-scale nature of the WindWizard output and the limitations of FARSITE.

Mapping Fire Hazard

The ability to model fire intensity and fire spread gives agencies the tools to create fire hazard maps and to identify areas where firefighters could not safely defend property. Fire hazard maps have been created in the past with overlay analysis, such as by Chuvieco and Congalton (1989), who used vegetation (classified according to fuel class, stand conditions and site), elevation, slope, aspect, proximity to roads and trails, campsites or housing as layers in their analysis of hazard in a forested area of Spain (1989). The various factors were weighted by their importance to fire hazard according to literature review (Chuvievo & Congalton, 1989).

The Fire Spread Probability Computation Procedure, employed by the U.S. Forest Service (USFS) in incident management, uses Monte Carlo to generate wind, fuel and moisture time series data. Fire spread simulations are then conducted for various weather scenarios, and the resulting fire spread probability is calculated (Fujioka, 2008). California's AB 337 required that California Department of Forestry and Fire Protection (CDF) work with Local Responsibility Areas to produce maps of Very High Fire Hazard Severity Zones. These maps were intended to support roofing and vegetative clearance requirements, as well as providing information for the real estate disclosure statements required by AB 1195 (Radtke et al., 2000). The low, medium, and high Fire Hazard Severity Zones for the state, adopted in 2008, were constructed incorporating "fire history, existing and potential fuel, flame length, blowing embers, terrain and typical weather" and fire behavior model results (FRAP-CDF, 2007, 2).

This information is of the utmost importance in planning for fire preparedness, including choosing locations where specific fuel management techniques may be applied. Previous studies (FireModels.org, 2009) have used fire hazard models embedded within a geographic information system (GIS) to map regional and neighborhood risk, and to assist decision makers to better mitigate future fires. GIS provides a systematic framework to estimate potential fire hazard over several jurisdictions, and can bring attention to areas where agencies and private landowners may have overlapping concerns and responsibilities for fire management that should be managed under collaborative policies (Radtke, 1995). Predictive models which measure rates of change in fuels can also track the success of mitigation efforts that have been implemented to reduce fire hazard (Radtke, 1995). Fire spread models are commonly compatible with GIS software for further analysis. This technological compatibility allows analysis of the data and the ability to create maps which can be distributed to a wider audience.

It is critical that hazard maps used for decision-making be as accurate as possible. Errors in fire spread modeling are often hard to identify and measure for spatially and temporally dependent data. The USFS has identified model misspecification, erroneous model inputs and measurement error as the most common problems in their own modeling experiences (Fujioka, 2008). Albini and Anderson (1982) found that predictions of fire hazard in Mediterranean systems were extremely sensitive to wind speed, and cited modest errors in wind speed as a major source of error. As wind speed on an acting flame increased, the forward rate of fire spread increased. Efforts have been made to quantify the errors and uncertainties of predictions based on fire spread models (Fujioka, 2004). Fujioka measured errors based on spread distances at points on the perimeters of actual and simulated fires, including for the 1996 Bee Fire, in the San Bernardino National Forest. A probability model was used to bound the errors in fire spread, and this error ratio was then used as a correction factor for the bias of the spread model (Fujioka, 2004).

WindWizard

WindWizard, developed by the Fire Behavior Project at the Fire Sciences Laboratory in Missoula, Montana, is a fluid dynamics model used to simulate the effect of terrain on wind (Stratton, 2006). The WindWizard program provides information about local surface wind regimes at 100 to 300 meters above ground (FireModels.org, 2009). Currently, weather information can be downloaded from Remote Automated Weather Stations (RAWS), which operate at a reference height of 6.1 meters (Peterson, et al., 2009). WindWizard simulates surface air flow by incorporating detailed information about the terrain, in the form of digital elevation model (DEM) files, and user-specified prevailing air flow and direction (FireModels.org, 2009). WindWizard software can run on desktop or laptop computers with at least 512 MB of RAM (Random Access Memory) and a Windows 2000 or newer operating system. This would allow land managers to incorporate wind into fire spread models without having to use supercomputers. Additionally, WindWizard output can be used to incorporate more detailed wind information into FARSITE and HFire simulations (FireModels.org). The gridded wind model can be used to identify areas of exceptionally high surface wind velocity during SAW events in the SMMs, such as on ridgetops.

The gridded wind produced by WindWizard gives a “snapshot” of the wind flow at one moment in time and is not a forecast model. WindWizard assumes a neutral stable atmosphere and does not take into account density driven flows such as diurnal winds or fire-induced winds (Forthofer et al., 2003). Not considering these flows introduces error into the resulting predicted winds. Additionally, WindWizard simulations can predict surface wind direction and magnitude given general area prevailing wind information. The interaction between wind and topography is not captured in broader scale wind. The wind grids created by WindWizard have been compared against historic data, and the results indicate that WindWizard speed predictions are close to reality (Butler & Forthofer, 2004). Predictions are most accurate for winds greater than 8 kilometers per hour (kph) (5 mph) at ridgetops of cold fronts, foehns like the SAWs and onshore/offshore winds. The accuracy of WindWizard predictions of surface wind speeds during SAW events can be determined using historical wind gauge data from past SAW events.

VI. METHODS

In order to propose recommendations for SMMNRA on the future usage of gridded wind in fire spread modeling, the project assessed the added benefits, if any, of incorporating gridded wind into fire spread modeling through a multi-step process:

1. conduct a wind direction analysis of historic SAW events;
2. compare fire simulations using gridded wind to fire simulations using prevailing winds for a historic fire within SMMNRA;
3. model fire hazards in HFire incorporating WindWizard output with historic and random ignition points; and
4. create a fire hazard index map for SMMNRA from HFire and WindWizard outputs.

Data Received from SMMNRA

To begin our analysis, SMMNRA provided us with the following data for the study area:

- digital elevation model (DEM),
- vegetation map,
- eight WindWizard wind grids and
- coordinates for ignition locations within SMMNRA from 1982 to 2008.

Overall Approach

Our overall project methods are shown in Figure 4. First we compiled the topographic (elevation, slope, aspect), vegetative, fire ignition locations and weather data necessary for fire spread modeling. We then ran multiple fire simulations on both a local scale, for the 2007 Corral Fire, and on the Recreation Area-wide scale. The local historic fire was used to validate whether or not gridded wind inputs improved fire simulations when compared to prevailing wind inputs. We used the Recreation Area-wide scale to attempt to map spatial variations in fire hazard during SAW events.

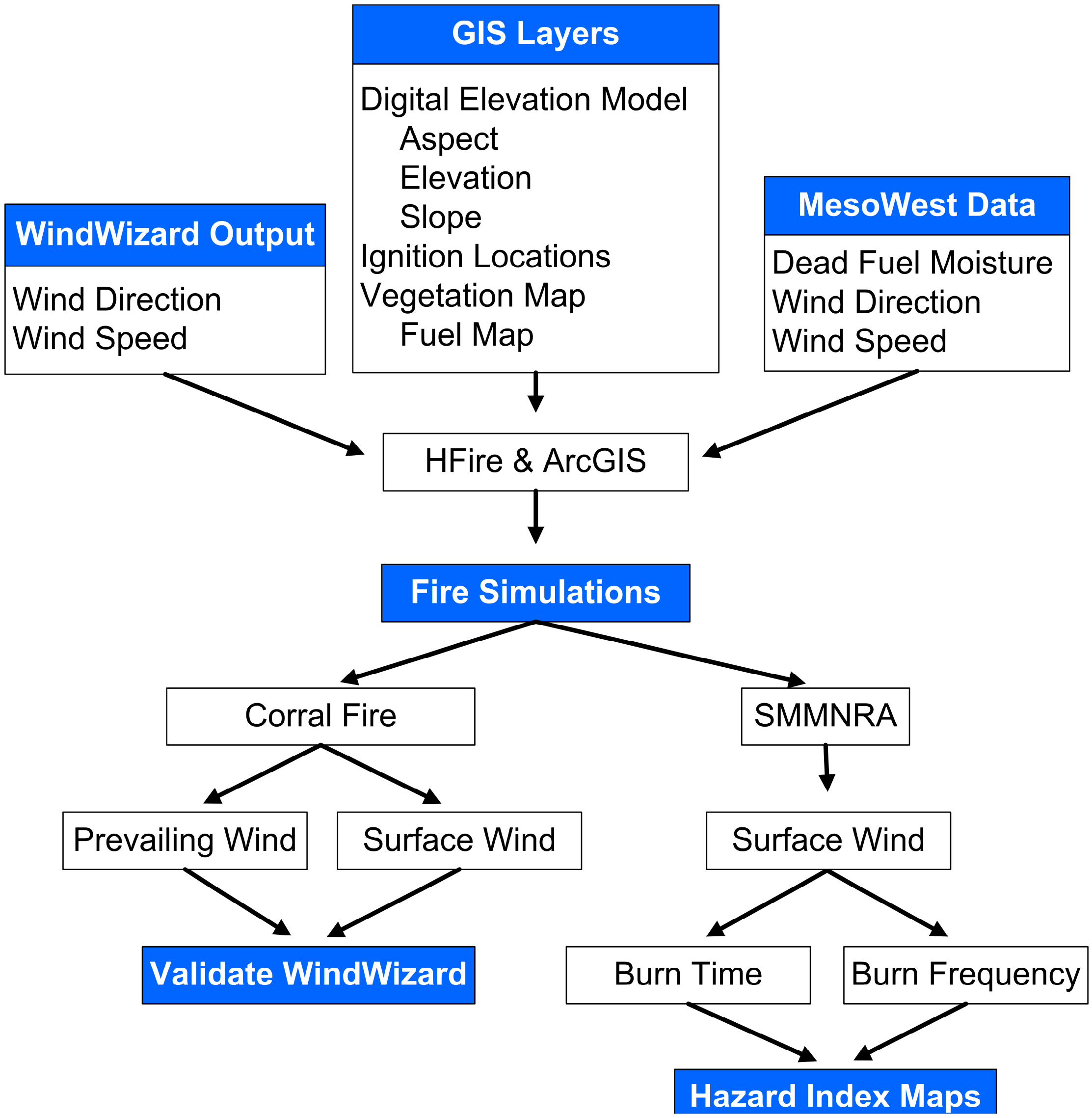

Figure 4: Flow chart overview of methods.

Wind Direction Analysis

Before running any simulations or analysis, we conducted an assessment of historical weather conditions during SAW events in SMMNRA using data acquired from MesoWest. MesoWest is a cooperative project between researchers at the University of Utah, forecasters at the Salt Lake City NWS office, the NWS Western Region Headquarters, and personnel of participating agencies, universities and commercial firms (University of Utah, 2009). RAWS in the MesoWest network, which operate at a reference height of 6.1 meters, take one measurement per hour of prevailing wind speed and direction, and dead ten-hour fuel moisture. We downloaded MesoWest data for the months of October and November, from 2004 to 2008, from the following stations: Agoura Hills, Cheeseboro, Circle X Ranch, Leo Carrillo, Los Angeles, Malibu Canyon, Malibu Hills, Thousand Oaks and Woodland

Hills. However, some of the stations listed above (Agoura Hills, Circle X Ranch, Los Angeles, Malibu Canyon and Woodland Hills) did not provide the complete set of data (fuel moisture, wind direction, wind speed and temperature) required for our analysis for those dates. We selected the months of October and November because these months represent peak SAW conditions. We used the temperature and humidity data from MesoWest to assist in identifying SAW events, but temperature and humidity were not used as inputs into the HFire model.

To model fire hazard for a worst-case scenario, we used the following criteria to identify an extreme SAW event: temperatures greater than 26° C (79°F), relative humidity less than 15 percent, wind direction between 330° and 110°, wind speeds greater than 25 kph (15 mph) and dead fuel moisture levels less than 10 percent. Based on the above criteria, we selected and analyzed the hourly wind directions for four different multiple day Santa Ana events (Table 3).

Table 3: RAW stations and dates of the multiple day Santa Ana events used to compile weather data.

	October 4-7, 2005	**October 21-23, 2007**	**November 5-8, 2008**	**November 13-19, 2008**
Stations	Thousand Oaks	Thousand Oaks	Thousand Oaks	Thousand Oaks
	Cheeseboro	Cheeseboro	Cheeseboro	Cheeseboro
	Malibu Hills	Malibu Hills	Malibu Hills	Malibu Hills
	Leo Carrillo	Malibu Canyon	Leo Carrillo	Leo Carrillo

Source: MesoWest

We calculated the mean, median and mode of the prevailing wind direction, wind speed and dead fuel moisture levels for an average SAW event. The historical wind direction of an average SAW event was used to weight the wind directions (0°, 45°, 90°, 337.5°) for the fire hazard index map.

We also compiled weather data from MesoWest to model the 2007 Corral Fire, the historic fire we recreated for our analysis. The Corral Fire began on November 24, 2007, and was contained on November 27, 2007. We downloaded data from three weather stations that were in close proximity to the fire: Malibu Hills, Leo Carrillo and Cheeseboro. We calculated the mean, median and mode of the prevailing wind direction, wind speed and dead fuel moisture levels during this period.

Fire Simulations

We used HFire to run numerous fire simulations within SMMNRA under SAW conditions. For the purposes of this study, the landscape was divided into 30-meter by 30-meter cells, a relatively fine resolution that still allowed data processing on standard desktop computers.

HFire

In HFire, the configuration file (.cfg) informs the batch file (.bat) where to find the necessary inputs to run the desired simulation (see Appendix A for a more detailed explanation of HFire file types). Computer simulation of fire spread is based on topographic data, weather data, fuel data and ignition location. The configuration file determines the start and end of the fire in one hour time-steps. Also included in the configuration file are details on the conditions that would extinguish a fire. For example, if a simulated fire does not spread to a new cell within three hours, HFire will extinguish the fire.

Several assumptions were made when running the HFire program. One major assumption was that our SAW data is representative of conditions in the study area. We limited our weather data to four years, which was restricted because of the data made available by the local weather stations. The fuel model we used is a simplification of the diverse landscape in the study area. We assumed that the fuel models used in the fire spread model accurately represent the vegetation communities in SMMNRA. When possible we used fuel models that were specific to the Recreation Area's vegetation communities (Weise & Regelbrugge, 1997), but we were limited to what fuel models are currently available. We also assumed that developed areas and roads within SMMNRA are unburnable. However, small burnable holes were created in U.S. Highway 101 and U.S. Highway 23 in order to simulate "spotting." Spotting occurs when embers are transported by the wind beyond the fire front and ignite vegetation ahead of the fire. Creating small burnable holes in the freeways allowed the fire to spread across roads that would have otherwise acted as barriers to the simulated fires. Smaller roads were not incorporated into the fuel model; therefore, they were not barriers to fire spread. Simulations for the study-area were limited to 24 hours, rather than 72 hours, which is the average length of a SAW event. Most boundaries of historic fires remain static after the first 24 hours, likely due to firefighting efforts. During a SAW event, winds do not blow continuously from the northeast quadrant for 72 hours, but fluctuate frequently. When winds die down or shift periodically to other quadrants, fire fighters are able to begin containment actions. HFire cannot model firefighting, and the limited number of grids we were given prevented hourly variation of the wind parameter. For this analysis, we assumed that four wind directions and two wind speeds (for a total of eight wind grids) can be used to model fire spread in the SMMs during SAW events.

Input Files

The model required several input files. SMMNRA provided us with a database of ignition locations within the Recreation Area (Appendix B1), as well as a DEM of the Recreation Area. We created ASCII (.asc) text files for elevation, slope and aspect from the provided DEM, all with identical area, cell size and number of cells. Additionally, the vegetation map SMMNRA provided us with served as the basis for the fuel model map. The WindWizard gridded wind data was supplied to SMMNRA by the Fire Sciences Laboratory in Missoula, Montana. The prevailing wind input data (hourly wind speed and direction) used to compare against the gridded wind inputs, were downloaded from MesoWest. Cloud cover was assumed to be zero during SAW events, and live fuel moisture was held constant at 60 percent of oven-dry weight for live herbaceous material and for live woody material (Peterson, et al., 2009). Some of the input files were slightly more complex. The processes for creating these files are described in detail below.

Wind Data

Wind modeling of historic fires requires simulating combinations of wind speeds and directions. Typically the simulations would match a forecasted or historic wind (Forthofer et al., 2003). WindWizard generates surface wind by accounting for the topography of a region. The Fire Sciences Laboratory used WindWizard to model SAW conditions (direction and speed) at a 100-meter resolution for SMMNRA. However, only four wind directions and two speeds were provided (Table 4).

Table 4: Prevailing wind direction and speed used by Missoula Fire Sciences Laboratory to produce wind grids for SMMNRA.

Wind Direction	Speed in kph (mph)
337.5° (NNW)	24 (15)
337.5° (NNW)	40 (25)
0° (N)	24 (15)
0° (N)	40 (25)
45° (NE)	24 (15)
45° (NE)	40 (25)
90° (E)	24 (15)
90° (E)	40 (25)

Given a particular prevailing wind speed and direction for the study area, WindWizard assigns a speed and direction value to every cell in the study area, based on the local topography. In effect the wind speed is scaled down from the prevailing wind speed in most cells, and scaled up in a small proportion of cells, as shown in the speed distribution figures below (Figure 5, Figure 6).

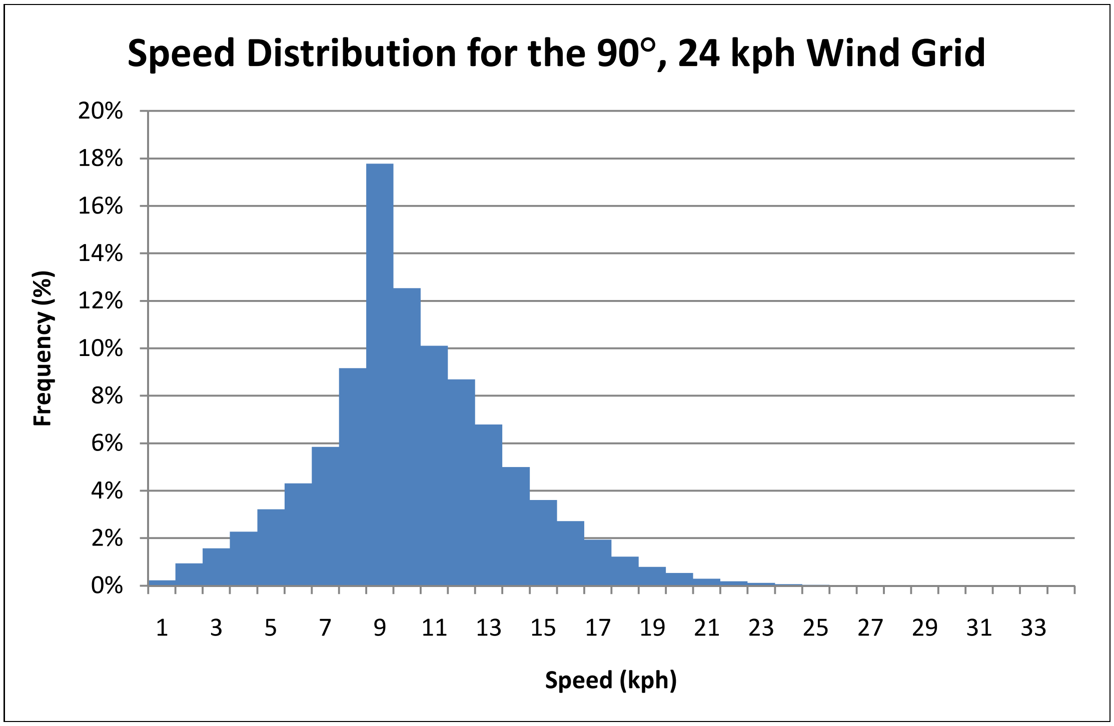

Figure 5: The distribution of wind speed in cells within the study area ,90°, 24 kph wind grid.

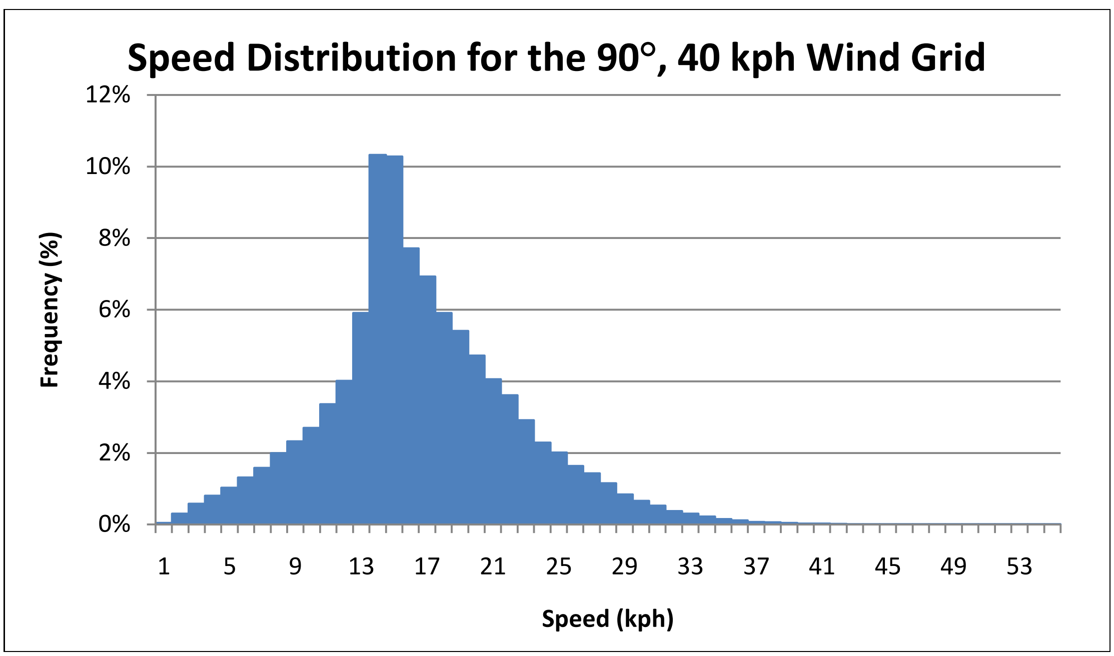

Figure 6: The distribution of wind speed in cells within the study area, 90°, 40 kph wind grid.

The most common wind speed at 100-meters from the surface, according to WindWizard for a 24 kph (15 mph) wind coming from due east (90°), is 9 kph (6 mph) (Figure 5). For a 40 kph (25 mph) wind from the same direction, the most common wind speeds are 14 and 15 kph (8 and 9 mph) (Figure 6).

Since the SMMs encompass a rather large area, two wind grids were required to cover the study area. The outer 10 to 20 percent of the wind modeling domain may be significantly affected by the boundary effect, particularly on an inflow side (Forthofer J., 2009). To account for the edge effect in the center of the Recreation Area, a third central grid was generated for each wind speed and direction combination. To create seamless wind grids for the whole study area, we clipped 20 percent from the right and left sides of the center grid to reduce edge effects, and then combined the three grid sections using the Mosaic tool in ArcGIS. However, there was no buffer between the ocean and the southern coast of the Recreation Area. Since the southern edge of the wind grids did not extend past the park boundaries, Point Dume and other areas along the southern coast of the Recreation Area are subject to edge effects.

Randomized Ignitions

A set of 200 random ignition locations was created using the ArcGIS Random Points tool. A map of the randomized ignitions is located in Appendix B2. The locations were placed within 500 meters of major roads in portions of SMMNRA with burnable fuel model classifications. Previous studies have found a higher probability of ignition based on proximity to roads, trails, housing developments and vegetation type (Syphard, et al., 2008).

Fuel Model Map

Vegetation Map

A National Vegetation Classification System was developed by managers in order to document the state of vegetation within the National Park Service. SMMNRA used this system, including photo-interpretation, automation and accuracy assessments, to produce a map of the vegetation resources in the Recreation Area. This map served as the basis of the fuel map that we created for the study area.

Existing Fuel Models

A fuel model consists of a variety of characteristics of a given vegetation type, measured during experimental burn tests. These values are used as inputs in fire spread modeling programs that simulate fire spread and intensity across a landscape. Initially, there were 13 non-dynamic fuel models built based on Rothermel’s work. Five more fuel models were added to the original 13 in 1997 (Weise & Regelbrugge, 1997). In total, the Federal Land Management Agencies recognize 18 different non-dynamic fuel models, including five classifications for shrublands.

Construction of Fuel Model Map

To create a fuel map for SMMNRA, the diverse vegetation assemblages were grouped into the most similar existing fuel classifications. For example, Fuel Model 16, “Ceanothus”, was used to represent 25 specific vegetation classifications including various species in the genus *Ceanothus*, as well as the "Bushpoppy Alliance." A complete list of the fuel models used to represent each vegetation community in SMMNRA is provided in Appendix C.

Because the fuel map represents the entire study area, developed and road areas were also given fuel classifications. In all simulations, developed areas and major roads were set as "unburnable" (i.e., fires would extinguish when reaching these areas) in the fuel map. Large roads can act as a barrier to fires, but large, wind-driven fires often "jump" even large freeways. FARSITE, the fire spread model used by SMMNRA, simulates spotting, which allows a fire to cross roads. Since HFire does not simulate spotting, the Raster Editor tool in ArcGIS was used to create small "burnable" gaps in U.S. Highway 101 and U.S. Highway 23. These burnable gaps were placed in areas where historic fires have spotted across these two freeways. For input into HFire, this information was compiled as an ASCII (.asc) grid text file with 30-meter cells.

Dead Fuel Moisture

The dead ten-hour fuel moisture level input file was built using data downloaded from MesoWest. Ten-hour fuels are fuels that take ten hours to absorb enough moisture to get two-thirds of the way to equilibrium with the ambient moisture level. HFire also used the ten-hour fuel moisture level to calculate the amount of moisture in fuels for one-hour and 100-hour fuels. We examined fuel moisture levels from multiple SAW events that took place during the months of October and November 2005 to 2008. To create the HFire input file, the average of the dead fuel moisture levels for the Cheeseboro, Leo Carrillo and Malibu Hills stations was taken, one reading per hour, from an strong SAW event that took place on November 14 to 15, 2008. The values for this event were found to be well within the range of November SAW events of the past four years.

<u>Validation Using One Historic Fire (Corral Fire)</u>

In order to test how well the model represents reality, we chose to recreate a historic fire at a local scale. The Corral Fire of 2007 was chosen because it took place completely within the study area, and weather data for that period was available from MesoWest. Hourly wind speed, wind direction and dead fuel moisture inputs for the Corral Fire were used to change parameters from the previous simulations. Given that the Corral Fire burned close to the ocean, we took the dead fuel moisture inputs for the simulations from one MesoWest station, Leo Carrillo, because of its proximity to the ocean.

To recreate the fire as accurately as possible, we used the conditions closest to the observed event (Table 5). First, in simulation C1, we varied wind speed, wind direction and dead fuel moisture every hour based on data from local weather stations. We were not able to do the same for gridded wind since we were limited to the grids that were available. To compare gridded wind inputs to prevailing wind inputs, for simulation C2 we varied the hourly prevailing wind inputs, using prevailing winds only from the four wind directions we had (0°, 45°, 90°, 337.5°).

For simulation C3, we used gridded wind inputs varied hourly, but limited to the four wind directions, as with C2. Simulations C4 to C11 used a constant gridded wind input, each with one of the four wind directions and two wind speeds. Simulations C12 to C19 are similar, but used prevailing wind inputs.

Table 5: Corral Fire simulations.

Run Number	Prevailing or Gridded Wind Input	Historic Values and Approximate of Historic Values *	Constant or Hourly Input	Grid Used (direction_ speed)	Notes
C1	Prevailing	Historic	Hourly	NA	Customary HFire Simulation
C2	Prevailing	Approximate	Hourly	Various	Prevailing winds set to match grid values in C3
C3	Gridded	Approximate	Hourly	Various	Gridded winds nearest to historic wind values
C4	Gridded	Approximate	Constant	0_24	Constant Grid
C5	Gridded	Approximate	Constant	0_40	Constant Grid
C6	Gridded	Approximate	Constant	45_24	Constant Grid
C7	Gridded	Approximate	Constant	45_40	Constant Grid
C8	Gridded	Approximate	Constant	90_24	Constant Grid
C9	Gridded	Approximate	Constant	90_40	Constant Grid
C10	Gridded	Approximate	Constant	338_24	Constant Grid
C11	Gridded	Approximate	Constant	338_40	Constant Grid
C12	Prevailing	Approximate	Constant	0_24	Constant Prevailing
C13	Prevailing	Approximate	Constant	0_40	Constant Prevailing
C14	Prevailing	Approximate	Constant	45_24	Constant Prevailing
C15	Prevailing	Approximate	Constant	45_40	Constant Prevailing
C16	Prevailing	Approximate	Constant	90_24	Constant Prevailing
C17	Prevailing	Approximate	Constant	90_40	Constant Prevailing
C18	Prevailing	Approximate	Constant	338_24	Constant Prevailing
C19	Prevailing	Approximate	Constant	338_40	Constant Prevailing

*Approximate historic values selects the closest of the four gridded wind directions (0°, 45°, 90°, and 337.5°) given to us by Missoula Fire Sciences Laboratory.

<u>Study Area-Wide Fire Hazard Index Modeling</u>

To model potential fire hazard throughout the study area under SAW conditions, we simulated fires using four wind grid scenarios (Table 6). All wind grids used were based on a 24 kph prevailing wind speed, because this best approximated the observed wind speeds in the wind analysis (Wind Analysis, Section VII). For each wind grid, we conducted a "historic run" consisting of 190 distinct fire simulations using the historic ignition locations. Each individual fire was modeled for a 24-hour period because WindWizard input to fire spread models was found to be most accurate for the first day of a fire simulation (Butler et al., 2006). Each ignition point was placed into a separate ignition text file with X- and Y-coordinates in Universal Transverse Mercator (UTM) North American Datum (NAD) 1983 Zone 11.

Table 6: Study area simulations.

Run Number	Wind Direction*	Ignition Location Database Used
S1	0°	historic
S2	90°	historic
S3	45°	historic
S4	337.5°	historic
S5	90°	historic
S6	90°	random

*all simulations used 24 kph wind grids, with the exception of S5, which used a 40 kph wind grid.

Creating Hazard Index Maps

Each HFire simulation resulted in an image (.png) file for each simulated hour, for a total of 24 image files based on the 24-hour fire simulation. The image file was then imported into ArcGIS to create maps for two different measures of hazard, burn frequency and burn time, or how rapidly a given cell burned in simulations. These two measures, described further below, were combined to produce a hazard index map.

<u>Hazard Index Map Based on Historic Runs</u>

Output 1: Burn frequency

For each run we found the frequency with which a cell burned across all simulated fires (190 for historic ignition locations, 200 for random ignitions). For each individual fire, the image file from the last hour was reclassified into binary data. The 24th hour, or final hour of the simulation, image file included all areas burned in the simulated fire. Each cell was given a value of 1 if it burned or 0 if it did not burn in a fire. The mean for all fires in the run, approximately 190 fires, was calculated using the ArcGIS Cell Statistics tool, to yield a burn frequency map for all ignitions in that run. The burn frequency was calculated using the following formula:

$$Output\ 1 = \left(\frac{Number\ of\ times\ burned}{Number\ of\ ignitions}\right)$$

Output 2: Burn time

For each run, we found the mean amount of time it took for a cell to burn. Fires are often measured in terms of the rate of spread, or the distance the fire travels over time. As a proxy for rate of spread, we excluded distance and only used the hour in which a cell burned, or “burn time.” This metric is not equivalent with rate of spread and does not truly indicate how fast a fire traveled. However, the burn time metric does indicate at what point in time the cell burned. For instance, a cell that burned in hour 15 of the fire simulation is considered a less hazardous location than a cell which burned in hour five of the same fire simulation. The method for finding burn time is explained in greater detail below.

We automated the processing of the HFire output image files into a single band fire progression image (that could be opened in ArcGIS) using ENVI/IDL, a program for processing and analyzing geospatial imagery. All cells that ignited within a given time step were given a value for that hour of the fire. We then found the sum of the time it took each cell to burn using the Cell Statistics tool in ArcGIS. Using the ArcGIS Single Output Map Algebra tool, this value was then divided by the total number of times each cell burned to find the mean time for a given cell to burn, if it burned at all. This calculation is shown below:

$$\frac{\sum Burn\ time}{number\ of\ times\ burned} = average\ burn\ time$$

The score based on the burn time was calculated to give a value of 24 to cells that burned in the first hour and a value of 1 to cells that burned in the last hour. We used the following equation to create the burn time scores:

$$Output\ 2 = 25 - \frac{\sum Burn\ time}{Number\ of\ times\ burned}$$

Fire Hazard Index Map for Each Run

To create a fire hazard index map for a given run of simulations, we multiplied the burn frequency (Output 1) by a score based on the average burn time for each cell (Output 2) using the Single Output Map Algebra tool. This weighted the burn time by the burn frequency:

$$H = Output\ 1 * Output\ 2 = \left(\frac{Number\ of\ times\ burned}{Number\ of\ ignitions}\right) \times \left(25 - \frac{\sum Burn\ time}{Number\ of\ times\ burned}\right)$$

Overall Fire Hazard Index Map

Three steps were involved in creating the overall hazard index map based on historic ignition locations, using 24 kph wind grids. First, we used the Single Output Map Algebra tool to create a weighted average of the burn frequencies based on each wind direction. Each grid was weighted based on the proportion of time the wind blew from that direction in the wind analysis (Figure 8). This calculation is shown below. We used the same method to create a weighted average of the burn time for all four directions. Finally, to create an index map based on both measures of hazard, we used the Single Output Map Algebra tool to multiply the two weighted average maps.

$$Weighted\ Average = 0°\,(46\%) + 45°\,(40\%) + 90°\,(8.9\%) + 337.5°\,(5.1\%)$$

$$Un - weighted\ Average = (0° + 45° + 90° + 337.5°)/4$$

Hazard Index Map Based on Random Runs

All of the processes described above were used to determine hazard indices based on the runs using random ignition locations for the 90° wind grid at 24 kph.

Analysis

Estimating Sample Size Adequacy

To determine how many ignitions points should be included to ensure that all burnable areas of the Recreation Area were burned, we conducted an analysis based on the number of ignitions simulated. Simulated fire ignitions were randomly selected in groups of: 1, 10, 20, 40, 60, 80, 100 and 120. Ten separate, randomly created groups of each size were added into ArcGIS and combined into one shapefile. We then recorded and plotted the average number of cells burned by each group (Appendix J).

Sensitivity Analysis

Study Area-Wide

We conducted simulations in order to evaluate how sensitive HFire is to ignition location, gridded wind direction and gridded wind speed.

To test the sensitivity of the model to grids representing different prevailing wind directions, we compared the hazard index maps produced for the four simulations. The fuel model, ignition locations and prevailing wind speeds were held constant for these four simulations.

To test the sensitivity of the model to grids representing different prevailing wind speeds we compared the hazard index maps produced for two simulations. We used the 90° wind direction grid for 24 kph and 40 kph prevailing wind speeds. We chose to use the 90° wind grid based on the wind analysis discussed in Section VII.

To test the sensitivity of the model to ignition location, we compared the hazard index maps produced for two simulations. We used the 90° wind direction grid at 24 kph using the historic ignition locations, and the same wind direction grid using the 200 random ignition locations. In this random run, all other factors, such as fuel model, wind speed and wind direction, were held constant. The results for the grids were compared to evaluate the effect of using historic versus randomized ignitions in the hazard index.

The relative importance of wind speed, wind direction and ignition location was determined based on absolute differences in hazard, and with regard to spatial location for cells in the study area. We calculated the raw differences in hazard by subtracting two raster maps of interest using the Single Output Map Algebra tool. Additionally, multiple regressions were conducted to find correlations between the spatial distribution of hazard with respect to input parameters.

Corral Fire

The Corral Fire was modeled in 14 additional ways. Seven of the simulations (C4 to C7, C9 to C11) used a constant gridded wind input, and another seven simulations (C12 to C15, C17 to C19) used prevailing wind inputs from the same directions the wind grids are based on (0°, 45°, 90°, 337.5°at 24 kph and 90° at 40 kph).

The sensitivity of the simulations recreating the local Corral Fire was tested for the same parameters of interest. For each simulation, we calculated the Sørenson metric for the total area burned, area burned outside the actual Corral Fire boundary (overburned), and area within the Corral Fire boundary that did not burn (underburned) to evaluate the accuracy of each. The Intersect tool in ArcGIS was used to find the area of overlap between the polygons for each simulated fire and the actual Corral Fire boundary polygon.

THIS PAGE INTENTIONALLY LEFT BLANK

VII. Results

Wind Direction Analysis

We analyzed the hourly wind directions for four different SAW events from five weather stations (Table 3). These four SAW events were assumed to be representative of most SAW events that occur in the study area. The result of the wind direction analysis demonstrated that, in past SAW events, winds have blown primarily from the northeast quadrant, or 330° to 110° (Figure 7).

Out of the four gridded wind directions (0°, 45°, 90° and 337.5°), the winds blew most often from the directions of 0° and 45° (Figure 8). We used the results of this analysis to weight the wind directions for the fire hazard index map.

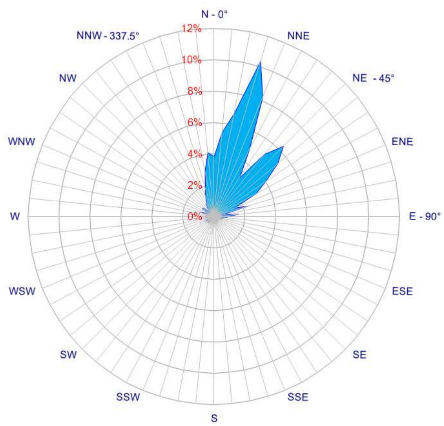

Figure 7: SAW wind rose. SAW event data were analyzed from weather stations within SMMNRA for the last four years. The wind rose depicts a compilation of wind frequency from each direction during the four SAW events during that period.

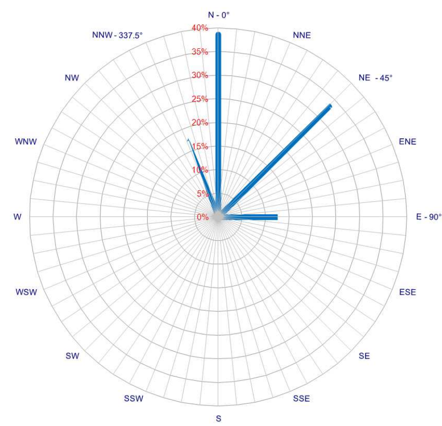

Figure 8: SAW simplified wind rose. SAW frequencies were generalize into one of the four directions (0°, 45°, 90°, 337.5°). These frequencies were used to weight our fire hazard index maps. SAWs blow more often from 0° and 45° than from the other two directions.

Fire Simulations

Modeling One Historic Fire (Corral Fire)

In recreating the Corral Fire, we used the weather conditions closest to the observed event (Figure 9, Figure 10), within the limitations of our data, and ran our simulations to recreate the first 14 hours of the fire.

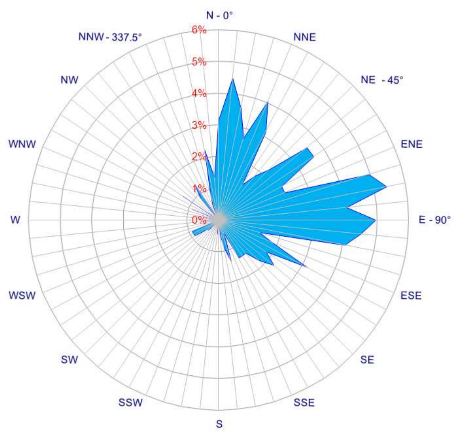

Figure 9: Corral Canyon Fire wind rose. Wind directions during the Corral Canyon Fire were compiled into this wind rose which depicts the frequency of wind from each direction during the event.

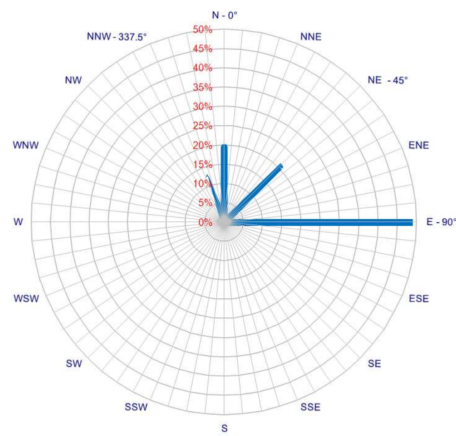

Figure 10: Corral Canyon Fire simplified wind rose. Wind directions during the Corral Fire were combined into one of the four directions (0°, 45°, 90°, 337.5°). SAWs blew most frequently from 90° during the Corral Fire.

The resulting fire boundaries from all simulations are shown in Appendix D. For simulation C1, we varied wind speed, wind direction and dead fuel moisture every hour based on data from local weather stations. The fire resulting from simulation C1 burned to the north and slightly west of the Corral Fire (Figure 11).

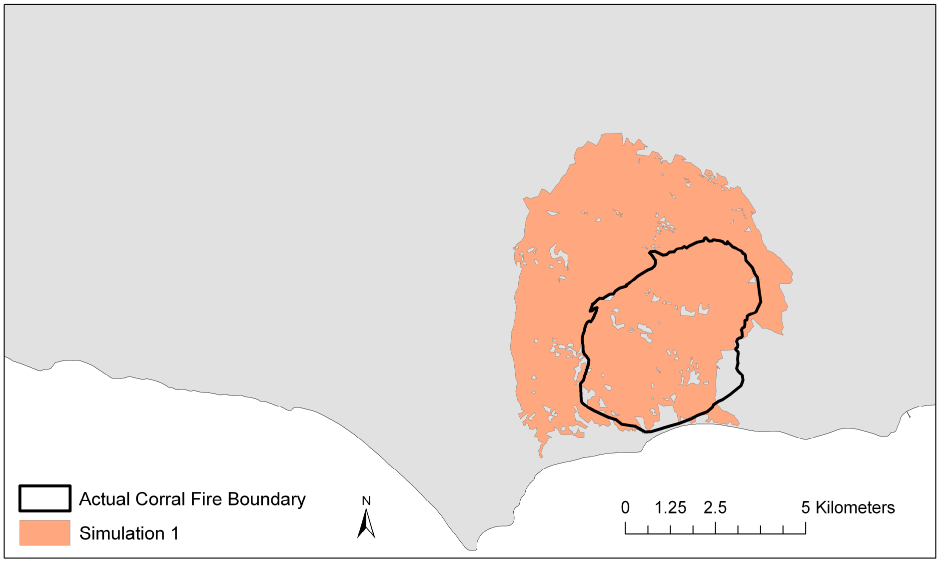

Figure 11: Corral Fire simulation, prevailing wind input, varied hourly.

We varied the hourly prevailing wind inputs using only values that matched the wind grids for simulation C2. The fire resulting from simulation C2 burned approximately three times the size of the actual fire (Figure 12). The simulated fire spread considerably north and west of the historic fire boundary, in addition to burning over the Corral Fire.

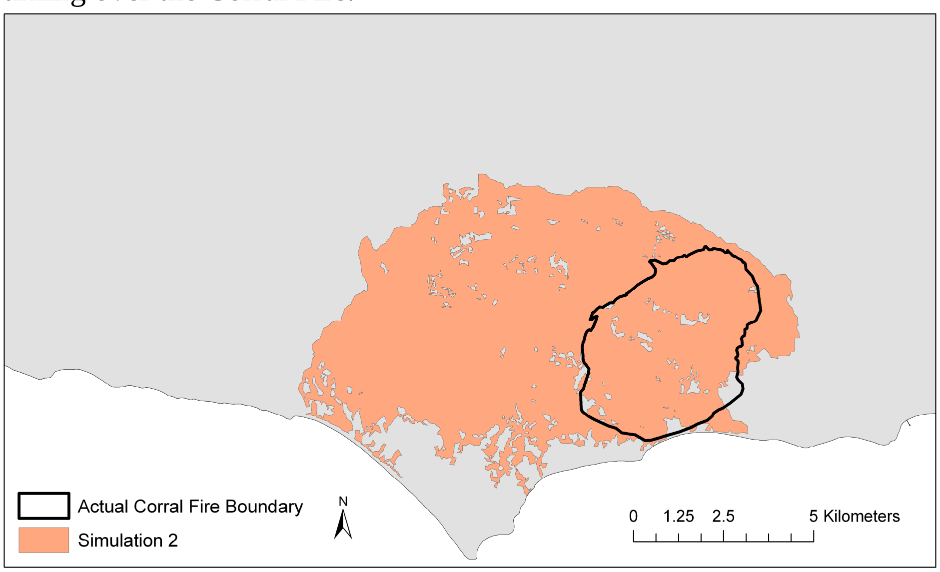

Figure 12: Corral Fire simulation, prevailing wind inputs varied hourly for the wind directions 0°, 45°, 90° and 337.5° and wind speeds of 24 or 40 kph.

Simulation C3 varied wind grids hourly, using the grid which most closely matched the historic data for each hour in MesoWest. The simulated fire burned over most of the Corral Fire, but also burned the area northwest of the Corral Fire boundary (Figure 13). The simulated fire is slightly larger than the historic fire.

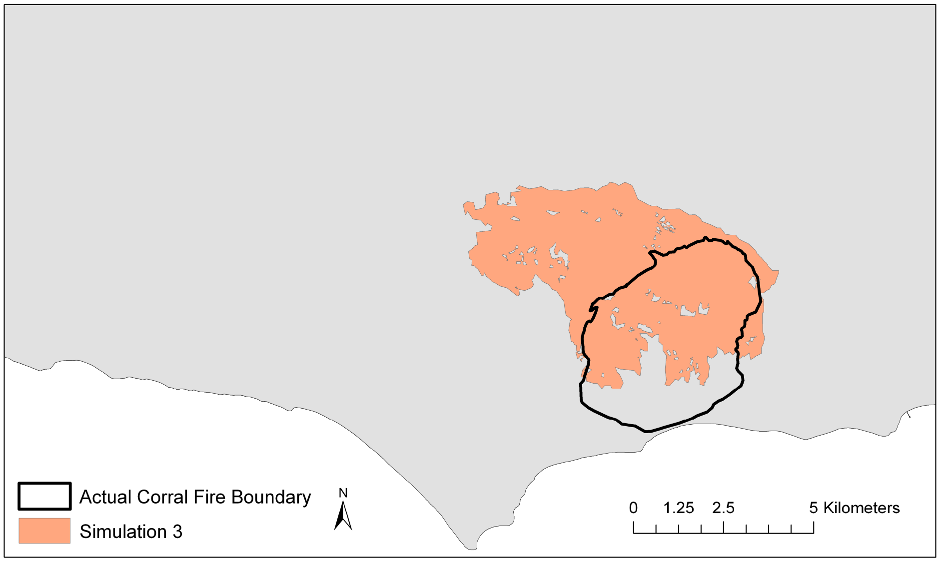

Figure 13: Corral Fire simulation using gridded wind inputs varied hourly for the wind directions 0°, 45°, 90° and 337.5° and wind speeds of 24 or 40 kph.

For simulation C8, we used a constant gridded input, with wind direction 90° and wind speed of 24 kph. The fire resulting from simulation C8 spread west, and intersects only a small area of the northwest corner of the Corral Fire (Figure 14).

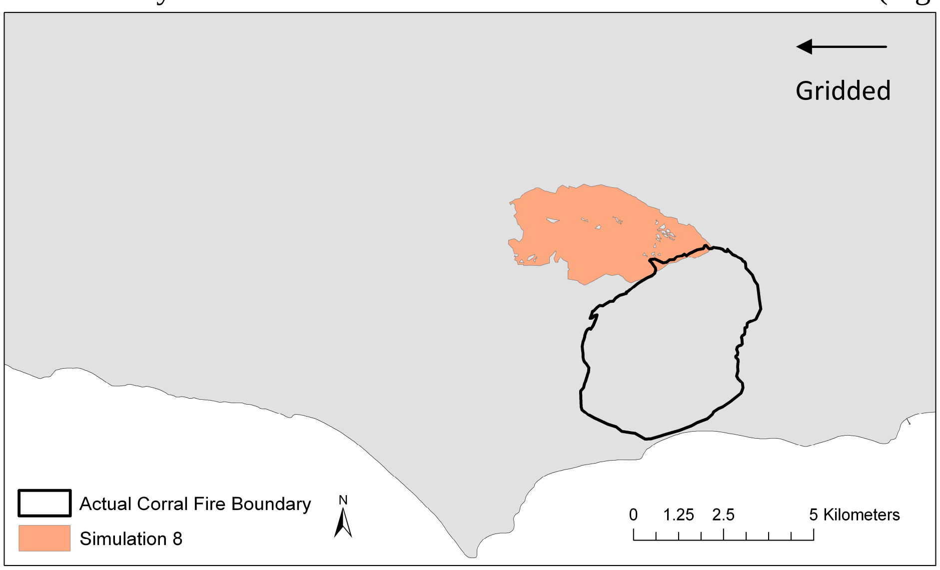

Figure 14: Corral Fire simulation using the 90° wind grid at a wind speed of 24 kph.

For simulation C16, we used a prevailing wind input from 90° with wind speed 24 kph. The fire resulting from simulation C16 burned approximately two times the size of the actual fire (Figure 15). The simulated fire spread west of the historic fire boundary, and intersects a small portion of the northwest corner of the Corral Fire.

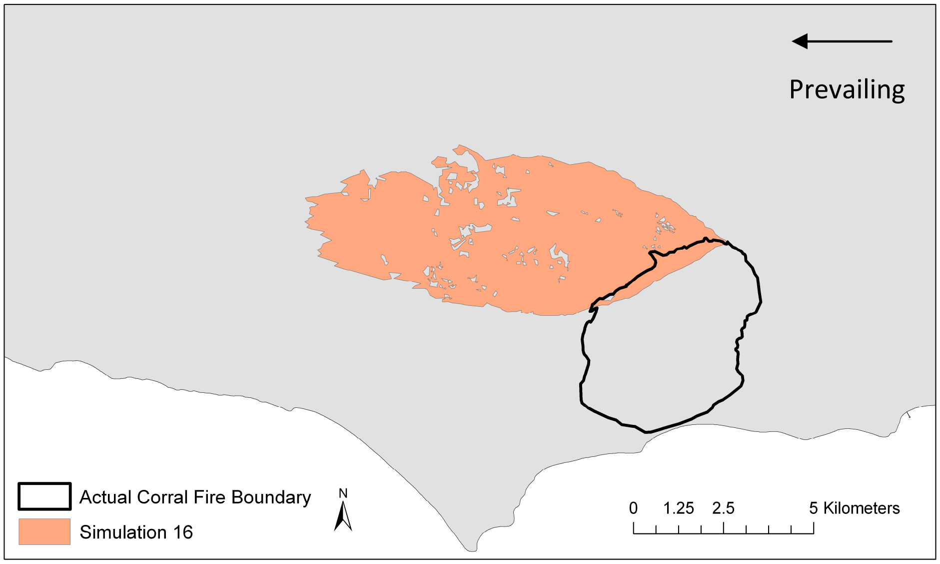

Figure 15: Corral Fire simulation produced by using prevailing wind for wind direction of 90° at a wind speed of 24 kph.

Hazard Index Map Based on Historic Runs

Hazard index maps for simulation S2, a historic run based on the 90° wind grid and 24 kph speed, are shown below. The hazard index maps for Simulations S1, S3, S4 and S5 are in Appendix E.

Output 1: Burn Frequency

Figure 16 is an example of a burn frequency map for the 90° wind grid at 24 kph. For all runs, fires tended to burn most frequently in the center of SMMNRA (Appendix E). Fires tended to burn least frequently in the northwestern, northeastern and eastern sections of the Recreation Area. The burn frequency for the 90° grid at 40 kph varied the most from the other burn frequency maps, in that the fires burned most frequently in the southern central portion of SMMNRA (Appendix E5).

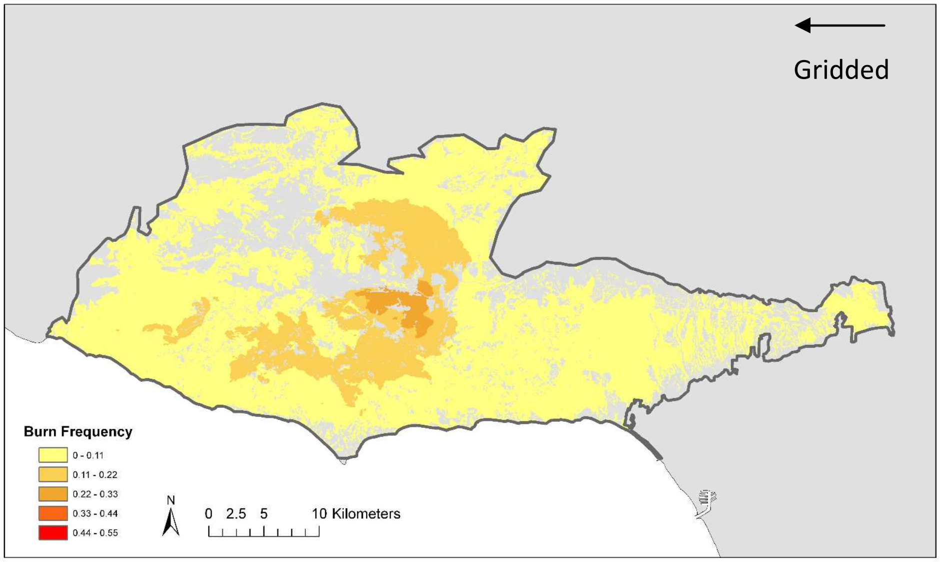

Figure 16: Burn frequency map for study area using the 90° wind grid at a wind speed of 24 kph using historic ignition locations.

Output 2: Burn Time

Figure 17 shows the burn time map for S2. Overall, fires burned moderately quickly throughout central SMMNRA (Appendix F). The 90° wind grid at 40 kph burned a greater area more rapidly (Appendix F5).

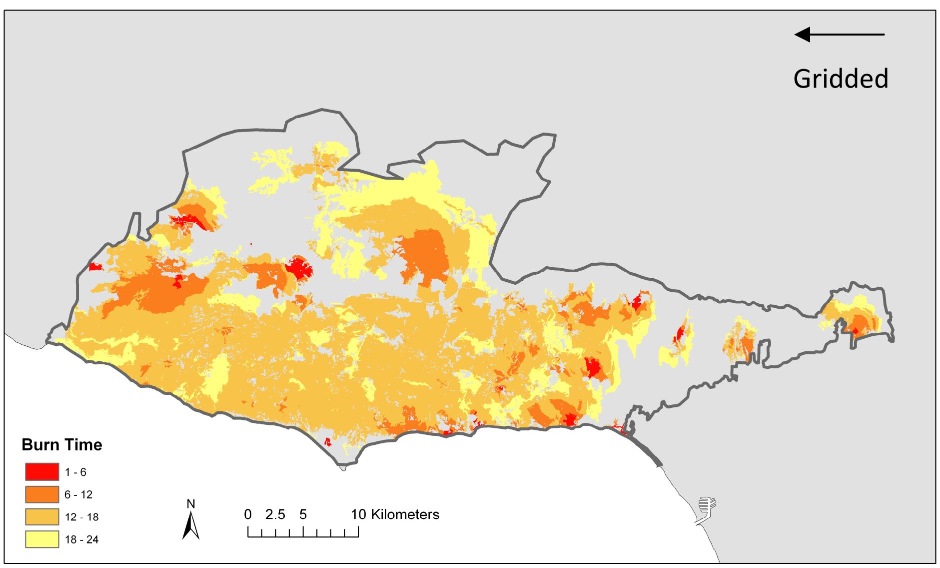

Figure 17: Burn time map for study area using the 90° wind grid at a wind speed of 24 kph using the historic ignition locations.

Fire Hazard Index Map for Each Run

Overall, fire hazard is highest in the central part of SMMNRA for all wind grids (Appendix G). Below, the fire hazard index map for S2 is shown (Figure 18).

When wind speed is increased for the 90° wind grid from 24 to 40 kph, the hazard shifts to the southern central portion of SMMNRA (Appendix G5).

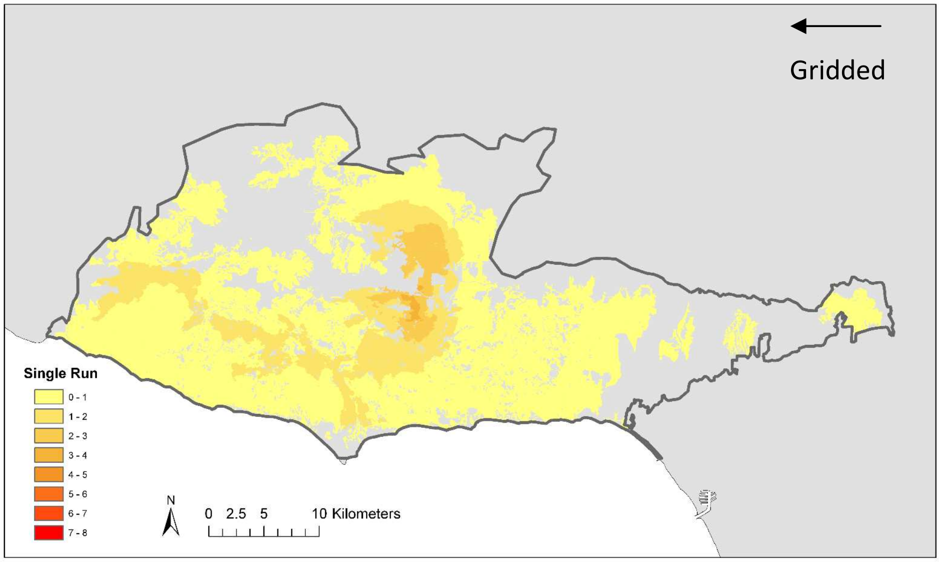

Figure 18: Fire hazard index map for the 90° wind grid at a wind speed of 24 kph using historic ignition locations.

Overall Fire Hazard Index Map

The overall fire hazard index map combines all four fire hazard index maps using a wind speed of 24 kph and historic ignition locations. In the un-weighted overall fire hazard index map (Figure 19), each wind grid is given equal weight. The map of the un-weighted overall fire hazard index shows that fire hazard is highest in the central portion of SMMNRA, and fire hazard is lowest in the eastern portion of the Recreation Area and along the coast.

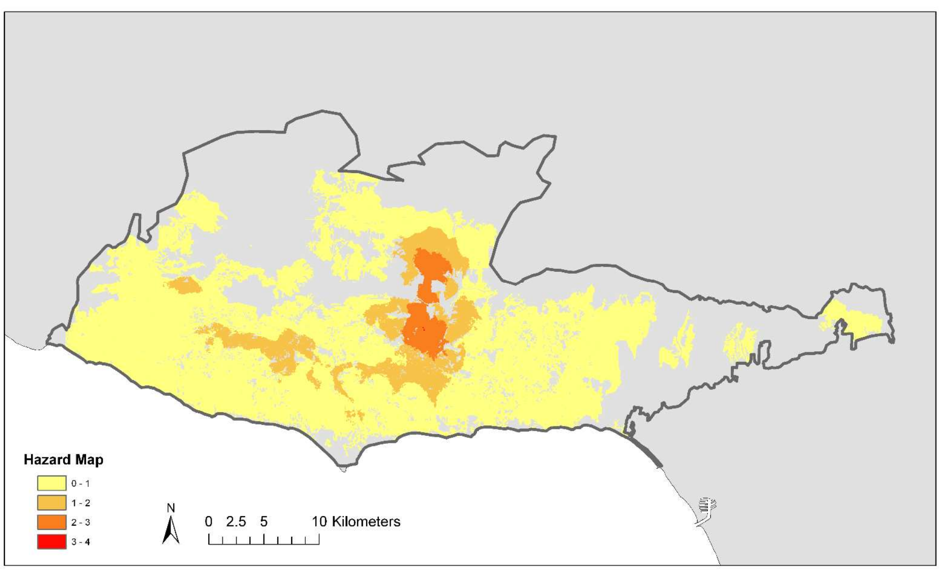

Figure 19: Un-weighted overall fire hazard index map using historic ignition locations.

The weighted overall fire hazard index map combines all four fire hazard index maps using a wind speed of 24 kph and historic ignition locations. Fire hazard is still highest in the central area of the Recreation Area, and fire hazard is still lowest in the eastern portion of SMMNRA and along the coast (Figure 20). The main difference between the two maps (Figure 19, Figure 20) is that the fire hazard is higher in the weighted overall map.

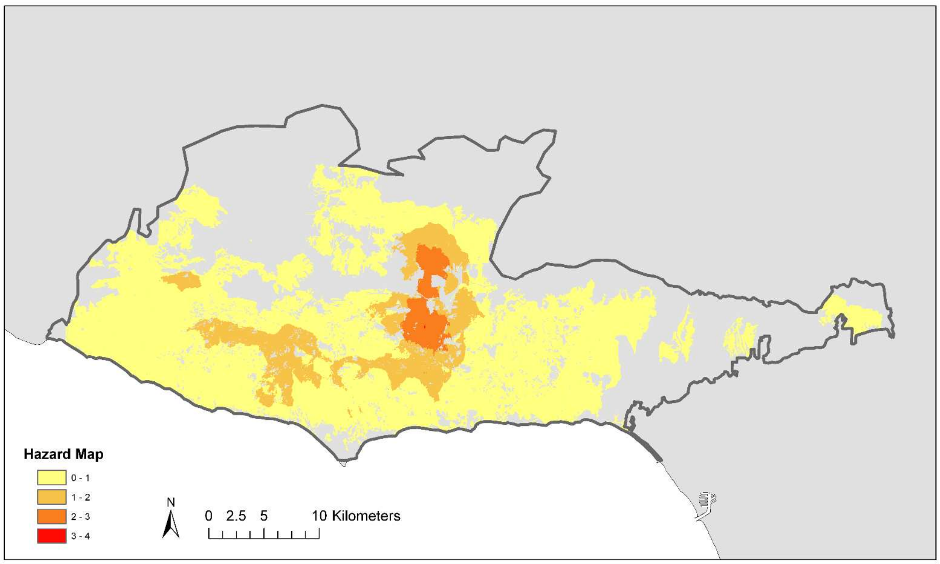

Figure 20: Weighted overall fire hazard index map for historic ignition locations.

<u>Hazard Index Map Based on Random Ignition Points</u>

Output 1: Burn Frequency

Overall, the burn frequency for the 90° wind grid at 24 kph is relatively low. The highest burn frequency is in the southern portion of SMMNRA (Figure 21). Fires burned less frequently in the northeastern, northwestern and eastern sections of the Recreation Area, and along the coast.

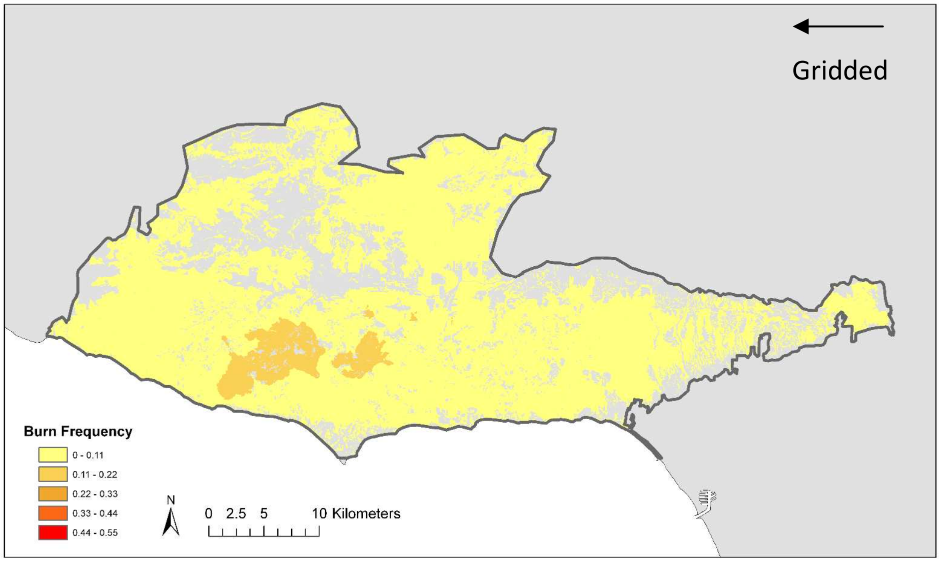

Figure 21: Burn frequency map using the 90° wind grid at a wind speed of 24 kph using random ignition locations.

Output 2: Burn Time

In the burn time map for S6, the study area burned at varying speeds. There are areas with lower burn time values interspersed with areas of higher intensity hot spots scattered throughout (Figure 22).

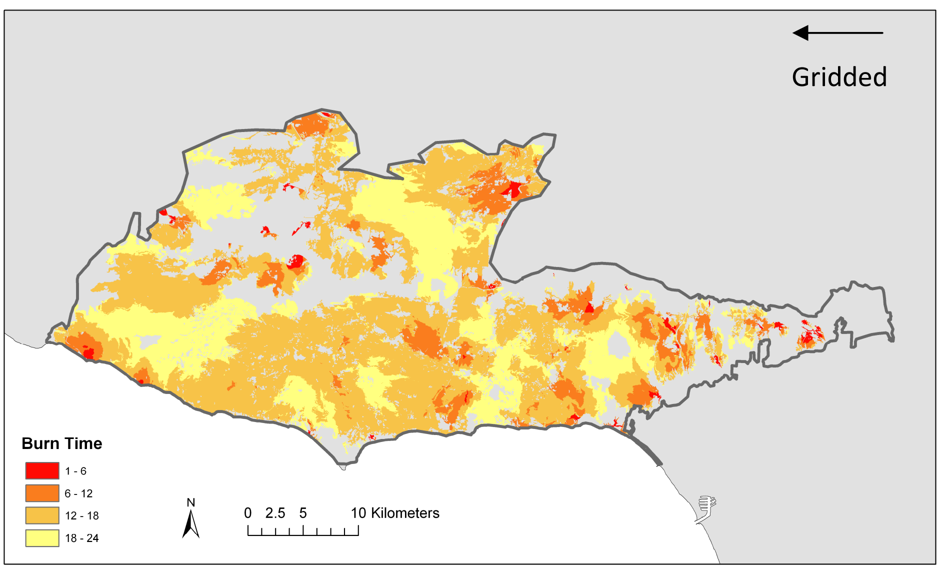

Figure 22: Burn time map using the 90° wind grid at a wind speed of 24 kph using random ignition locations.

Fire Hazard Index Map for Each Run

The fire hazard index map for S6 shows that fire hazard is highest in a small portion of the southern central SMMNRA (Figure 23). The map is very similar to the burn frequency map (Figure 21).

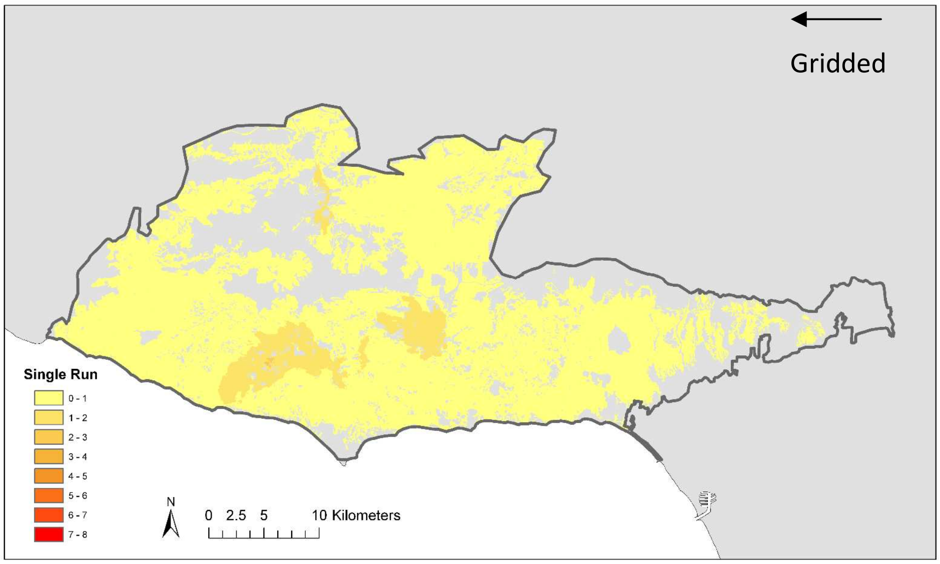

Figure 23: Fire hazard index map for the 90° wind grid at a wind speed of 24 kph using random ignition locations.

<u>Analysis</u>

Sensitivity Analysis

Corral Fire

In order to compare the accuracy of the gridded wind inputs to prevailing wind inputs, we compared the resulting fire boundaries from the simulations of the Corral Fire. The Sørenson Metric (Greig-Smith, 1983; Perry et al., 1999) was used to compare the agreement between each simulated fire and the boundary of the actual Corral Fire (Table 7). See Appendix I for a complete summary of the Corral Fire simulations.

Table 7: Comparison of Corral Fire simulations using the Sørenson metric.

Run	**Description**	**Sørenson Metric***
C1	Prevailing input, varied hourly	0.668631
C2	Prevailing input, using only 0°, 45°, 90°, 337° directions at 15 and 25 mph, varied hourly	0.381595
C3	Gridded input, varied hourly	0.522065
C4	0°, 15mph wind grid, held constant	0.488179
C8	90°, 15mph wind grid, held constant	0.016974
C9	90°, 25mph wind grid, held constant	0.024579
C16	90°, 15mph prevailing input, held constant	0.055548
C17	90°, 25mph prevailing input, held constant	0.042896
*The Sørenson Metric is calculated as S = 2a/(2a+b+c), where a is the intersection of the area burned by the two fires, b is the area burned in fire 1 but not fire 2 and c is the area burned in fire 2 but not fire 1. A Sørenson metric value of zero indicates no agreement, while a value of 1 indicates perfect agreement.		

Figure 24 shows simulations C1 and C2, both using prevailing wind inputs, except that C2 is limited to the direction of the eight wind grids. This comparison allowed us to see how limiting prevailing wind inputs to the four wind grid directions would affect the fire spread. Both simulations burned over and larger than the Corral Fire (Figure 24). The fire in simulation C1 burned mostly to the north and slightly west of the Corral Fire, whereas the fire in simulation C2 burned to the west of the Corral Fire. Both simulations overlap the boundary of the Corral Fire but burn larger than the historic fire.

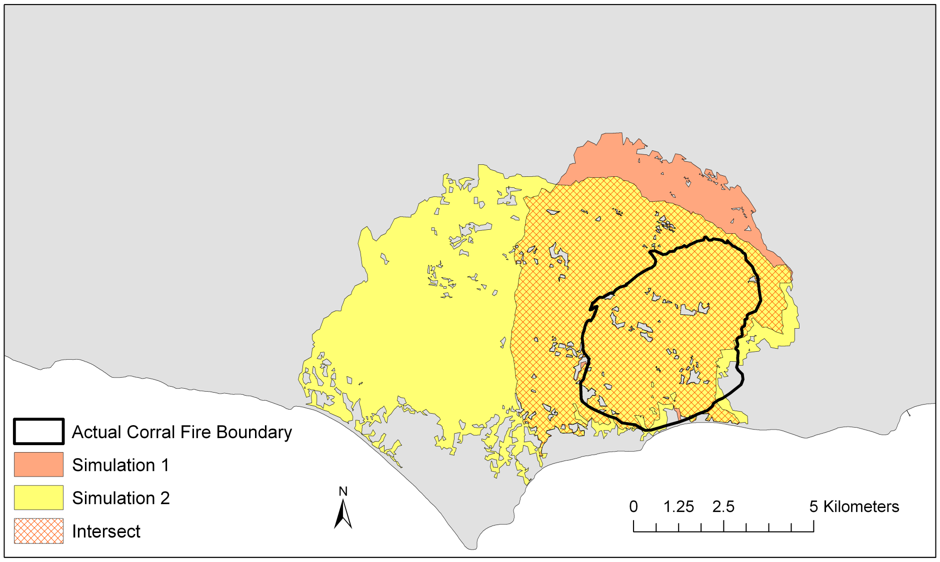

Figure 24: Corral Fire simulations using prevailing wind inputs varied hourly (red) and prevailing wind inputs varied hourly and set to match the four wind grids (0°, 45°, 90° and 337.5°) (yellow). C2 overlaps with most of C1 (red cross-hatching).

We then compared simulations C2 and C3 to determine how prevailing wind inputs set to match the four wind grids and varied hourly differed from gridded wind inputs varied hourly (Figure 25). The fire resulting from simulation C2 burned approximately three times the size of the historic fire and spread considerably to the south and west of the Corral Fire. The fire in simulation C3 was much smaller than simulation C2, but burned north from the northern edge of the Corral Fire.

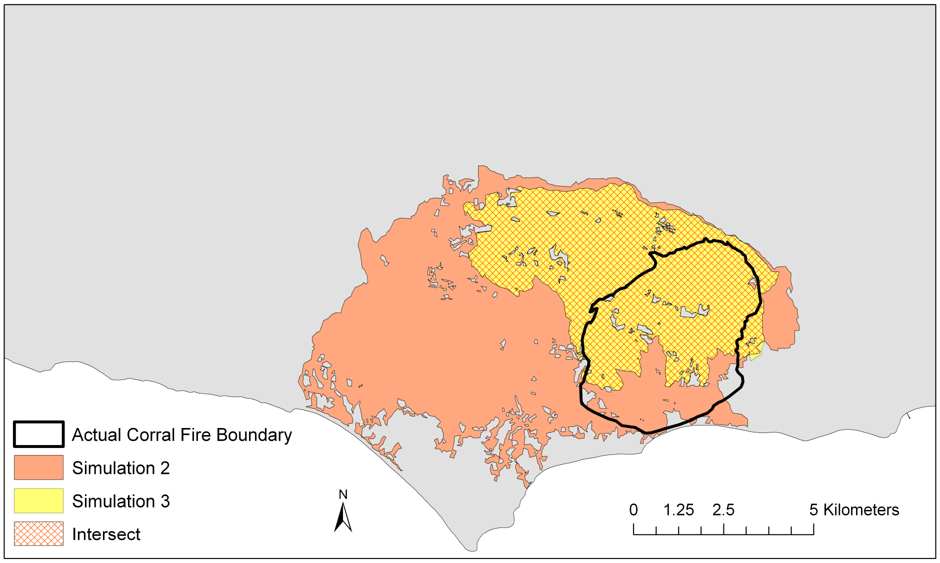

Figure 25: Corral Fire simulations using prevailing wind inputs varied hourly and set to match the four wind grids (red) (0°, 45°, 90° and 337.5°) and gridded wind inputs varied hourly and set to match the four wind grids (yellow) (0°, 45°, 90° and 337.5°). C2 overlaps with most of C1 (red cross-hatching).

Figure 26 shows simulations C1 and C3 comparing prevailing wind inputs and gridded wind inputs varied hourly. Even though C3 is only using four wind directions, it does closely model the historic fire.

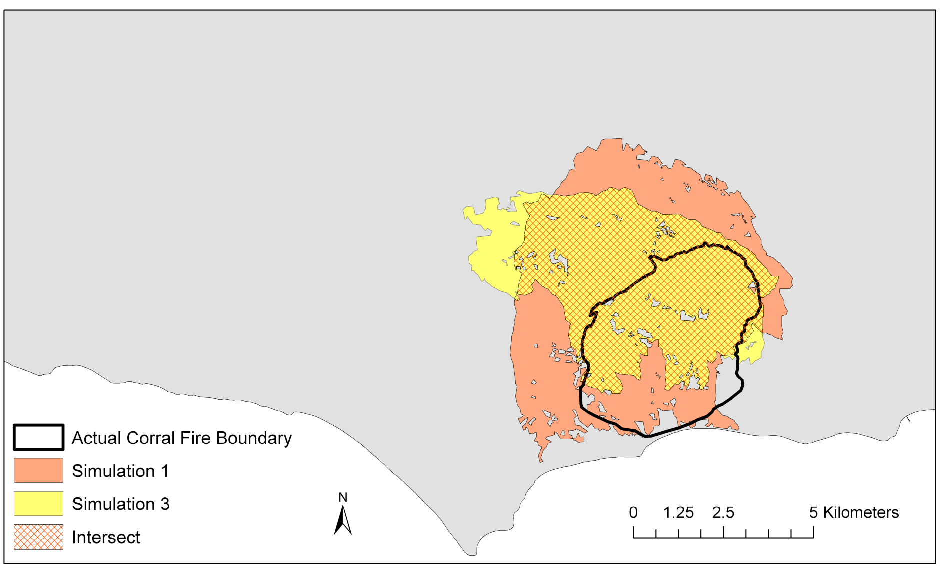

Figure 26: Corral Fire simulations using prevailing wind inputs varied hourly (red) and gridded wind inputs varied hourly (yellow). C1 overlaps with most of C3 (red cross-hatching).

Figure 27 shows simulations C8 and C16 comparing a gridded wind input to a prevailing wind input using a constant wind speed and wind direction for both. C8 and C16 both spread entirely to the west of the Corral Fire. C16 overlaps slightly with the historic fire. However, the fire from simulation C16, the prevailing wind input, spread further west than the fire from simulation C8, the gridded wind input.

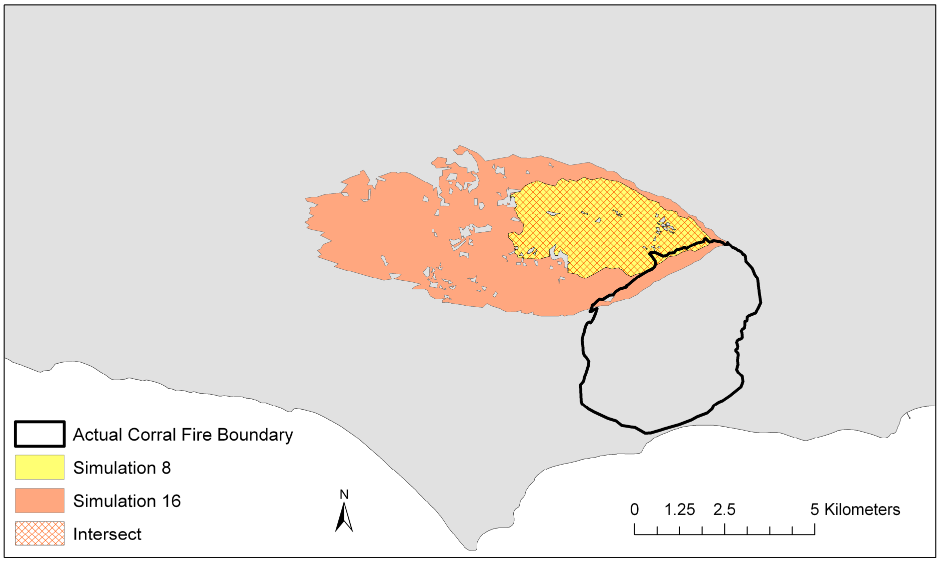

Figure 27: Corral Fire simulations using a constant, gridded wind input of 90° and 24 kph (yellow) and a constant, prevailing wind input of 90° and 24 kph (red). C16 overlaps entirely with C8 (red cross-hatching).

We then compared how wind speed affects fire spread using the gridded wind input. The fire from simulation C8 (wind speed 24 kph) spread to the west, and is smaller than the actual Corral Fire (Figure 28). The fire from simulation C9 (wind speed 40 kph) spread to the west, and is almost the same size as the Corral Fire. When comparing Figure 27 to Figure 28, the gridded wind input at the higher wind speed (C9) is still smaller than the prevailing wind input at the lower speed (C16).

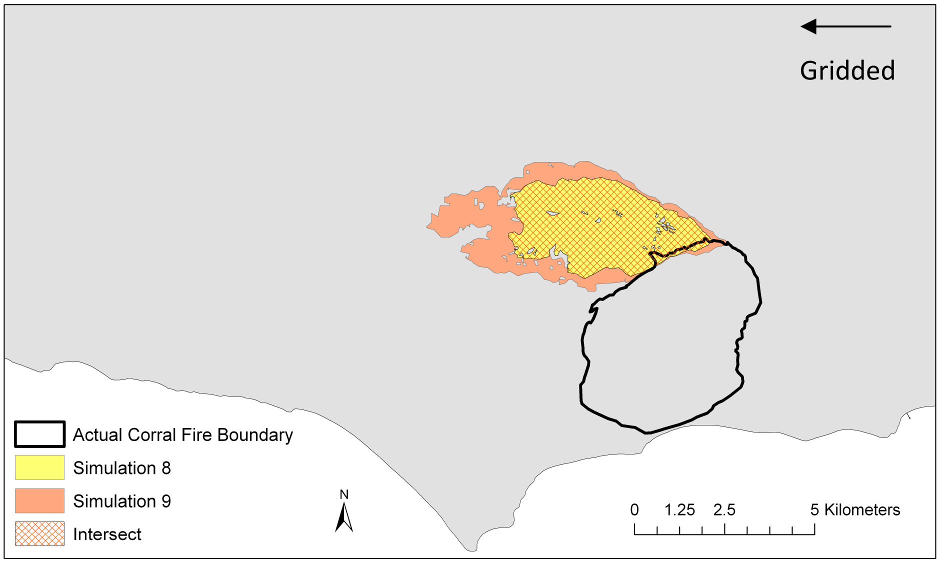

Figure 28: Corral Fire simulations using a constant, gridded wind input of 90° and 24 kph (yellow) and a constant, gridded wind input of 90° and 40 kph (red). C9 overlaps entirely with C8 (red cross-hatching).

Figure 29 shows simulations C16 and C17, which compares how wind speed affects fire spread using the prevailing wind input. Both simulated fires spread west of the Corral Fire, and both were larger than the Corral Fire. However, the fire from simulation C17, which had the higher wind speed (40 kph), spread further west than the fire from simulation C16 (24 kph).

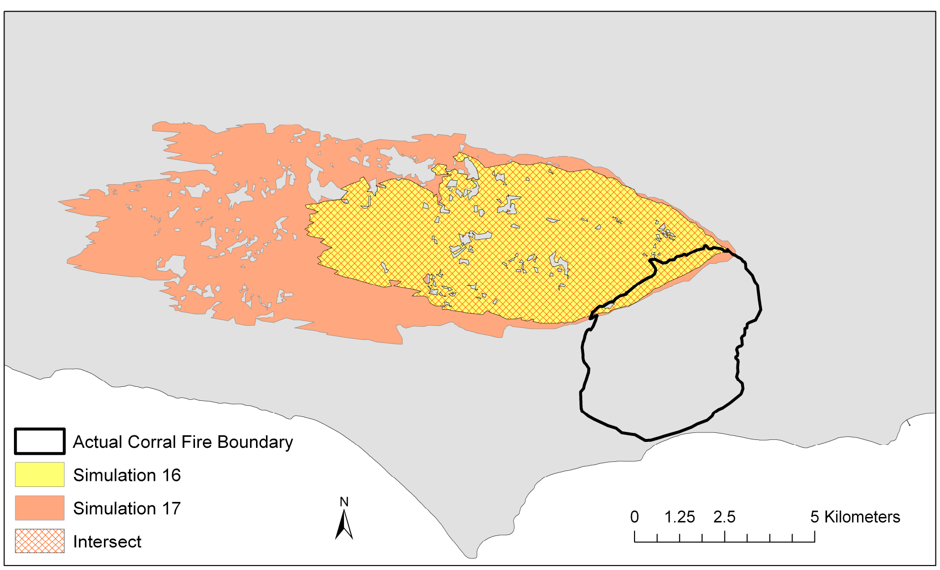

Figure 29: Corral Fire simulations using a constant, prevailing wind input of 90° and 24 kph (yellow) and a constant, prevailing wind input of 90° and 40 kph (red). C17 overlaps entirely with C16 (red cross-hatching).

Study Area-Wide

We compared the fire hazard index maps for fire simulations using each of the four wind grids and using historic ignition locations, and one simulation based on random ignition locations. We tested the sensitivity of the model to wind direction, wind speed and ignition location. A raw difference in magnitude of hazard was calculated for each cell using the Single Output Map Algebra tool to subtract the values in one map from another.

Figure 30C shows the difference between the fire hazard index maps created based on S2 90° wind grid and S4, the 337.5° wind grid both at 24 kph.

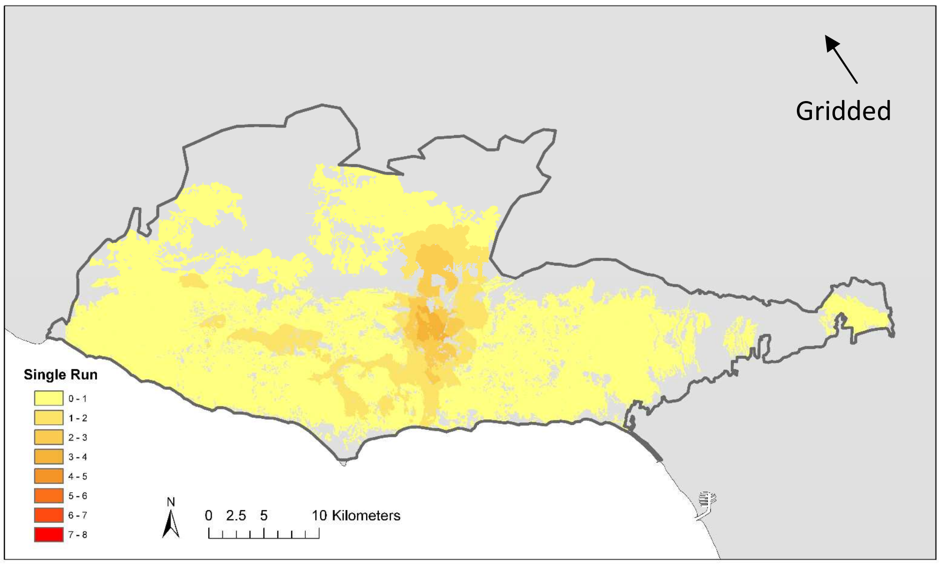

Figure 30A: Fire hazard index map for a gridded wind input of 337.5° at 24 kph using historic ignition locations.

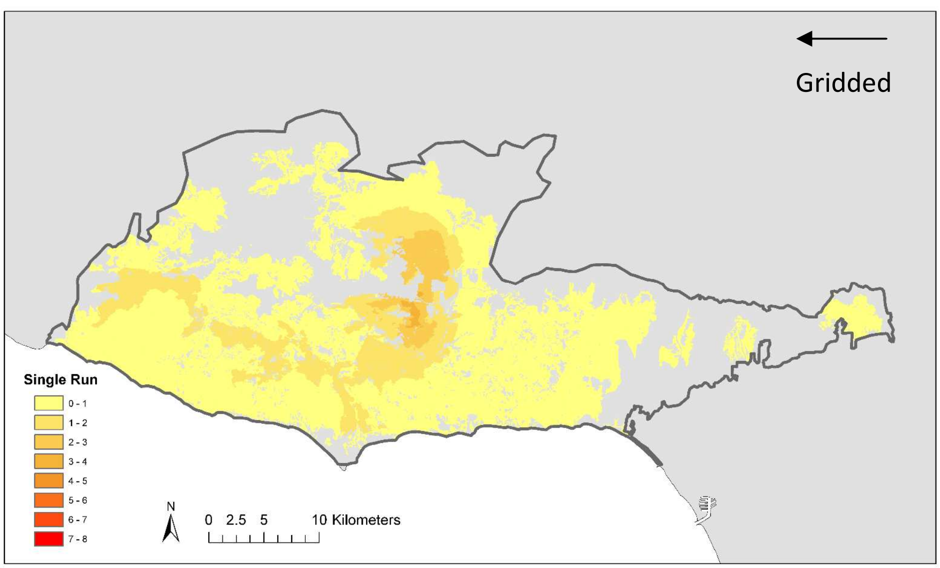

Figure 30B: Fire hazard index map for a gridded wind input of 90° and 24 kph using historic ignition locations**.**

Difference maps were produced to show the spatial location and magnitude of difference in hazard between the cells for two hazard maps, based on two wind different directions.

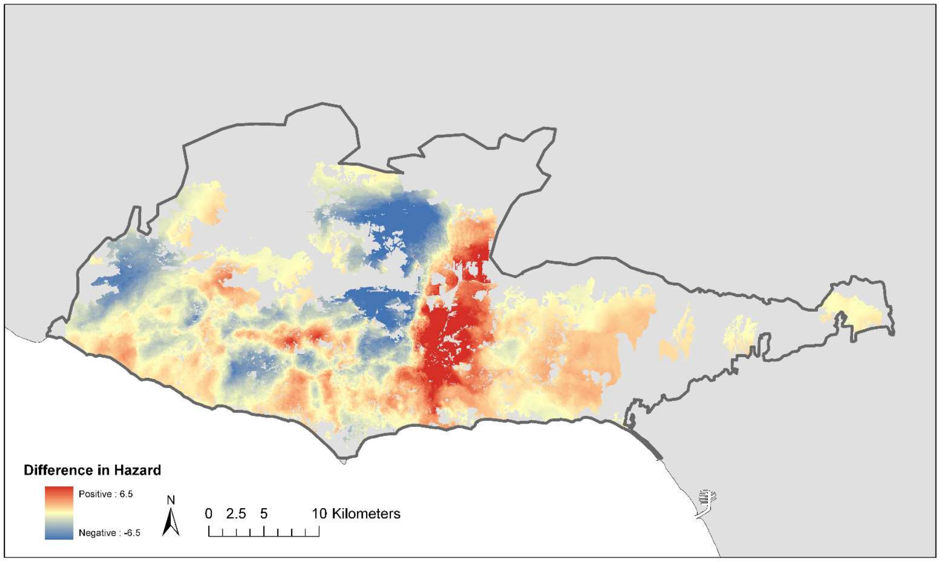

Figure 30C: Spatial location of difference in hazard for a gridded wind direction of 337.5° at 24 kph minus the 90° wind grid at 24 kph.

Overall, the difference map demonstrates that the location of fire hazard differs for each wind direction. As shown in Figure 30C, these two wind grids (337.5° and 90°) were chosen because they represent the greatest range in wind direction that we evaluated in our simulations. Of all of the wind direction comparisons, they also showed the greatest difference in the magnitude and location of hazard. A positive value indicates areas where S2 had the higher fire hazard compared to S4. The greatest positive difference (red) is located in the central northern and southern portion of the Recreation Area. The greatest negative difference (blue) is in the central northern and western portion of the Recreation Area.

We also tested the sensitivity of the model to grids representing different prevailing wind inputs by comparing the fire hazard index maps for S2 (Figure 31A) for the 90° wind grid at 24 kph, and S5 (Figure 31B), the same wind grid but at 40 kph. Figure 31C shows the difference between the hazard maps for S2 and S5.

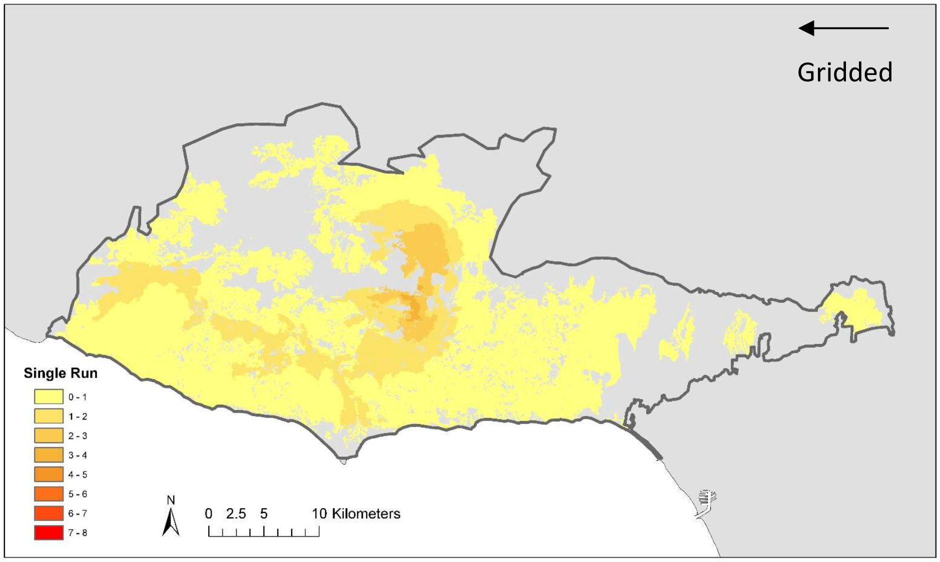

Figure 31A: Fire hazard index map for a gridded wind input of 90° and 24 kph using historic ignition locations.

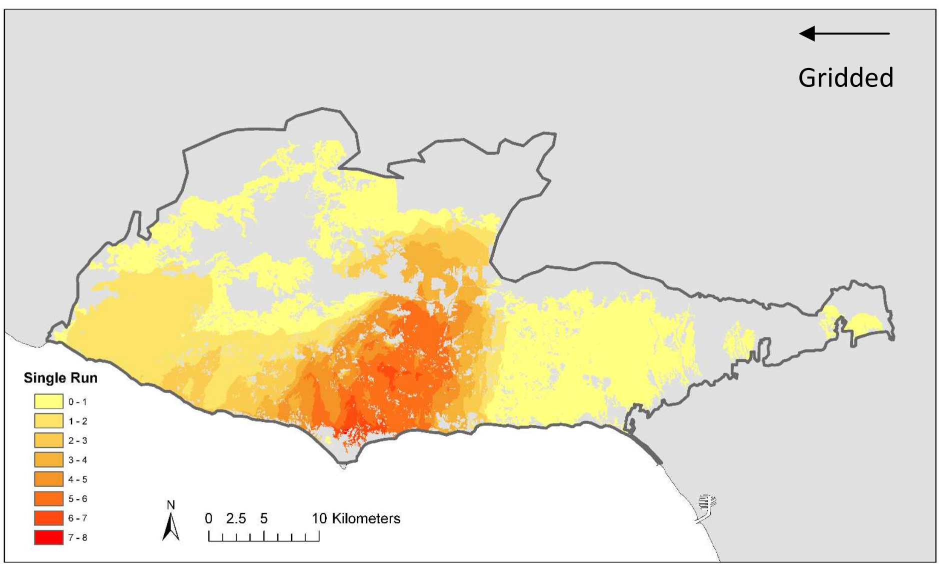

Figure 31B: Fire hazard index map for a gridded wind input of 90° and 40 kph using historic ignition locations.

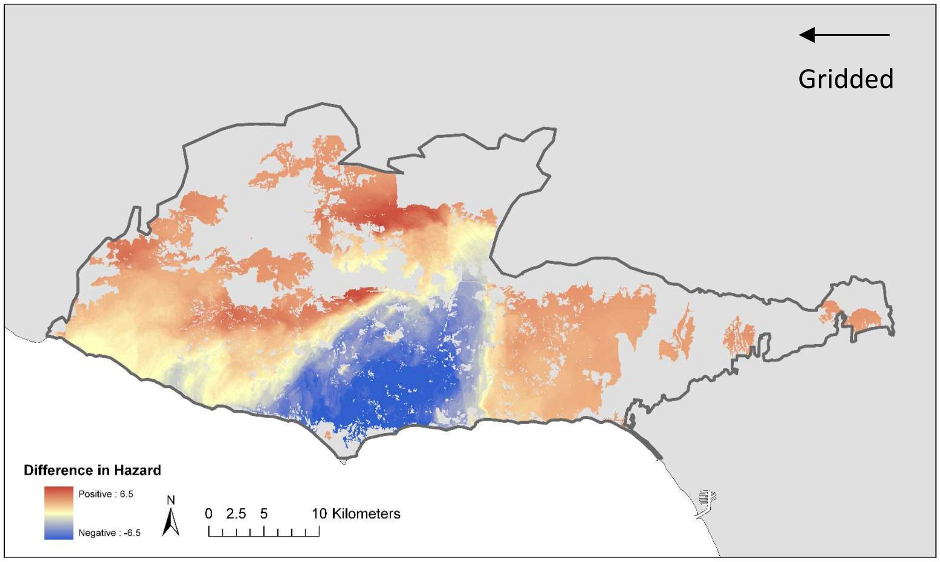

Figure 31C: Fire hazard index map showing the difference in raw magnitude of hazard between simulations for a gridded wind input of 90° at 24 kph and a gridded wind input of 90° at 40 kph.

The comparison of the two fire hazard index maps representing the two wind speeds showed the greatest magnitude of difference. The higher wind speed in S5 (Figure 31B) appears to push simulated fires in the same direction the wind blows, concentrating the fire hazard in the southern central portion of SMMNRA. In contrast, S2 (Figure 31A), with a wind speed of 24 kph, had lower fire hazard in this same portion of the Recreation Area, and the hazard was more spatially dispersed.

To test the sensitivity of the model to ignition location, we compared the fire hazard index Maps of S2 and S6, where S2 uses historic ignition locations and S6 uses random ignition locations. Figure 32 is the difference map for these two simulations.

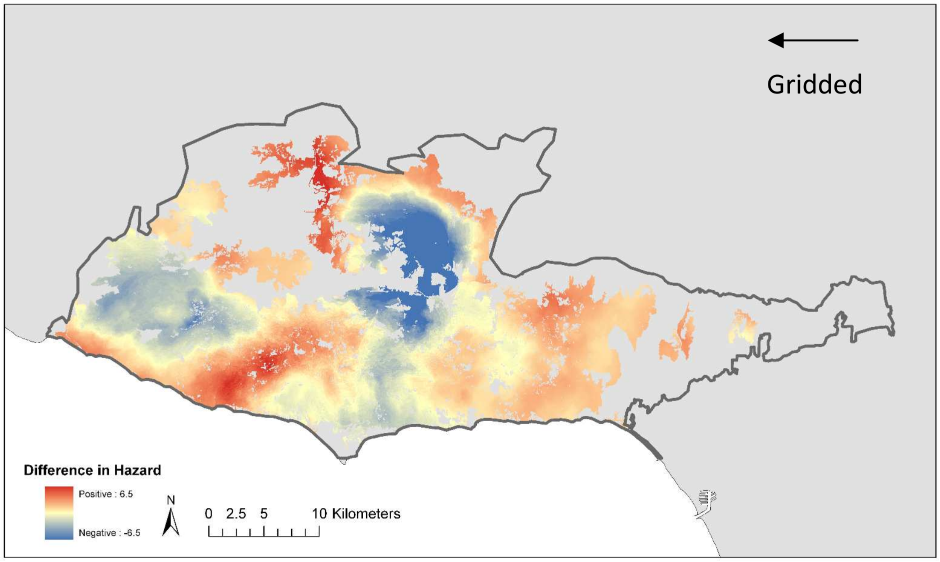

Figure 32: Difference in raw magnitude of hazard for gridded wind input for the 90° wind direction grid at 24 kph using historic and random ignition locations.

The difference map shows that the location of ignitions does have an effect on the spatial distribution of hazard. The greatest positive difference (red) is located in the southern and northern portion of the Recreation Area. The greatest negative difference (blue) is in the central northern portion of the Recreation Area.

It may be valuable from a management perspective to know the relative importance of wind direction, wind speed and ignition location. We measured this in two ways. First, to determine the magnitude of hazard, we computed the absolute value of the difference in hazard associated with each variable for each cell in the study area (Figure 33). Although we only conducted a difference operation for speed based on one grid direction (90°), this comparison showed the greatest spread of absolute difference values, with the greatest proportion of cells showing a high degree of difference. Varying the wind grid and ignition locations also seems to affect hazard index values to a lesser extent (Figure 33).

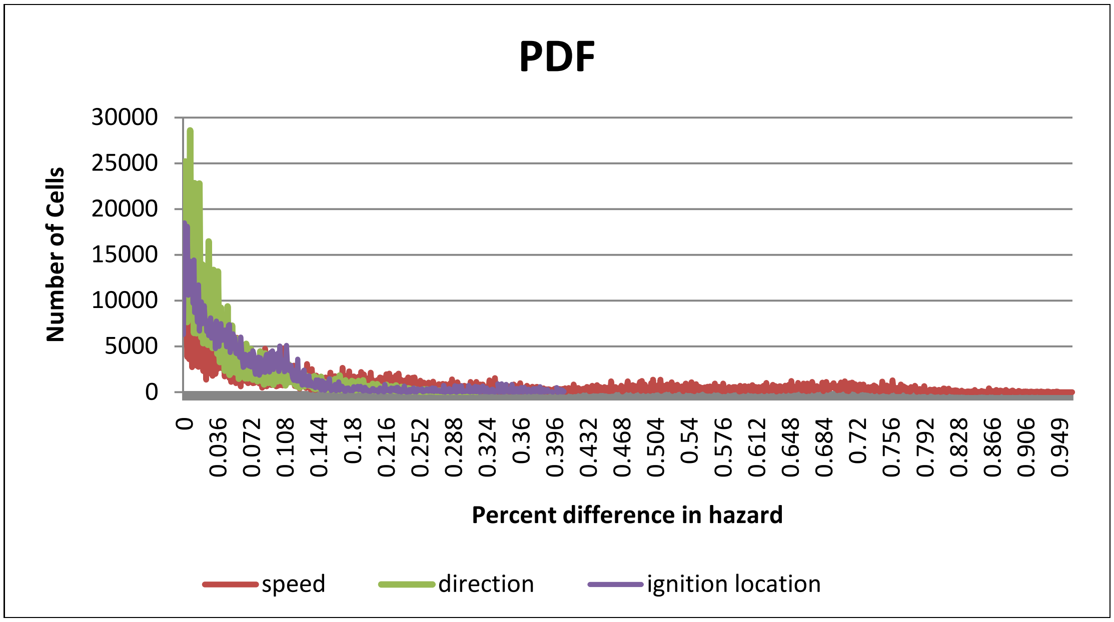

Figure 33: Probability distribution function of change in hazard due to varying wind speed, wind direction and ignition location.

A subsequent spatial analysis was performed to determine correlations between the location of hazard values created by different wind directions, speeds and ignition locations in individual cells in the study area. ANOVA F-tests and multiple regressions were conducted in R (Hornik, 2010), a free statistical analysis package, to analyze input parameters with respect to their variance and their importance as predictors of the spatial distribution of fire hazard. The R-scripts used for the analyses are included in Appendix K.

Table 8 shows the results of an ANOVA F-test of the input parameters used in the model to produce the overall weighted fire hazard map. Because this map incorporates results of simulations using multiple wind grids, wind speed and direction values were not considered. Aspect was also not included in the analysis because of complications due to circular statistics (values ranging from 0 to 360°).

Table 8: ANOVA F-test of input parameters for overall weighted hazard index.

Parameter	**Elevation**	**Slope**	**Distance from Ignition Point**	**Fuel Model**
F value	20068.17	165.11	192943.46	2986.69
Pr(>F)	2.2e-16 ***	2.2e-16 ***	2.2e-16 ***	2.2e-16 ***
Significance codes: 0 *** 0.001** 0.01* 0.05⁺ 0.1# 1’				

Large F values and low probability values indicate significant differences in the datasets for the input variables. Due to the results of the F-test, coefficients for each parameter in the regression (Table 9) were re-scaled by their standard deviations. This removes magnitude effects and makes the regression spatially-based.

Table 9: Regression of overall weighted hazard index regressed on input parameters.

Parameter	Elevation	Slope	Distance from Ignition Point	Fuel Model
Coefficient	-1.574e-03	-1.574e-03	-2.322e-04	many
Rescaled Coefficient	0.081436333	-0.007261987	-0.237110736	
p-value	< 2e-16 ***	< 2e-16 ***	< 2e-16 ***	
Adjusted R-squared: 0.2417 Significance codes: 0*** 0.001** 0.01* 0.05^{+} $0.1^{\#}$ 1'				

All parameters were highly significant (p<0.0001) predictors of overall weighted fire hazard index values. The distance from ignition point was the most influential predictor, explaining approximately 19 percent of the variation in hazard index values when a single regression was performed.

In order to examine the importance of wind speed and wind direction parameters, the same tests were run for the fire hazard index map based on the 90°, 24 kph wind grid. To remove circular statistics issues associated with wind direction and aspect, a difference between the two parameters was calculated for this analysis. The results of the F-test for the parameters are shown in Table 10 and Table 11.

Table 10: ANOVA F-test of input parameters for 90°, 24 kph wind grid hazard index.

Parameter	Elevation	Slope	Degrees Difference (Aspect – Wind Direction)	Wind speed	Distance from Ignition Point	Fuel Model
F value	17598.5	2111.5	2040.1	7326.1	177417.9	3213.7
Pr(>F)	<2.2e-16 ***	<2.2e-16 ***	<2.2e-16 ***	<2.2e-16 ***	<2.2e-16 ***	<2.2e-16 ***
Significance codes: 0*** 0.001** 0.01* 0.05^{+} $0.1^{\#}$ 1'						

The F-test showed significant differences in the spread of the different data layers used to produce the fire hazard index values based on the 90°, 24 kph wind grid. Distance from ignition point showed the greatest variance of all of the parameters. Coefficients were re-scaled in the regression (Table 11) to remove the effect of differing variance.

Table 11: Regression of hazard index for simulations using a 90°, 24 kph wind grid, regressed on input parameters.

Parameter	Elevation	Slope	Degrees Difference (Aspect – Wind Direction)	Wind speed	Distance from Ignition Point	Fuel Model
Coefficient	132.659	-45.951	45.167	85.593	-421.210	many
Rescaled Coefficient	0.08507611	-0.02833854	0.02633206	0.05184054	- 0.2465004	many
p-value	< 2e-16 ***	< 2e-16 ***	< 2e-16 ***	< 2e-16 ***	< 2e-16 ***	
Adjusted R-squared: 0.222 Significance codes: 0*** 0.001** 0.01* 0.05⁺ 0.1# 1'						

Consistent with the overall weighted fire hazard index map, all parameters were highly significant (p<0.0001) predictors of hazard. While the fuel model was a significant predictor of hazard, some of the specific model types were less significant or insignificant predictors. This included fuel models 3 (tall grass), 4 (chaparral up to four feet) and 6 (dormant brush/hardwood slash).

We also used a pair-wise principle component analysis to find the correlations between the hazard outputs of the 90°, 24 kph wind grid and the 337.5°, 24 kph wind grid, the 90°, 24 kph wind grid with historic and random ignition locations, and the 90°, 24 kph and 90°, 40 kph. This analysis found the highest correlation value between the different wind directions and the smallest correlation values between the ignition locations (Table 12). Therefore, different wind directions had the least effect on spatial hazard variations and different ignition locations had the largest effect.

Table 12: Correlation values for hazard outputs for different wind directions, wind speeds and ignition locations.

	Input Grid 1	Input Grid 2	Correlation Value
Wind Direction	90° 15 mph Historic Ignitions	337.5° 15 mph Historic Ignitions	0.65327
Ignition Location	90° 15 mph Historic Ignitions	90° 15 mph Random Ignitions	0.39549
Wind Speed	90° 15 mph Historic Ignitions	90° 25 mph Historic Ignitions	0.48696

THIS PAGE INTENTIONALLY LEFT BLANK

VIII. Discussion

Scales of Fire Hazard Prediction

Although limited by the number of wind grids, the analysis of the Corral Fire simulations show that gridded wind inputs have the potential to improve fire spread simulations of historic fires. The third Corral Fire simulation (Figure 13, Section VII), using only eight wind grids, was nearly as accurate as simulating the fire with the prevailing wind input, which is currently used (Figure 11, Section VII). In other words, using a limited number of wind grids produced a fire simulation that is comparable to the current state of the art in fire spread modeling. This gives us confidence in the use of a similar method for assessing fire hazard at a larger scale.

Weighted Overall Fire Hazard Index Map (for Historic Runs)

As shown in Figure 20 (Section VII), the highest hazard areas predicted in our simulations are in the central portion of SMMNRA. This is consistent with the majority of the hazard maps (both burn frequency and burn time) for the study area based on the different wind grids (Appendix E, Appendix F).

The observed hazard concentration in this portion of SMMNRA may be due to various factors. There may be characteristic differences in this part of the Recreation Area with respect to topography, fuels, weather and ignition locations. Steeper topography, greater fuel loads and high wind speed are all expected to correlate with higher fire hazard. Recent research has indicated that there are spatial relationships between high fire danger and mountain passes that channel SAWs (Moritz et al., 2010). Furthermore, a higher density of ignition locations could also contribute to the hazard level. Part of the hazard pattern could also be explained by the limitations of our model inputs and is discussed in greater detail below.

Analysis

Sensitivity Analysis

Corral Fire

Gridded Wind Inputs versus Prevailing Wind Inputs

The fact that the hourly gridded wind inputs produced a smaller fire than the prevailing wind inputs (Figure 25, Section VII) may indicate that using gridded wind inputs will improve fire spread and fire hazard predictions. Although the fire from the prevailing wind input had more area of overlap with the Corral Fire, it also overburned a greater area, whereas the fire from the gridded wind input had less overlap, but predicted the size of the fire much more accurately. This could be because gridded wind reduces wind speed to account for the influences of topography (i.e., scaling wind speed up or down depending on the topography).

One of the major limitations of our project was that we only had eight wind grids. As shown in Figure 14 (Section VII), the simulated fire based on only one wind speed (the mean wind speed for this event), and one wind direction did not match up with the Corral Fire boundary. Figure 25 (Section VII) shows both the prevailing wind and gridded wind inputs varied hourly based on eight wind grids. Comparing Figure 14 (Section VII) to the fire using the gridded wind input in Figure 25 (Section VII), we see that the simulated fire with more than one wind grid is more accurate in modeling both the direction and size of the historic fire. Based on the result of the gridded wind inputs varied hourly, having more wind grids available that mimic the historic weather data should more accurately model the Corral Fire.

Speed

Increasing the speed resulted in an increase in the size of the simulated Corral Fire (Figure 28, Figure 29 Section VII), while maintaining the same fire spread trajectory. The direction values in individual cells in a wind grid do not change with increased speed. As a result, the size of the fire will increase but the direction of fire spread will remain the same. Using the prevailing wind input, as the constant wind speed increases in the same direction, the size of the fire increases dramatically compared to the boundary of the Corral Fire. In contrast, when using the gridded wind input, as the speed increases in the same direction, the fire size still increases, but when compared to the prevailing wind input at the same speed, gridded wind more closely captures the size of the historic fire.

Study Area-Wide

Direction

The difference maps and the statistical analyses indicate that wind direction is an important predictor of the magnitude and spatial pattern of fire hazard, although not the most significant predictor. Figures 30A, B and C (Section VII) illustrate this. Since we are limited to four wind directions, the overall weighted hazard map is limited to winds from the northeast.

After analyzing the historic weather data for four years of SAW conditions, we grouped the winds out of the northeast into the four directions (0°, 45°, 90°, 337.5°) that we were given. From this analysis we found that 0° and 45° were the two most common wind directions. However, even though the wind grids were weighted based on their frequency, there was minimal difference in spatial pattern or magnitude of fire hazard between the overall weighted hazard map and the un-weighted hazard map. With the amount of variation observed in hazard between our four wind grids, it is expected that having more wind grids could produce a map that takes more of this hazard variation, due to direction, into account.

Speed

Figures 31A, B and C show that changes in wind speed have a large effect on the magnitude and spatial arrangement of modeled fire hazard. Using a 90° wind grid, we would have expected the fire hazard to increase to the west when wind speed was increased from 24 kph to 40 kph. However, fire hazard increased in the southern portion of the Recreation Area. This is due to the influence of topography on wind. Major canyons in SMMNRA run north to south, and SAWs are known to be more intense within north to south canyons.

Ignition Locations

Fire hazard varies with respect to magnitude and spatial distribution when different sets of ignition location are used in the simulations (Figure 32). According to the results of the multiple regression, distance to ignition location was the best indicator of spatial distribution of hazard. Still, this factor only explains approximately 20 percent of the spatial pattern. Furthermore, the low R squared value (0.2417) indicates that the model results are more than simply the sum of the inputs. Given that ignitions are the starting points of fires, it follows that areas around an ignition location generally burn earlier. Furthermore, areas with a high concentration of ignition points would be expected to have a higher burn frequency.

Fixed Inputs

Fixed inputs, including the topography and the fuel model map, were significant predictors of fire hazard, according to the multiple regression. This is expected, given that these are basic components of the fire spread model.

Limitations

Inputs

Wind Grids

As stated previously, we only had eight wind grids. The Corral Fire simulations demonstrated that using the eight wind grid inputs varied hourly modeled the fire more accurately than the prevailing wind inputs. However, we realize that using only four wind directions at two wind speeds is a gross oversimplification of weather data.

In addition to the limited number of wind grids, there is also an edge effect to consider. Due to the size of the Recreation Area, the study area was divided into three segments, and a wind grid was created for each of these segments. Each wind grid is most accurate at the center, with accuracy decreasing toward the edges. To compensate for this decrease in accuracy, a buffer should be applied around the study area. Unfortunately, there is no buffer between the Pacific Ocean and the Recreation Area and the wind grids end at the southern tip of Point Dume. As a result, the southern portion of the study area may be influenced by edge effects, which could affect the Corral Fire simulations.

Ignition Points

There are limitations to using the historic ignition locations dataset provided by SMMNRA. First of all, the dataset may be incomplete because recordkeeping and data management have changed over time. Using this dataset in simulations also assumes that future fires will start in very similar locations. Additionally, fires which started outside of the Recreation Area boundary, but caused significant damage within the Recreation Area, are not reflected in this dataset. Furthermore, the ignition locations used in this study did not all occur during SAW events. We used these historic ignition locations because we knew that fires had started in these areas in the past and it gave us a starting point to begin our fire simulations.

Fuel Models

The fuel model was based on the best available vegetation map for the study area. It is a snapshot in time, so the fuel model map cannot represent past or future vegetation conditions. The vegetation map is at a 30-meter scale, which is the finest scale we had available to us, so all of our other input layers were constrained to a 30-meter resolution.

The fuel model map contains assumptions about how different land types will burn. One major assumption is that developed land is unburnable, our best proxy for firefighting efforts. However, in highly fragmented parts of the Recreation Area, particularly in the eastern portion, this assumption means that more of the simulated fires are very restricted in spread. We also did not have a vegetation map for areas surrounding the Recreation Area; therefore we could not model fires outside the Recreation Area boundaries, even though they are likely to occur.

Weather Data

Hourly weather records from MesoWest were available from one month to 10 years in the past, depending on the weather station. However, wind speed and direction can change rapidly, so hourly measurements may not accurately depict wind conditions. Hourly weather data is currently the standard for modeling fires. Fires have been modeled reasonably accurately using these hourly wind inputs; therefore, we believe the hourly measurements to be accurate enough for the purposes of this study.

Wind information from RAWS was recorded from a less than 10-meter height from the surface, yet WindWizard models wind from 100-meters off the ground. The lack of information about wind at 100-meters from the surface during SAWs was a major limitation. Currently, there is no way to validate the output from WindWizard.

We also expect that four years of data can give a reasonable approximation of recent weather conditions, but is not a long enough period to cover larger planetary processes that alter wind and weather conditions, such as the El Niño Southern Oscillation (ENSO) and the Pacific Decadal Oscillation (PDO). Both of these events have return intervals of over four years. Therefore the ‘characteristic’ SAW data used in our project may not be an accurate depiction of long-term average SAW conditions.

Fragmentation

The decision to make developed areas unburnable in the model had an unforeseen impact on the eastern areas of SMMNRA. The area of SMMNRA east of Interstate 405 (Appendix L) is interspersed with large developed areas and became extremely fragmented in the model. This fragmentation drastically limited the ability of fires to spread in these areas and therefore may not be a reasonable approximation of reality.

The large unburnable developed areas in and around the City of Thousand Oaks may also have created unrealistic limits to the spread of fire. Urban fire ignitions and the ability of a wildfire to spread over and through a small developed area are not included in this study and may have limited the spread of some simulated fires.

Models

There are limitations to the models that we used in our analysis. HFire does not incorporate the effects of firefighting or the probability of fire containment into the model. Boundaries showing fire progression, such as the 2007 Corral Fire, tended to remain relatively static after the first day of the fire due to firefighting efforts.

WindWizard attempts to model surface winds based on topography. In this case, 100-meter cells were used at 20 feet off the ground. Surface roughness, based on vegetative cover, and topographic scale may result in very different resulting wind grids. Additionally, WindWizard has not been tested in the SMMs, and no validation has been done with high wind speeds for the study area. There is also a question of whether WindWizard can accurately represent surface wind conditions near a large body of water, such as the ocean. On-shore winds could influence the surface winds of the nearby landscape because of the wind dynamics over the ocean. Gridded wind inputs have been tested in fire spread studies using the FARSITE model. However, there is no literature documenting the coupling of WindWizard with HFire.

By combining two different models, each with their own limitations, it is important to recognize how these limitations combine together and interact with each other and how that affects the usefulness of these results. Errors from one model can compound with the errors of the other model, which can limit their uses. The models are a snapshot of conditions at one point in time and are not predictive in nature. Therefore, the results should be viewed as scenarios and not absolute.

THIS PAGE INTENTIONALLY LEFT BLANK

IX. Conclusions & Future Research

The SMMs are characterized by a fire-prone Mediterranean-climate ecosystem that often experiences intense fires due to extreme fire weather. These devastating fires are frequently associated with short episodes of hot, dry winds, such as SAW events (Moritz et al., 2010). Land managers are responsible for protecting both natural resources and the lives and property of those residents living within the boundaries of SMMNRA. The gridded wind program, WindWizard, was identified by SMMNRA land managers as a potential tool for improving both the accuracy of current fire spread modeling efforts and mapping spatial differences in fire hazard.

In our study, we compared fire simulations for the 2007 Corral Fire using both prevailing and gridded wind inputs. The results of these simulations and statistical analysis indicated that gridded wind inputs improve the accuracy of a fire spread model when compared to prevailing wind inputs. A fire hazard map for the study area was created based on additional fire simulations. Our research represents a preliminary assessment of the use of gridded wind inputs in a fire spread model. Furthermore, we have developed a method that can be replicated by SMMNRA. Based on the results of our analysis, we conclude that the WindWizard program is an effective tool that could be utilized by SMMNRA land managers.

Clark et al. (2008) conducted a global-sensitivity analysis on the HFire model and determined that under extreme weather conditions, wind speed was more important than any other model input in determining the predicted fire size. Consistent with this result, wind speed was the most important predictor of the magnitude of fire hazard in our model output. However, distance to ignition location was the most important predictor of the spatial pattern of fire hazard, as determined by our analysis. Fixed inputs, including the topography and fuel model map, were also significant predictors of hazard in our model.

SMMNRA land managers could use our model to assess the effectiveness of specific management options in reducing fire hazard. Limiting fire ignitions and reducing development in and around high fire hazard areas could decrease the probability of large fires occurring (Moritz et al., 2010), and would help prevent catastrophic loss of property and life. We have identified the following opportunities to improve our model and to apply it to answer management questions in SMMNRA.

<u>Further Analysis of Weather, Ignition Sources and Patterns and Fire History</u>

More data of historic SAW events and a more formal analysis would be useful in refining the model. A 20-year record of data would provide greater confidence that climatic variations, such as ENSO and PDO events, are captured in the model. Additionally, past weather station data for wind speed, wind direction and fuel moisture values could be analyzed to determine the range of variation within past events. Knowing the number and degree of these fluctuations could assist with further refinement of the fire spread model. For instance, the HFire season simulator could incorporate this historical weather data and randomize within the ranges identified to simulate the various conditions experienced during these events.

In addition to analyzing weather information, pattern analysis of past ignitions would be useful. An ignition occurring during the peak of a SAW event is a simplification in our current model. Many of the historic ignition points used did not ignite during a SAW event. Analysis of ignition points, with respect to time of day the ignition began and association with particular landscape features, could refine the probability space used for randomizing ignition locations and improve the accuracy of the model's fire spread predictions.

Lastly, the overall fire hazard index map could be compared to other fire hazard maps and with SMMNRA's fire history. Mortiz et al. (2010) reconstructed weather data for the study area and overlaid it with the Fosberg Fire Weather Index to determine if high fire severity coincided with weather patterns and fire history. This same method could be used with our model to further validate if it can accurately predict areas of high fire hazard.

Validation of the WindWizard Output

Validation of the WindWizard output would increase confidence in its utility for fire spread modeling within SMMNRA. One way to accomplish validation would be to collect measurements of speed and direction at specific locations (e.g., canyon bottoms, ridges and coastal canyon mouths) while weather stations record data during a Santa Ana event. These data could then be compared with the WindWizard output for the same locations.

Fire Spread Model Refinement

We have identified several potential improvements for our fire spread model. Most importantly, additional wind grids representing more wind speeds and directions should be added. Although our use of the eight wind grids showed promise in improving the accuracy of fire spread predictions, it does not account for the full range of variation within a SAW event. The season simulator module in HFire could be reprogrammed to incorporate gridded wind, and vary the inputs on an hourly basis. This would allow much more realistic fire spread simulations. Ideally, the effect of ignitions located outside of the Recreation Area should also be incorporated. The Topanga Fire, one of the most devastating SAW-driven fires on record, ignited just north of the Recreation Area boundary. Including areas outside of the boundary would also lessen the extreme fragmentation effect we observed, particularly in the eastern portion of the Recreation Area.

There are also other opportunities for further sensitivity analysis. For example, we did not test the model's sensitivity to topography. To conduct this analysis, fire simulations could be conducted using one fuel model and varying the wind grid. Doing so would isolate the effect of topography, separate from the effects that different types of vegetation have on fire spread rates.

To make the model useful in the future, the fuel model map and inputs will have to be modified in order to take changes in vegetation and weather variation into account.

Climate change projections, such as increasing temperatures and decreasing precipitation, might also be utilized to assess how the fire regime may change. This would make the model applicable for answering an entirely different suite of research questions.

<u>Assessment of Land Management Policies Using HFire</u>

The areas mapped as high fire hazard are the areas that have the highest probability of being burned in a wildfire under the specified model conditions. Although our model does not provide a metric for fire intensity at a given location, it does give the likelihood of a particular area burning when a wildfire occurs. Since SMMNRA faces issues with existing development and pressure for future development at the boundaries as well as on in-holdings within the Recreation Area, the high fire hazard areas defined by our model could indicate where development should not occur. Although not within the exclusive control of NPS, further refinement of the model and confirmation of its accuracy will allow SMMNRA to evaluate the impact of development scenarios, property acquisition, development mitigation programs, regulations for defensible space, implementation of local versus regional building code policies and strategies to limit ignitions. SMMNRA can also use the model to assess the effectiveness of specific management strategies and scenarios, such as evaluating the location and size of strategic fuel reduction and modification zones.

SMMNRA can use a refined model to evaluate and compare the impact of various development scenarios (i.e., different intensities and configurations). Conversely, properties might be prioritized for acquisition based on the results of fire spread modeling. Organizations such as Mountains Restoration Trust (MRT) and Santa Monica Mountains Conservancy (SMMC) work to preserve, protect, restore and enhance the natural resources of the SMMs, in part through land acquisition and conservation easements (Mountains Restoration Trust, 2005-2009). Land trusts such as MRT often have limited funding, so land acquisitions are usually prioritized based on the biodiversity and connectivity of parcels. Currently, MRT's priority acquisitions include: Cold Creek watershed properties, properties acquired for transfer to park agencies and properties with outstanding resource value (Kitz, 2009). It would be interesting to determine if there are specific parcels that could serve both the goal of natural area preservation and hazard reduction (i.e., limiting exposure to fire hazard by preventing development in areas more likely to burn). The results of fire spread modeling could be overlaid with MRT's priorities to answer such a question.

Development mitigation programs could also be examined in the fire spread model. Though it might be very complex to model, theoretically the impact of fire-resistant versus standard homes could be evaluated. This type of simulation would require that different WUI fuel models be created for the two types of structures.

With these new WUI fuel models, it would also be possible to determine whether a blanket regulation for defensible space (if enforced) would reduce fire hazard of homes on SMMNRA in-holdings. Similarly, the implementation of building code policies on a local and regional scale can also be evaluated. Additionally, limiting ignitions, such as by closing roads or limiting access to hazardous areas during high wind periods, could also be modeled using HFire.

Location, size and effective hazard reduction of strategic fuel reduction and modification zones could also be evaluated in our model. SMMNRA previously identified locations for strategic fuel reduction zones in their 2007 Fire Management Plan. These areas were identified by overlaying GIS layers of slope, vegetation type and housing density. This method could be further refined by using the fire hazard areas identified from fire spread modeling outputs or overlaying areas predicted to have high wind speeds according to the WindWizard output. The effective size of fuel reduction and modification zones could also be assessed to determine if an appropriate reduction in fire hazard can be achieved.

Economic Analyses to Inform Fire Management Decisions

The outputs from fire spread simulations could additionally be used to answer economic questions. For example, it would be possible to use cost effectiveness analysis (CEA) to determine the most cost effective method to reduce fire hazard from an array of alternative policy options. One example could be to use CEA to evaluate if it is less costly to buy in-holdings or to build and maintain defensible space or fuel reduction and modification zones.

A cost-benefit analysis could also be used to compare alternative policy decisions and resource allocation decisions. This method takes non-use value into consideration, which can be useful when cost is not the only consideration. Some possible questions might include analyzing the costs and benefits of:

- paving permanent fuel breaks or maintaining traditional fuel breaks over a specific time horizon;
- revenues versus service costs and potential fire losses associated with both existing and new development;
- fire safe building features, structures or standard home designs; and
- decreasing the fire return interval by limiting ignitions or allowing the current fire return interval to continue or decrease.

Improving Current Education Programs

One of the ways that SMMNRA can influence fire hazard outside the Recreation Area managers' control is to effectively communicate with stakeholders. For example, if the value of one policy over another can be quantified and visualized, it may make a more compelling case to present to the public and decision makers. Policies could be evaluated based on their ability to increase or decrease hazard levels at the boundaries of development. Increased coordination and education could also increase general awareness about fire hazard and risk or the promotion of community-based action groups such as Fire Safe Councils. SMMNRA is currently creating a community wildfire protection plan that will allow local communities to identify areas of concern and mitigation strategies for reducing wildfire risk. Arson watch programs that train local volunteers to watch for suspicious behavior exist in Topanga Canyon and other communities. The results from our project could inform these community-based action groups on where to target their resources, especially on red-flag warning days when fire danger is highest.

THIS PAGE INTENTIONALLY LEFT BLANK

REFERENCES

Anderson, H. E. (1983). *Predicting Wind-Driven Wildland Fire Size and Shape.* Ogden, Utah: U.S. Department of Agriculture, Forest Service, Intermountain Forest and Range Experiment Station, Res. Pap. INT-RP-305.

Beer, T. (1991). The Interaction of Wind and Fire. *Boundary-Layer Meteorology , 54* (3), 287-308.

Burnham, K. P., & Anderson, D. R. (2002). *Model Selection and Multimodel Inference: A Practical Information-Theoretic Approach* (2nd ed.). New York: Springer-Verlag.

Butler, B. W., & Forthofer, J. (2004). *Gridded Wind Data: What is it and How is it Used?* Fire Sciences Laboratory, Fire Behavior Project, Missoula, MT.

Butler, B. W., Finney, M., Bradshaw, L., Forthofer, J., McHugh, C., Stratton, R., et al. (2006). A New Tool for Fire Management Decision Support. *Fuels Management - How to Measure Success, March 28-30, 2006* (p. 10). Portland, Oregon: U.S. Department of Agriculture, Forest Service, Rocky Mountain Research Station, Proceedings, RMRS-P-41.

Butler, B. W., Forthofer, J. M., Finney, M. A., Bradshaw, L. S., & Stratton, R. (2006). High Resolution Wind Direction and Speed Information for Support of Fire Operations. *USDA Forest Service Proceedings, RMRS-P-42CD* , 595-602.

[CDF] California Department of Forestry and Fire Protection. (2007). *California Fire Siege '07: Overview Appendix 2.* Retrieved February 20, 2010, from California Department of Forestry and Fire Protection: http://www.fire.ca.gov/fire_protection/downloads/siege/2007/Overview_Appendix_2.pdf

Chuvievo, E., & Congalton, R. T. (1989). Application of Remote Sensing and Geographic Information Systems to Forest Fire Hazard Mapping. *Remote Sensing of the Environment , 29*, 147-159.

City of Agoura Hills. (2009). *City of Agoura Hills Municipal Code.* Retrieved September 29, 2009, from http://www.municode.com/resources/gateway.asp?pid=11934&sid=5

Clark, R. E., Hope, A. S., Tarantola, S., Gatelli, D., Dennison, P. E., & Moritz, M. A. (2008). Sensitivity Analysis of a Fire Spread Model in a Chaparral Landscape. *Fire Ecology , 4* (1), 1-13.

Cohen, J. D., & Stratton, R. D. (2008). *Home Destruction Examination: Grass Valley Fire, Lake Arrowhead, CA.* United States Department of Agriculture, R5-TP-026b.

Conard, S. G., & Weise, D. R. (1998). Management of Fire Regime, Fuels, and Fire Effects in Southern California Chaparral: Lessons from the Past and Thoughts for the Future. In T. L. Pruden, & L. A. Brennan (Eds.), *Fire in ecosystem management: Shifting the paradigm from suppression to prescription* (pp. 342-350). Tall Timbers Fire.

[FRAP-CDF] California Department of Forestry and Fire Protection. (2007). *Fire Hazard Severity Zone Model: A Non-Technical Primer*. Office of the State Fire Marshal.

Hornik, K. (2010, ISBN 3-900051-08-9). *The R FAQ*. Retrived March 9, 2010, from http://cran.r-project.org/doc/FAQ/R-FAQ.html

Joint Fire Science Program. (2007, October). *The Fire-Climate Connection*. Retrieved April 22, 2009, from Fire Science Digest: http://www.firescience.gov/Digest/FSdigest1.pdf

Kearns, F. R., Golstein, N. C., Pederson, B., & Moritz, M. A. (2007). The Fire Information Engine: A Web-Based Toolkit for Wildfire-Related Needs. *Journal of Map & Geography Libraries , 4* (1), 195-206.

Keeley, J. E. (2005). *Fire as a Threat to Biodiversity in Fire-Type Shrublands*. USDA Forest Service Gen. Tech. Rep. PSW-GTR-195.

Keeley, J. E. (2002). Fire Management of California Shrubland Landscapes. *Environmental Management , 29* (3), 395-408.

Keeley, J. E., & Fotheringham, C. J. (2001). Historic Fire Regime in Southern California Shrublands. *Conservation Biology , 15* (6), 1536-1549.

Keeley, J. E., & Zedler, P. H. (2009). Large, High Intensity Fire Events in Southern California Shrublands: Debunking the Fine-Grain Age Patch Model. *Ecological Applications , 19* (1), 69-94.

Kitz, J. (2009, December). Mountains Restoration Trust. *Personal communication with Kyung Koh regarding MRT activities* .

Los Angeles Almanac. (2008). *Median Home Prices: Cities/Communities of Los Angeles County*. Retrieved August 10, 2009, from http://www.laalmanac.com/economy/ec37b.htm

Los Angeles County Burn Area Recovery Task Force. (2007). *Corral Fire: Los Angeles County Burn Area Recovery Task Force Report*. Retrieved February 20, 2010, from California Emergency Management Agency: http://www.oes.ca.gov/Operational/OESHome.nsf/PDF/Fire%20-%20BARTF/$file/Corral_LA.pdf

McCaffrey, S., & Rhodes, A. (2008). Public Response to Wildfire: Is the Australian "Stay and Defend or Leave Early" Approach an Option for Wildfire Management in the United States? *Journal of Forestry* , 9-15.

McGrath, R. (2009, October 19). Residents of Santa Monica Mountains Invited to Fire Planning Meetings. *Ventura County Star* .

Morais, M. E. (2001). *Comparing Spatially Explicit Models of Fire Spread through Chaparral Fuels: A New Algorithm based upon the Rothermel Fire Spread Equation*. Masters thesis, University of California Santa Barbara, Geography Department.

Moritz, M.A., Moody, T.J., Krawchuk, M.A., & A. Hall. (2010). Spatial variation in extreme winds predicts large wildfire locations in chaparral ecosystems. *Geophysical Research Letters* .

Mountains Restoration Trust. (2005-2009). *Mountains Restoration Trust*. Retrieved August 2009, from http://www.mountainstrust.org/

National Fire Protection Association. (2009). *Firewise Communities*. Retrieved April 23, 2009, from National Fire Protection Association: http://www.firewise.org

National Oceanic and Atmospheric Administration, United States Department of Commerce. (2008). *Santa Ana Winds - Wildfires: NOAAWatch All Hazards Monitor*. Retrieved February 10, 2010, from National Oceanic and Atmospheric Administration, United States Department of Commerce: http://www.noaawatch.gov/2008/santa_ana.php

Natural Resources Conservation Science. (2002, June). *Conservation Practice Standard: Prescribed Burning.* Retrieved December 24, 2009, from United States Department of Agriculture, Natural Resources Conservation Science: http://efotg.nrcs.usda.gov/references/public/IA/N338_06-2002.pdf

Peterson, S. H., Morais, M. E., Carlson, J. M., Dennison, P. E., Roberts, D. A., Moritz, M. A., et al. (2009). *Using HFire for Spatial Modeling of Fire in Shrublands.* United States Department of Agriculture, Forest Service, Research Paper PSW-RP-259.

Radtke, J. (1995). *Spatial Decisions Support System for Urban/Wildland Interface Fire Hazards.* Retrieved 04 2009, from http://proceedings-esri-com_library_userconf_proc95_to200_p175-html.pdf

Radtke, J., Cova, T., Sheridan, M. F., Troy, A., Lan, M., & Johnson, R. (2000). Application Challenges for Geographic Information Science: Implications for Research, Education, and Policy for Emergency Preparedness and Response. *URISA Journal* , 12(2).

Radtke, K., Arndt, W. H., & Wakimoto, R. H. (1982). *Fire History of the Santa Monica Mountains.* USDA Forest Service General Technical Report, PSW-58, Pacific Southwest Forest and Range Experiment Station, Berkeley, California.

Randall, C. K. (2003). *Fire in the Wildland-Urban Interface: Understanding Fire Behavior.* Retrieved April 22, 2009, from School of Forest Resources and Conservation, Florida Cooperative Extension Service, Institute of Food and Agricultural Sciences, University of Florida: http://www.edis.ifas.ufl.edu

Raphael, M. N. (2003). The Santa Ana Winds of California. *Earth Interactions , 7* (8), 1-13.

Rothermel, R. C. (1972). A Mathematical Model for Predicting Fire Spread in Wildland Fuels. *USDA Forest Service, Intermountain Forest and Range Experiment Station Research Paper, INT-115* , 40.

Rundel, P. W., & Parson, D. J. (1979). Structural Changes in Chamise (Adenostoma fasciculatum) Along a Fire-Induced Age Gradient. *Journal of Range Management 32 (6)* , 462-466.

Santa Monica Mountains National Recreation Area. (2005). *Final Environmental Impact Statement for a Fire Management Plan.* United States Department of the Interior - National Park Service.

State Board of Forestry and Fire Protection. (2006). *General Guidelines for Creating Defensible Space.* California Department of Forestry and Fire Protection.

Adopted by BOF on February 8, 2006 pending filing with the Office of Administrative Law.

Stephens, S. L., Adams, M. A., Handmer, J., Kearns, F. R., Leicester, B., Leonard, J., et al. (2009). Urban-Wildland Fires: How California and Other Regions of the U.S. can Learn from Australia. *Environmental Research Letters , 4*, 1-5.

Stratton, R. D. (2006). *Guidance on Spatial Wildland Fire Analysis: Models, Tools, and Techniques.* U.S. Department of Agriculture, Forest Service, Rocky Mountain Research Station, Gen. Tech. Rep. RMRS-GTR-183.

Sutherland, S. (2004). *Structure Fires in the Wildland-Urban Interface.* Retrieved April 22, 2009, from USDA Forest Service, Rocky Mountain Research Station: http://www.fs.fed.us/rm/pubs/rmrs_rn023_03.pdf

Syphard, A. D., Clarke, K. C., & Franklin, J. (2007). Simulating Fire Frequency and Urban Growth in Southern California Coastal Shrublands, USA. *Landscape Ecology , 22*, 431-445.

Syphard, A. D., Radeloff, V. C., Keeley, J. E., Hawbaker, T. J., Clayton, M. K., Stewart, S. I., et al. (2007). Human Influence on California Fire Regimes. *Ecological Applications* , 1388 - 1402.

Syphard, A. D., Radeloff, V. C., Keuler, N. S., Taylor, R. S., Hawbaker, T. J., Stewart, S. I., et al. (2008). Predicting Spatial Patterns of Fire on a Southern California Landscape. *International Journal of Wildland Fire , 17* (5), 602-613.

Taylor, R. (2009, December 7). Personal communication to Erin Shapiro regarding the use of fire models.

Tibbits, A., & Whittaker, J. (2007). Stay and Defend or Leave Early: Policy Problems and Experiences During the 2003 Victorian Bushfires. *Environmental Hazards 7* , 283-290.

Troy, A., & Romm, J. (2007). Chapter 6: The Effects of Wildland Disclosure and Occurrence on Property Markets in California. In *Advances in the Economics of Environmental Resources.* Emerald Group Publishing Limited.

United States Census Bureau. (2010). Retrieved January 10, 2010, from U.S. Census Bureau: http://www.census.gov

University of Utah. (2009). *MesoWest*. Retrieved 2009, from MesoWest: http://mesowest.utah.edu

Ventura County Planning Division. (2005). *Lake Sherwood/Hidden Valley Area Plan.* Retrieved August 8, 2009, from http://www.ventura.org/rma/planning/pdf/plans/Lk_Sherwood_Area_Plan.pdf

Victorian Bushfires Royal Commission. (2009). *2009 Victorian Bushfires Royal Commission*. Retrieved February 24, 2010, from Interim Report: http://www.royalcommission.vic.gov.au/getdoc/f91ff31a-f477-4543-85ca-ead47f27c58f/Print-Friendly-Version

Wade, D. D., & Lunford, J. D. (1988). *A Guide for Prescribed Fire in Southern Forests.* United States Department of Agriculture, Forest Service Southern Region, Technical Publication R8-TP 11.

Wardell-Johnson, G. (2009). *Prescribed Burning is No Panacea for the New Extremes of Fire and Weather*. Retrieved December 24, 2009, from BNET Today | Management, Strategy, Work Life Skills & Advice for Professionals: http://findarticles.com/p/articles/mi_7735/is_200901/ai_n42041358/

Weise, D. R., & Regelbrugge, J. (1997). Recent Chaparral Fuel Modeling Efforts. *The Fire Element (Newsletter of the California Fuels Committee)* , 1.

Westerling, A. L., Cayan, D. R., Brown, T. J., Hall, B. L., & Riddle, L. G. (2004). Climate, Santa Ana Winds, and Autumn Wildfires in Southern California. *EOS Transactions, AGU , 85* (31), 289-300.

Witter, M., Taylor, R. S., & Davis, S. (2007). Vegetation Response to Wildfire and Fire History in the Santa Monica Mountains. *Flora and Ecology of Santa Monica Mountains: Proceedings of 32nd Annual Southern California Botanists Symposium* (pp. 173-194). Fullerton, CA: Southern California Botanists.

THIS PAGE INTENTIONALLY LEFT BLANK

APPENDIX

THIS PAGE INTENTIONALLY LEFT BLANK

In HFire, the configure file (.cfg) informs the batch file (.bat) as to where to find the necessary inputs to run the simulation desired. HFire simulations are begun by double clicking the batch file.

The configuration (.cfg) file:
The lines from the .cfg shown below are in blue, followed by an explanation in black.

```
SIMULATION_START_YEAR                2009
SIMULATION_START_MONTH               7
SIMULATION_START_DAY                 1
SIMULATION_START_HOUR                0

SIMULATION_END_YEAR                  3009
SIMULATION_END_MONTH                 11
SIMULATION_END_DAY                   30
SIMULATION_END_HOUR                  0
```

Simulation start and end can either cover a few hours to days for one fire simulation or a thousand years as shown in the season simulator.

```
SIMULATION_TIMESTEP_SECS             3600
```

Timestep is always one hour in seconds.

```
SIMULATION_RAND_NUM_SEED             1260624655
```

This line is used to generate random numbers, so it does not need to change.

```
FUELS_PROPS_TYPE                     ROTH
FUELS_PROPS_FMD_FILE                 samo_fuel_models.fmd
FUELS_PROPS_FM_NUMS_IMPORT
1;3;4;5;6;7;9;14;15;16;17;18;20;21
FUELS_PROPS_FM_NUMS_UNBURNABLE       0;98;99;255;-9999
```

This section details which fuel models will be used in the simulation. The .fmd file is explained below. It lists all burnable and unburnable model numbers used in the simulation.

```
# ELEV z units are assumed to be in meters.
ELEV_RASTER_FORMAT                   ASCII
ELEV_RASTER_MAIN_FILE                elev_ircutm.asc
ELEV_RASTER_HEADER_FILE              NULL
ELEV_RASTER_TYPE                     FLOAT

# SLOPE is rise/run expressed as percent (can be > 1).
SLOPE_RASTER_FORMAT                  ASCII
SLOPE_RASTER_MAIN_FILE               hfslope_pr.asc
SLOPE_RASTER_HEADER_FILE             NULL
```

```
SLOPE_RASTER_TYPE                    FLOAT

# ASPECT is expressed as 0-360 with -1 corresponding to perfectly
level terrain.
ASPECT_RASTER_FORMAT                 ASCII
ASPECT_RASTER_MAIN_FILE              aspectircutm.asc
ASPECT_RASTER_HEADER_FILE            NULL
ASPECT_RASTER_TYPE                   FLOAT
```

The elevation, slope and aspect of the terrain covered by the simulation are input into the simulation by the three ASCII files above. HFire can also take binary files, but ASCII outputs are just as effective and easier to create with ArcGIS. All three files must cover the same area, have the same cell size and the same number of cells. Also, HFire assumes that the files were in UTM NAD 83 projection.

```
EXPORT_FREQUENCY                     ANNUAL
EXPORT_FIRE_ID_RASTER_DIR
hfm_1100y_ifpyigs_safprsa_thresh\fire_id
EXPORT_FUELS_RASTER_DIR
hfm_1100y_ifpyigs_safprsa_thresh\fuels
EXPORT_STAND_AGE_RASTER_DIR
hfm_1100y_ifpyigs_safprsa_thresh\stand_age
EXPORT_FIRE_AREA_FILE
hfm_1100y_ifpyigs_safprsa_thresh\fire_area.txt
EXPORT_FIRE_PERIMTER_FILE            NULL
EXPORT_IGNITION_LOCS_FILE
hfm_1100y_ifpyigs_safprsa_thresh\ignition_locs.txt
EXPORT_SANTA_ANA_RASTER_DIR
hfm_1100y_ifpyigs_safprsa_thresh\santa_ana
EXPORT_SANTA_ANA_EVT_FILE
hfm_1100y_ifpyigs_safprsa_thresh\santa_ana_evt.txt
EXPORT_FIRE_INFO_FILE
hfm_1100y_ifpyigs_safprsa_thresh\fire_info_ifpyigs_safprsa_thresh.cs
v
EXPORT_AGE_AT_BURN_HIST_FILE
hfm_1100y_ifpyigs_safprsa_thresh\age_at_burn.csv
EXPORT_FIRE_ID_PNG_DIRECTORY
hfm_1100y_ifpyigs_safprsa_thresh\fire_id_png
EXPORT_FIRE_ID_PNG_ICM_FILE          fid_12clr.icm
EXPORT_FIRE_ID_PNG_IMG_WIDTH         1160
EXPORT_FIRE_ID_PNG_IMG_HGT           1283
EXPORT_FIRE_ID_PNG_TITLE_TXT         NULL
EXPORT_FIRE_ID_PNG_TITLE_FNT         MEDBOLD
EXPORT_FIRE_ID_PNG_TITLE_POS         LR
```

The above section details what files HFire will export for the simulation. The annual season simulation is shown. The rasters are exported as ASCII files that can be imported into ARCGIS.

```
FIRE_EXTINCTION_TYPE                 CONSUME
# Extinguish cells above maximum hours burning threshold.
FIRE_EXTINCTION_HOURS                3
```

```
# Extinguish cells below minimum rate of spread threshold.
FIRE_EXTINCTION_ROS_MPS                 0.005
```

Fire extinction details when a simulated fire will burn out.

```
# Enable regrowth and pnv options for multi-year simulations.
FUELS_REGROWTH_TYPE                     PNV
FUELS_FIXED_MODEL_NUM                   NULL
FUELS_PNV_RGR_FILE                      IRC_pnv2custom_nogr.rgr
FUELS_PNV_RASTER_FORMAT                 ASCII
FUELS_PNV_RASTER_MAIN_FILE              irc_pnv2.asc
FUELS_PNV_RASTER_HEADER_FILE            NULL
FUELS_PNV_RASTER_TYPE                   INT
FUELS_STATIC_RASTER_FORMAT              NULL
FUELS_STATIC_RASTER_MAIN_FILE           NULL
FUELS_STATIC_RASTER_HEADER_FILE         NULL
FUELS_STATIC_RASTER_TYPE                NULL
```

Regrowth details how vegetation will re-grow after a fire. The PNV Raster main file is an ASCII raster of the potential vegetation that would exist in the absence of fire on the landscape in question. The PNV RGR file details the progression of vegetation types as fuel models after a fire (Morais, 2001). For example, an area that would potentially be coastal sage scrub without fire will be modeled as short grass for the first few years after a fire.

Static raster is used in the single fire simulation and is where the fuel model map is imported as an ASCII raster.

```
# Stand age relates to regrowth.
STAND_AGE_TYPE                          SPATIAL
STAND_AGE_FIXED_AGE                     NULL
STAND_AGE_RASTER_FORMAT                 ASCII
STAND_AGE_RASTER_MAIN_FILE              stand_age_utm.asc
STAND_AGE_RASTER_HEADER_FILE            NULL
STAND_AGE_RASTER_TYPE                   INT
```

Stand age is also used for vegetation regrowth in the season simulation. This file is an ASCII raster of the age of vegetation patches at the start of the simulation. For a single fire the type is set at fixed, as the fuel model map should already incorporate the age of the vegetation in the fuel model choices.

```
IGNITION_TYPE                           RANDOM_SPATIAL
IGNITION_FIXED_IGS_FILE                 NULL
IGNITION_RSP_RASTER_FORMAT              ASCII
IGNITION_RSP_RASTER_MAIN_FILE           rd302.asc
IGNITION_RSP_RASTER_HEADER_FILE         NULL
IGNITION_RSP_RASTER_TYPE                FLOAT
IGNITION_FREQUENCY_PER_YEAR             .5
```

The ignition location is input as “Random_Spatial” to input a probability space raster, “Random_Uniform” to allow HFire to randomly place ignitions, or “Fixed” to place a fixed ignition location or locations. Probability rasters can be input as ASCII rasters with numbers from 0 to 1. Fixed locations are input as .igs (text) files with XY coordinates in UTM NAD 83, with each location on its own line.

```
WIND_AZIMUTH_TYPE                    RANDOM_HISTORICAL
WIND_AZIMUTH_HISTORICAL_FILE         IRC_Reg_Rand.waz
WIND_AZIMUTH_FIXED_FILE              NULL
WIND_AZIMUTH_SPATIAL_FILE            NULL

WIND_SPEED_TYPE                      RANDOM_HISTORICAL
WIND_SPEED_HISTORICAL_FILE           IRC_Reg_Rand.wsp
WIND_SPEED_FIXED_FILE                NULL
WIND_SPEED_SPATIAL_FILE              NULL
WIND_SPEED_UNIFORM_RANGE             NULL

DEAD_FUEL_MOIST_TYPE                 RANDOM_HISTORICAL
DEAD_FUEL_MOIST_HISTORICAL_FILE      IRC_Reg_Rand.10h
DEAD_FUEL_MOIST_FIXED_FILE           NULL
DEAD_FUEL_MOIST_SPATIAL_FILE         NULL
DEAD_FUEL_MOIST_D1H_INCREMENT        2.0
DEAD_FUEL_MOIST_D100H_INCREMENT      2.0
```

Weather data is input as wind speed, wind direction and dead 10 hour fuel moisture files. For a single fire the type is “Fixed” with 27 columns of data per day. The columns are the year, month, day and 24 columns of hourly data starting at hour 0 and going to hour 23 (see end of Appendix A for a more detailed description of the dead 10 hour fuel moisture file). Historical data is used for season simulation and includes all non-SAW days in at least one full fire season.

```
LIVE_FUEL_MOIST_TYPE                 RANDOM_HISTORICAL
LIVE_FUEL_MOIST_HERB_FILE            IRC_reg_randh_diff_const.lfh
LIVE_FUEL_MOIST_WOOD_FILE            IRC_reg_randh_diff_const.lfw
LIVE_FUEL_MOIST_SPATIAL_FILE         NULL
```

Live fuel moisture is input into the simulation through the .lfh and .lfw files. Live herbaceous fuel moisture is input as .lfh and live woody fuel moisture is input as .lfw. Both files are text files with three columns of data comprised of month, day and value. Live fuel moistures are measured and made available by local or regional fire departments.

```
# Enable occurrence of Santa Ana events.
#SANTA_ANA_FREQUENCY_PER_YEAR          safpr.0
SANTA_ANA_FREQUENCY_PER_YEAR         4
SANTA_ANA_NUM_DAYS_DURATION          2.5
SANTA_ANA_WIND_AZIMUTH_FILE          HFSEA_SA.waz
SANTA_ANA_WIND_SPEED_FILE            HFSEA_SA.wsp
SANTA_ANA_DEAD_FUEL_MOIST_FILE       HFSEA_SA.10h
```

SAW frequencies are only used in season simulations. Single fire weather data already encompasses Santa Ana data. For season simulations, the number of SAW events, the duration of the events in days and Santa Ana weather information is entered separately. SAW speed, direction and dead 10 hour fuel moisture is entered the same way as the historical weather data, but only Santa Ana days are used.

```
# values are relative to standard model of fire spread
# value < 1.0 = more circular
# value > 1.0 = more elliptical
FIRE_ELLIPSE_ADJUSTMENT_FACTOR      0.66

# choose between methods used to compute windspeed adjustment factor
# value of 'AB79' uses method of Albini and Baughman, 1979
# value of 'BHP' uses method of BEHAVEPLUS
# value of 'NOWAF' assumes windspeed supplied as input is at
midflame
WIND_SPEED_WIND_ADJUSTMENT_FACTOR   BHP

# Cells that are part of a fire where the number of cells is less
than
# or equal to the FIRE_FAILED_IGNITION_NUM_CELLS will be classified
as
# "failed ignitions".
FIRE_FAILED_IGNITION_NUM_CELLS      1
```

The Fuel Model (.fmd) file:

	D1H	D10H	D100	LH	LW	1HSAV	LHSAV	LWSAV	FDepth	Mex	DHC	LHC
21	5.50	0.70	0.00	1.60	3.00	19.37	45.42	19.37	91.44	25	21399	21399

The .fmd must first specify either metric or English units. The following explanation uses metric units. The .fmd file is a text file with a row for each fuel model used in the simulation. The first column is the fuel model number, and the second is the amount of dead one hour fuels in mega grams per hectare. The third and forth columns are dead ten hour and dead one hundred hour fuels respectively, also in mega grams per hectare. Live herbaceous and live woody fuel moisture levels, approximated based on known ranges from local fire departments, are in columns five and six, also in mega grams per hectare. The next three columns are the surface to area ratios for dead one hour fuels, live herbaceous fuels and live woody fuels in square centimeters / cubic centimeters. The tenth column is the fuel bed depth in centimeters, and the eleventh column is the moisture of extinction for the fuel type. Moisture of extinction is the ambient moisture level at which the fuel type will no longer burn, thereby extinguishing the fire. The last two columns are the heat content of the fuel type in kJ/kg.

THIS PAGE INTENTIONALLY LEFT BLANK

APPENDIX B – MAPS OF RANDOM AND HISTORIC IGNITION LOCATIONS

Appendix B1: Historic Ignition Locations

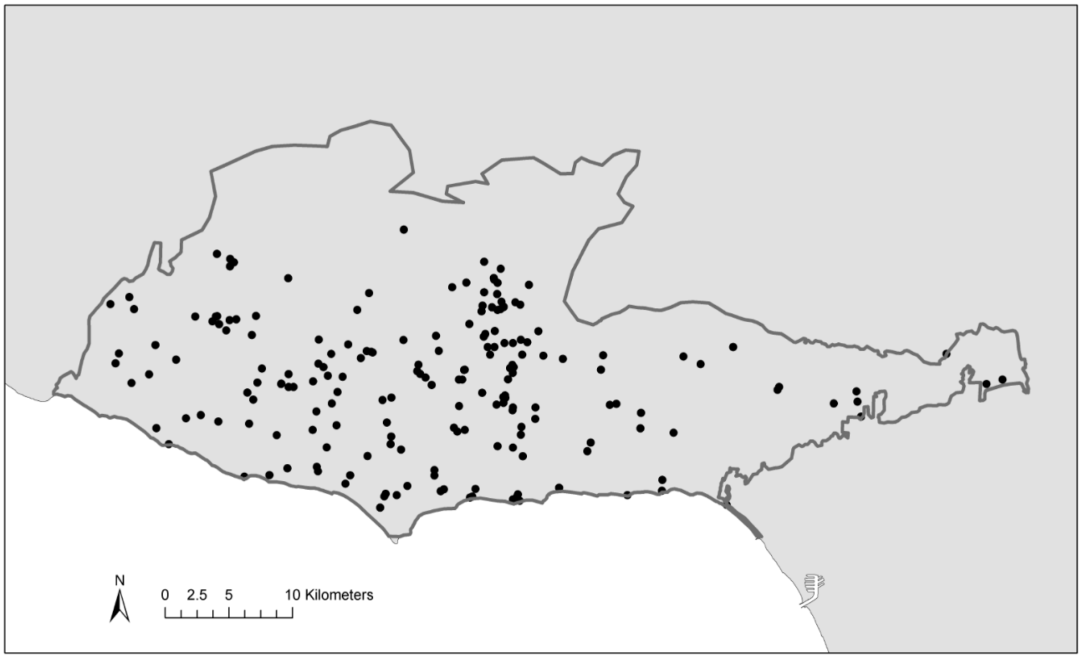

Appendix B2: Randomized Ignition Locations

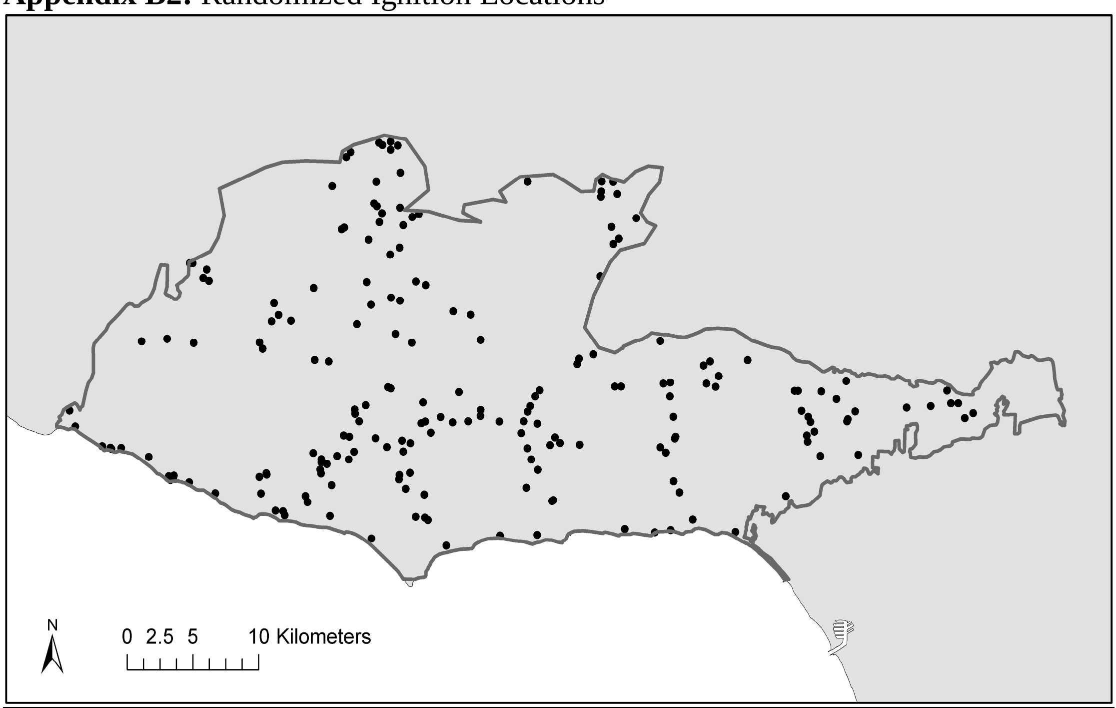

THIS PAGE INTENTIONALLY LEFT BLANK

Appendix C1: Background on Fuel Models

Fuel models consist of a variety of measured characteristics that fire spread modeling programs input into a fire behavior formula to simulate fire spread and intensity. A region's vegetation is input into a fire spread modeling program by categorizing the different habitat types into fuel model designations. The common fuel models used in southern California shrublands are described in Appendix C2. The measured characteristics that go into a fuel model are listed and explained in Appendix C3.

Appendix C2: Crosswalk for conversion of vegetation communities into fuel models

Vegetation Alliance	Fuel Model Type	Fuel Model Number
Native and Non-Native Herbaceous Superalliance Mapping Unit	Short Grass	1
Predominantly Shrubs on Firebreak		1
Predominantly Shrubs/Herbaceous on Artificial Cuts/Embankments		1
Saltgrass - Dune Burrweed		1
Saltgrass - Giant Reed Mapping Unit		1
Saltgrass Alliance		1
Urban - Herbaceous/Cleared		1
California Bulrush	Tall Grass	3
Cattail		3
Fennel Alliance		3
Fountaingrass - Giant Coreopsis - Chaparral Yucca		3
Fountaingrass Alliance		3
Giant Reed Alliance		3
Giant Wildrye		3
Pampas Grass		3
Spanish Broom on Artificial Cuts/Embankments		3
Spartium junceum (Spanish Broom)		3
Tall Shrubs Undifferentiated Superalliance Mapping Unit	Chaparral (up to 4 feet)	4
Ornamental Shrubs	Brush (up to 2 feet)	5
Post Fire or Post Clearing Regeneration Unidentifiable Shrubs		5
Urban - Shrub		5
Acacia redolens	Dormant Brush	6

	Hardwood Slash	
Iceplant	Closed Timber Litter	8
Pepper on Artificial Cuts/Embankments		8
Predominantly Trees on Artificial Cuts and Embankments		8
Urban - California Sycamore		8
Urban - California Sycamore-Coast Live Oak		8
Urban - California Sycamore-Willow spp.		8
Urban - Coast Live Oak		8
Urban - Valley Oak		8
Urban - Valley Oak-Coast Live Oak		8
Valley Oak - Arroyo Willow (provisional)		8
Valley Oak - Coast Live Oak / Annual Grass Herb		8
Valley Oak / Annual Grass - Herb		8
Valley Oak Alliance		8
Arroyo Willow / Laurel Sumac	Hardwood Litter	9
Arroyo Willow / Mulefat		9
Arroyo Willow Alliance		9
California Bay		9
California Bay - California Sycamore		9
California Bay - California Walnut / Greenbark Ceanothus		9
California Bay / Hairyleaf Ceanothus (provisional)		9
California Bay Alliance		9
California Sycamore - Coast Live Oak - Arroyo Willow South Coast		9
California Sycamore - Coast Live Oak / Mulefat South Coast		9
California Sycamore - Coast Live Oak South Coast		9
California Sycamore / Annual Grass - Herb		9
California Sycamore Alliance		9
California Sycamore South Coast Intermittent Stream		9
Conifers		9
Conifers on Artificial Cuts/Embankments		9
Eucalyptus		9
Eucalyptus on Artificial Cuts/Embankments		9
Exotic Trees Undifferentiated		9

Narrowleaf Willow Alliance		9
Other Trees		9
Red Willow Alliance		9
Red Willow and Arroyo Willow Superallliance Mapping Unit		9
Schinus molle (Pepper)		9
White Alder - California Sycamore		9
White Alder Alliance		9
Willow spp. / Mulefat Superalliance Mapping Unit		9
Willow spp. scrubby - California Sycamore scrubby / Mulefat Superalliance Mapping Unit		9
Willow spp./Giant Reedgrass Suballiance Mapping Unit (AruDon in: 1420/1430/1432 dense)		9
Bigberry Manzanita Alliance	Manzanita	14
Birchleaf Mountain Mahogany - Chamise		14
Birchleaf Mountain Mahogany - Laurel Sumac - California Sagebrush		14
Birchleaf Mountain Mahogany Alliance		14
Birchleaf Mountain-mahogany Alliance (Cercocarpus betuloides)		14
California Walnut / Annual Grass - Herb		14
California Walnut / California Sagebrush / Giant Wildrye		14
California Walnut / Greenbark Ceanothus		14
California Walnut / Laurel Sumac		14
California Walnut / Toyon		14
California Walnut Alliance		14
California Walnut-(Coast Live Oak)/Tall Shrub Superassociation Mapping Unit		14
Coast Live Oak - Arroyo Willow		14
Coast Live Oak - California Bay		14
Coast Live Oak - California Bay / Hairyleaf Ceanothus		14
Coast Live Oak - California Walnut		14
Coast Live Oak / Annual Grass - Herb		14
Coast Live Oak / Annual Grass - Herb		14
Coast Live Oak / Bush Monkeyflower Phase		14
Coast Live Oak / Chamise		14
Coast Live Oak / Poison Oak		14
Coast Live Oak / Purple Sage - California Sagebrush		14

Coast Live Oak / Purple Sage - California Sagebrush		14
Coast Live Oak / Scrub Oak		14
Coast Live Oak / Toyon		14
Coast Live Oak Alliance		14
Coast Live Oak South Coastal		14
Coast Live Oak Superassociation Mapping Unit		14
Eastwood Manzanita Alliance		14
Hollyleaf Cherry - Toyon		14
Hollyleaf Cherry Alliance		14
Laurel Sumac		14
Laurel Sumac - California Buckwheat		14
Laurel Sumac - Ashy Buckwheat		14
Laurel Sumac - Ashy Buckwheat - Black Sage Phase		14
Laurel Sumac - Black Sage		14
Laurel Sumac - California Sagebrush		14
Laurel Sumac - Lemonadeberry - Ashy Buckwheat - California Sagebrush Phase		14
Laurel Sumac - Sugarbush - Bigpod Ceanothus		14
Laurel Sumac / Annual Grass - Herb		14
Laurel Sumac / Annual Grass - Herb		14
Laurel Sumac Alliance		14
Lemonadeberry - Ashy Buckwheat - Chaparral Yucca - Giant Coreopsis Phase		14
Lemonadeberry - California Sagebrush - Ashy Buckwheat		14
Lemonadeberry - Coast Prickly Pear - Ashy Buckwheat		14
Lemonadeberry Alliance		14
Lemonadeberry Strongly Dominant		14
Mexican Elderberry - Toyon / Annual Grass - Herb		14
Mexican Elderberry / Giant Wildrye - Annual Grass - Herb		14
Mexican Elderberry Alliance		14
Scrub Interior Live Oak Alliance		14
Scrub Oak		14
Scrub Oak - Birchleaf Mountain Mahogany		14
Scrub Oak - Greenbark Ceanothus		14
Scrub Oak Alliance		14
Sugarbush		14
Sugarbush - Purple Sage - California Sagebrush		14

Sugarbush Alliance		14
Toyon - Laurel Sumac - Rhus spp.		14
Toyon Alliance		14
Bigpod Ceanothus	Ceanothus	16
Bigpod Ceanothus - Birchleaf Mountain Mahogany		16
Bigpod Ceanothus - Black Sage		16
Bigpod Ceanothus - Chamise		16
Bigpod Ceanothus - Laurel Sumac		16
Bigpod Ceanothus - Redshank		16
Bigpod Ceanothus Alliance		16
Bush Poppy Alliance		16
Ceanothus spp. and Birchleaf Mountain-mahogany Superalliance Mapping Unit		16
Greenbark Ceanothus		16
Greenbark Ceanothus Alliance		16
Greenbark Ceanothus and Bigpod Ceanothus and Birchleaf Mountain-mahogany Superalliance Mapping Unit		16
Hairyleaf Ceanothus		16
Hairyleaf Ceanothus - Redshank		16
Hairyleaf Ceanothus - Scrub Oak		16
Hairyleaf Ceanothus - Tall Shrubs Superassociation Mapping Unit		16
Hairyleaf Ceanothus - Toyon		16
Hairyleaf Ceanothus Alliance		16
Hoaryleaf Ceanothus		16
Hoaryleaf Ceanothus - Laurel Sumac		16
Hoaryleaf Ceanothus Alliance		16
Wedgeleaf Ceanothus - Scrub Oak		16
Wedgeleaf Ceanothus Alliance		16
Ceanothus spp. - Chamise Superalliance Mapping Unit		**16**
Wedgeleaf Ceanothus and Wedgeleaf Ceanothus - Chamise Superalliance Mapping Unit		16
Chamise	Young Chamise	17
Chamise - Bigberry Manzanita		17
Chamise - Bigpod Ceanothus		17
Chamise - Bush Monkeyflower		17
Chamise - California Buckwheat - (Deerweed)		17
Chamise - Eastwood Manzanita		17

Chamise - Eastwood Manzanita Alliance		17
Chamise - Laurel Sumac		17
Chamise - Laurel Sumac - Yerba Santa / Annual Grass - Herg		17
Chamise - Purple Sage (Provisional)		17
Chamise - Redshank - Hoaryleaf Ceanothus		17
Chamise - Redshank Alliance		17
Chamise - Scrub Oak		17
Chamise - Scrub Oak Alliance		17
Redshank Alliance		17
Riverine, Lacustrine, and Tidal Mudflat Mapping Unit		17
Chamise - Hoaryleaf Ceanothus - Laurel Sumac		17
Chamise - Hoaryleaf Ceanothus Alliance		17
Chamise - Wedgeleaf Ceanothus - Black Sage - Laurel Sumac		17
Alkali Heath - California Sealavender - Shoregrass - Pickleweed	Santa Monica Mountains Coastal Sage Scrub	21
Ashy Buckwheat		21
Ashy Buckwheat Alliance		21
Black Sage		21
Black Sage - Ashy Buckwheat		21
Black Sage - Laurel Sumac		21
Black Sage - Laurel Sumac and Black Sage - Sugarbush Superassociation Mapping Unit		21
Black Sage Alliance		21
Black Sage Superassociation Mapping Unit		21
Bush Mallow		21
Bush Mallow - Bigpod Ceanothus		21
Bush Mallow - Black Sage		21
Bush Mallow - Laurel Sumac		21
Bush Mallow - Purple Sage		21
Bush Mallow Alliance		21
Bush Mallow-Greenbark Ceanothus		21
Bush Monkeyflower		21
Bush Monkeyflower Alliance		21
Bush Monkeyflower and Poison Oak Superalliance Mapping Unit		21
California Buckwheat		21

California Buckwheat - Black Sage - Laurel Sumac		21
California Buckwheat - White Sage Alliance		21
California Buckwheat Alliance		21
California Encelia		21
California Encelia - Ashy Buckwheat		21
California Encelia - California Sagebrush		21
California Encelia - Laurel - Sumac - Black Sage		21
California Encelia - Lemonadeberry		21
California Encelia Alliance		21
California Encelia Superassociation Mapping Unit		21
California Sagebrush		21
California Sagebrush - Ashy Buckwheat - Black Sage		21
California Sagebrush - Black Sage		21
California Sagebrush - Black Sage Alliance		21
California Sagebrush - Bush Monkeyflower		21
California Sagebrush - California Buckwheat - Black Sage		21
California Sagebrush - California Buckwheat - Purple Sage		21
California Sagebrush - California Buckwheat / Annual Grass - Herb		21
California Sagebrush - California Buckwheat Alliance		21
California Sagebrush - Purple Sage - Ashy Buckwheat / Needlegrass		21
California Sagebrush - Purple Sage Alliance		21
California Sagebrush - Purple Sage codominance		21
California Sagebrush - Purple Sage Superassociation Mapping Unit		21
California Sagebrush / Giant Wildrye		21
California Sagebrush Alliance		21
Canyon Sunflower Alliance		21
Chamise - Black Sage		21
Chamise - Black Sage - Laurel Sumac		21
Chamise - Black Sage - Sugarbush		21
Chamise - Black Sage Alliance		21
Coast Prickly Pear - Mixed Coastal Sage Scrub		21
Coast Prickly Pear Alliance		21
Conejo Buckwheat Shrubland Unique Stands Mapping Unit		21
Coyotebrush - California Sagebrush		21

Coyotebrush / Annual Grass - Herb		21
Coyotebrush Alliance		21
Deerweed Alliance		21
Giant Coreopsis - California Sagebrush - Ashy Buckwheat		21
Giant Coreopsis - Dune Goldenbush - California Encelia		21
Giant Coreopsis Alliance		21
Mulefat - Riparian		21
Mulefat Alliance		21
PalmerÆs Goldenbush Shrubland Unique Stands Mapping Unit		21
Pickelweed / Algae		21
Pickleweed - Alkali Heath - California Seablite		21
Pickleweed - Alkali Heath - Saltwort PHase		21
Pickleweed - Black Mustard		21
Pickleweed - California Seablite Phase		21
Pickleweed - Marsh Jaumea		21
Pickleweed - Parish's Glasswort		21
Pickleweed Alliance		21
Poison Oak - Bush Monkeyflower		21
Poison Oak - California Sagebrush / Giant Wildrye		21
Poison Oak Alliance		21
Purple Sage		21
Purple Sage - Ashy Buckwheat / Annual Grass - Herb		21
Purple Sage Alliance		21
Quailbush Alliance		21
Rush Superalliance		21
Sawtooth Goldenbush - California Sagebrush / Grass		21
Sawtooth Goldenbush / Purple Needlegrass - Clustered Tarplant		21
Sawtooth Goldenbush Alliance		21
Scalebroom Alliance		21
Water	Unburnable (Water)	98
Wetland Undifferentiated Superalliance Mapping Unit		98
Agriculture	Unburnable	99
Beach Sand		99
Bushy Spikemoss / California Buckwheat		99
Cleared Land		99
Coast Live Oak in Agriculture		99

Landslide		99
Rock outcrop Mapping Unit		99
Rock outcrop/Herbaceous Mapping Unit		99
Rocky Streambed		99
Saltpan		99
Sand/Gravel Bar		99
Sparsely Vegetated Coastal Strand (Great Sand Dune)		99
Sparsely Vegetated to Non-vegetated Artificial Cuts and Embankments		99
Urban/Disturbed or Built-Up		99
Valley Oak in Agriculture		99
Valley Oak-Coast Live Oak in Agriculture		99

Appendix C3: Fuel Model Characteristics

Code	Description	Units	Notes
D1H	Dead One Hour Fuels	Mg/ha	Time it takes for fuel moisture to approach half of ambient humidity change
D10H	Dead Ten Hour Fuels	Mg/ha	Time it takes for fuel moisture to approach half of ambient humidity change
D100	Dead One Hundred Hour Fuels	Mg/ha	Time it takes for fuel moisture to approach half of ambient humidity change
LH	Live Herbaceous Fuels	Mg/ha	
LW	Live Woody Fuels	Mg/ha	
1HSAV	Dead One Hour Fuels Characteristic Surface Area to Volume Ratio	cm^2/cm^3	
LHSAV	Live Herbaceous Fuels Characteristic Surface Area to Volume Ratio	cm^2/cm^4	
LWSAV	Live Woody Fuels Characteristic Surface Area to Volume Ratio	cm^2/cm^5	
FDepth	Fuel Bed Depth	cm	70% of Average Stand Height
Mex	Moisture of Extinction of Dead Fuels	%	
DHC	Dead Fuels Heat Content	kJ/kg	
LHC	Live Fuels Heat Content	kJ/kg	

APPENDIX D – FIRE BOUNDARIES FROM CORRAL FIRE SIMULATIONS

Appendix D1: Fire boundary from simulation C1

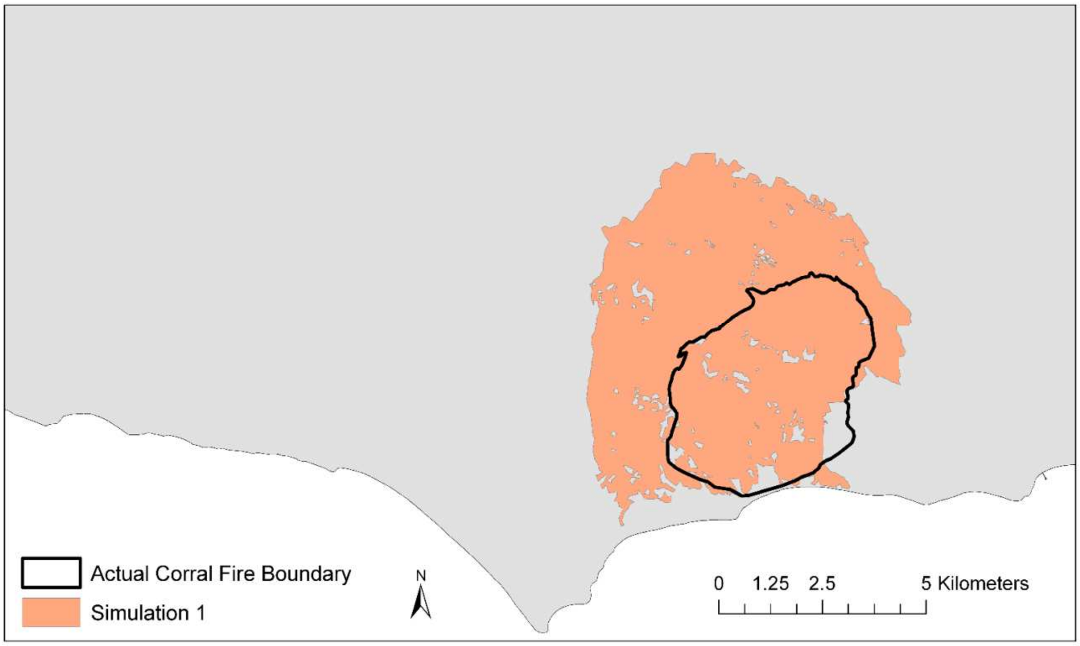

Appendix D2: Fire boundary from simulation C2

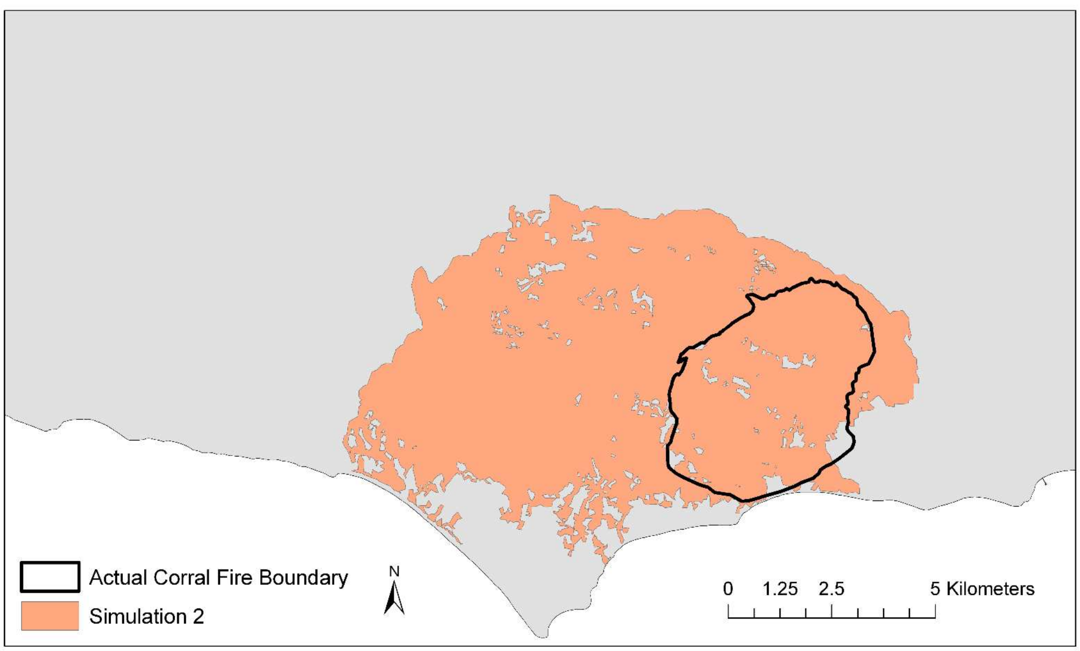

Appendix D3: Fire boundary from simulation C3

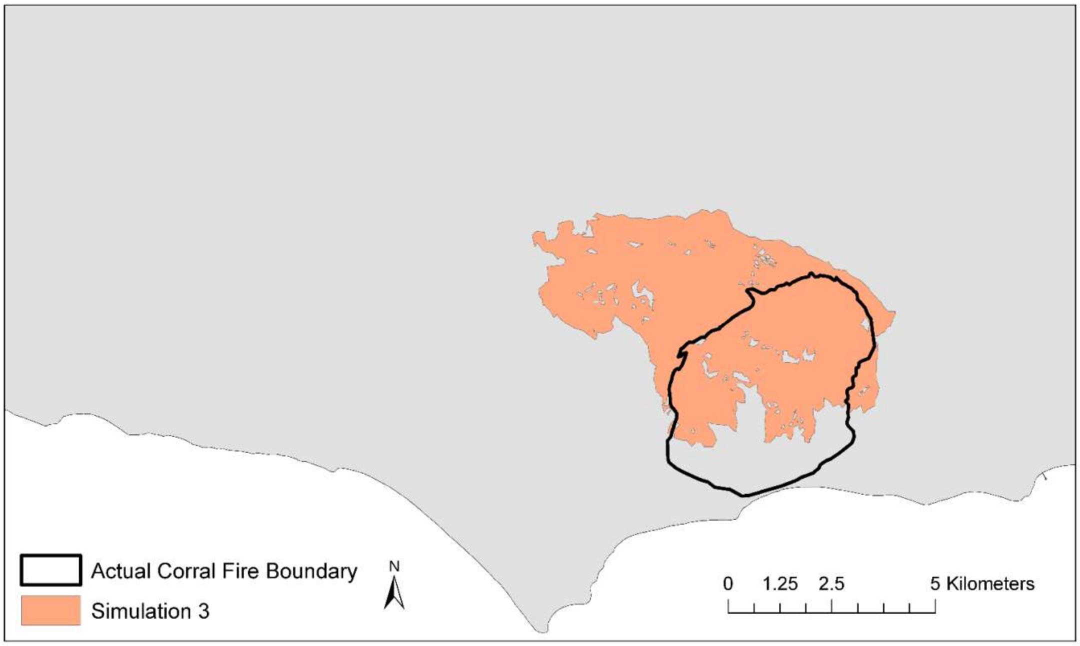

Appendix D4: Fire boundary from simulation C4

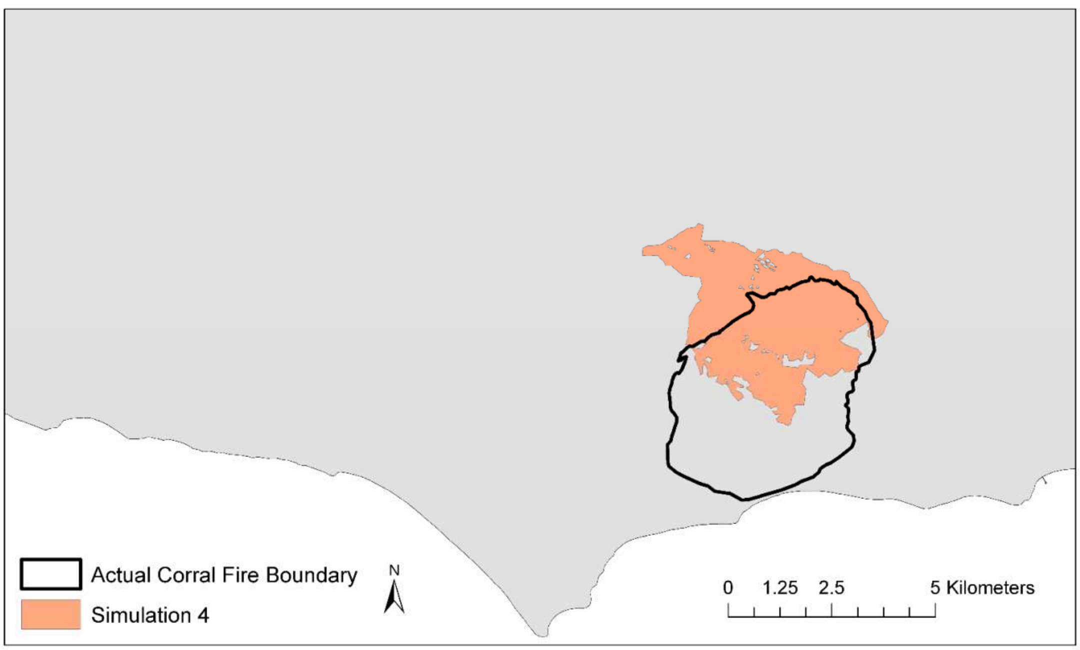

Appendix D5: Fire boundary from simulation C5

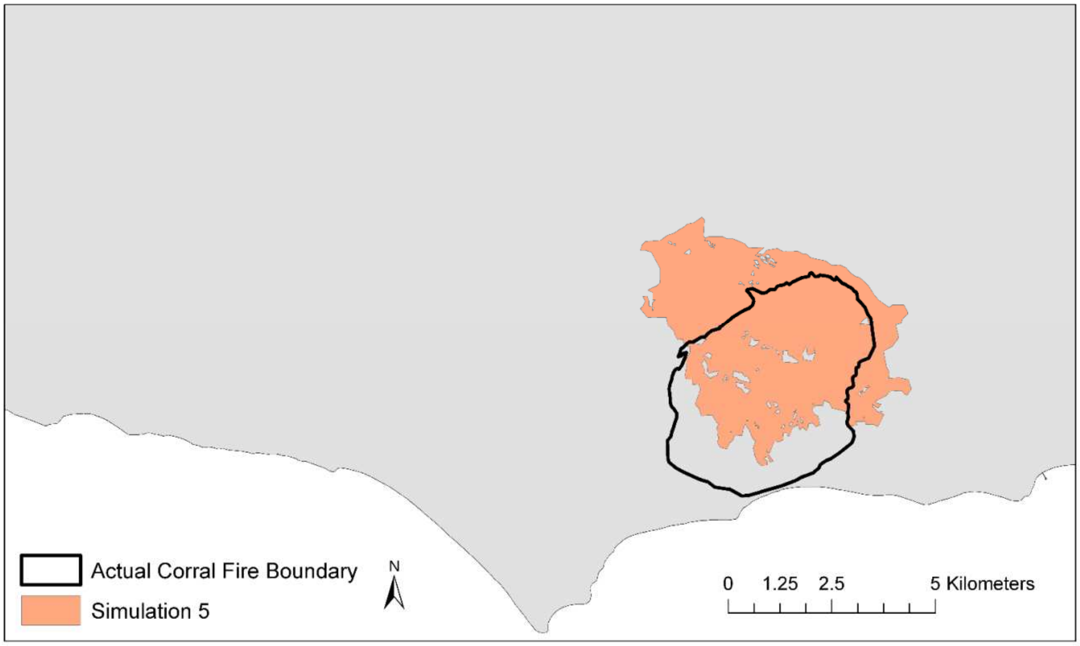

Appendix D6: Fire boundary from simulation C6

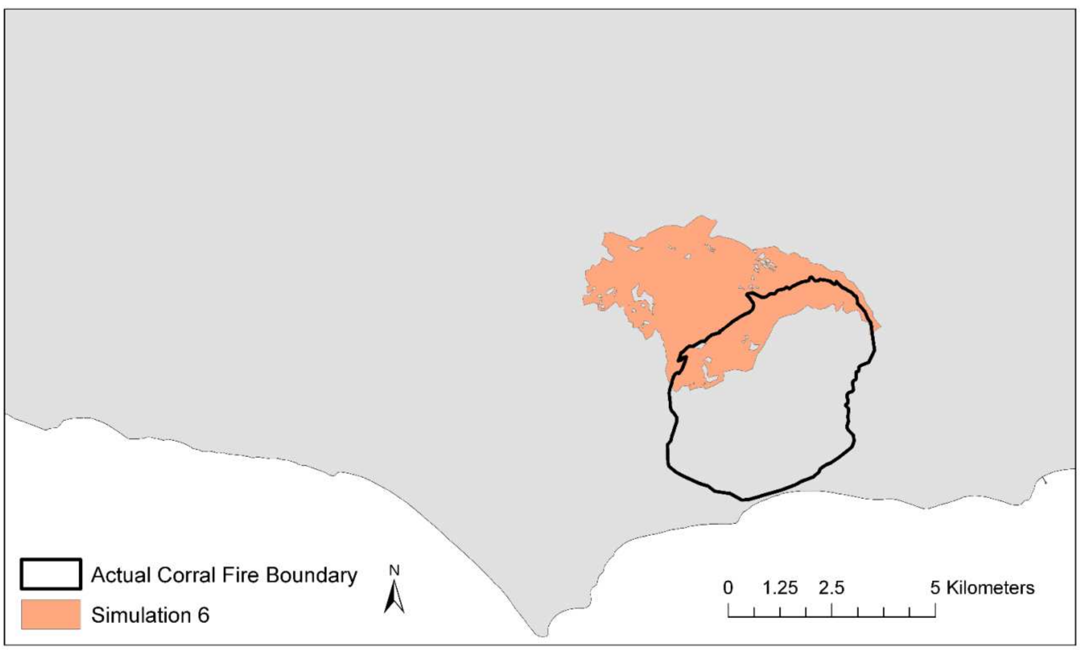

Appendix D7: Fire boundary from simulation C7

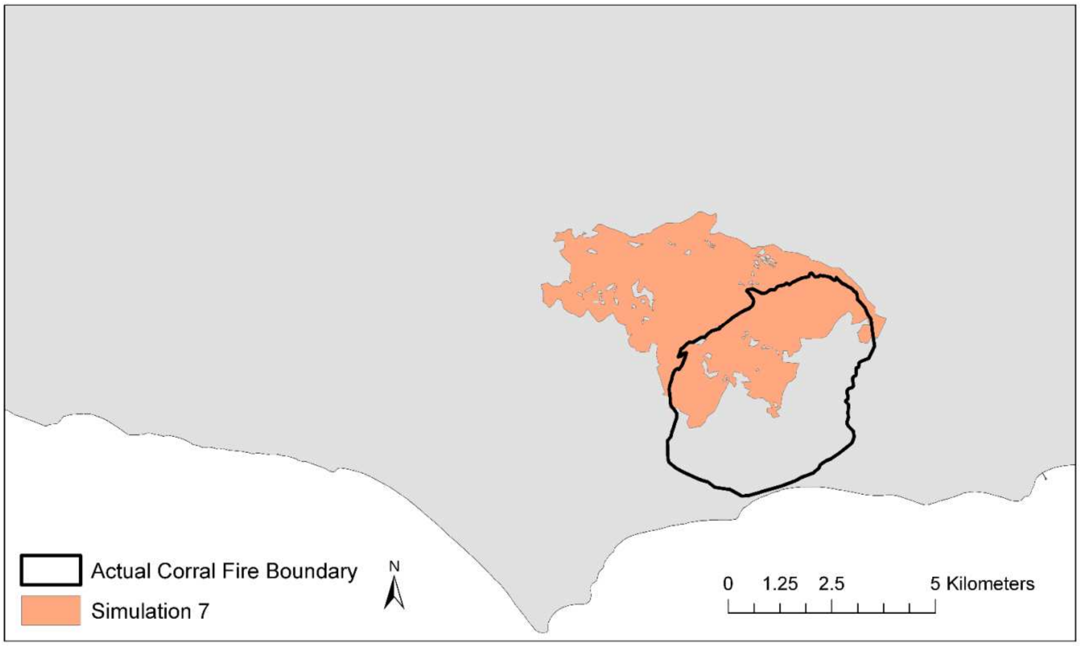

Appendix D8: Fire boundary from simulation C8

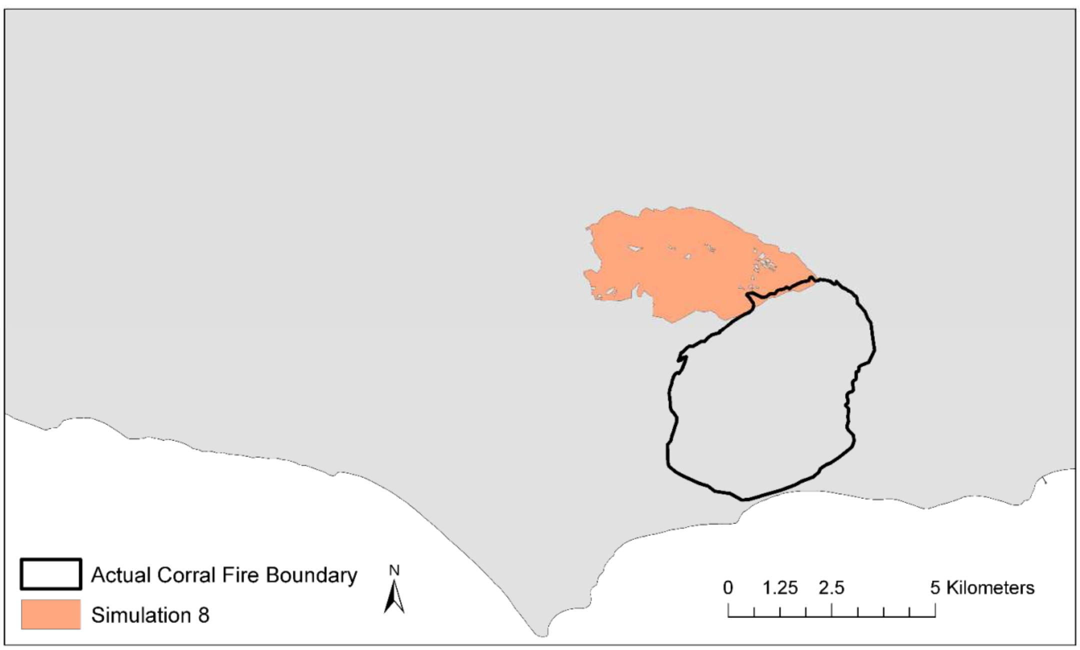

Appendix D9: Fire boundary from simulation C9

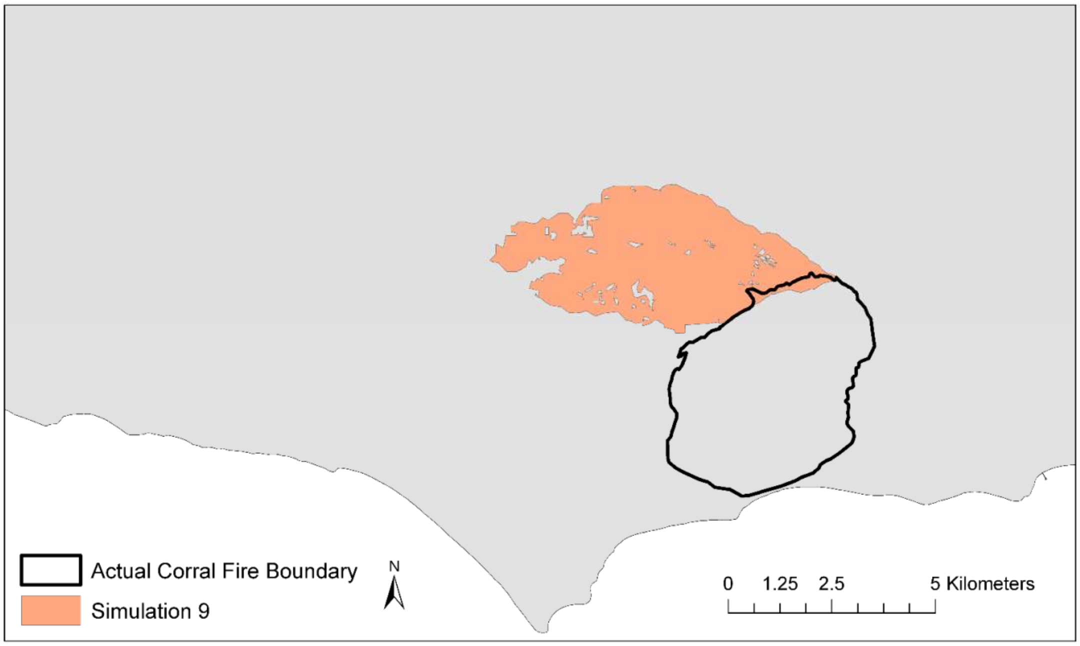

Appendix D10: Fire boundary from simulation C10

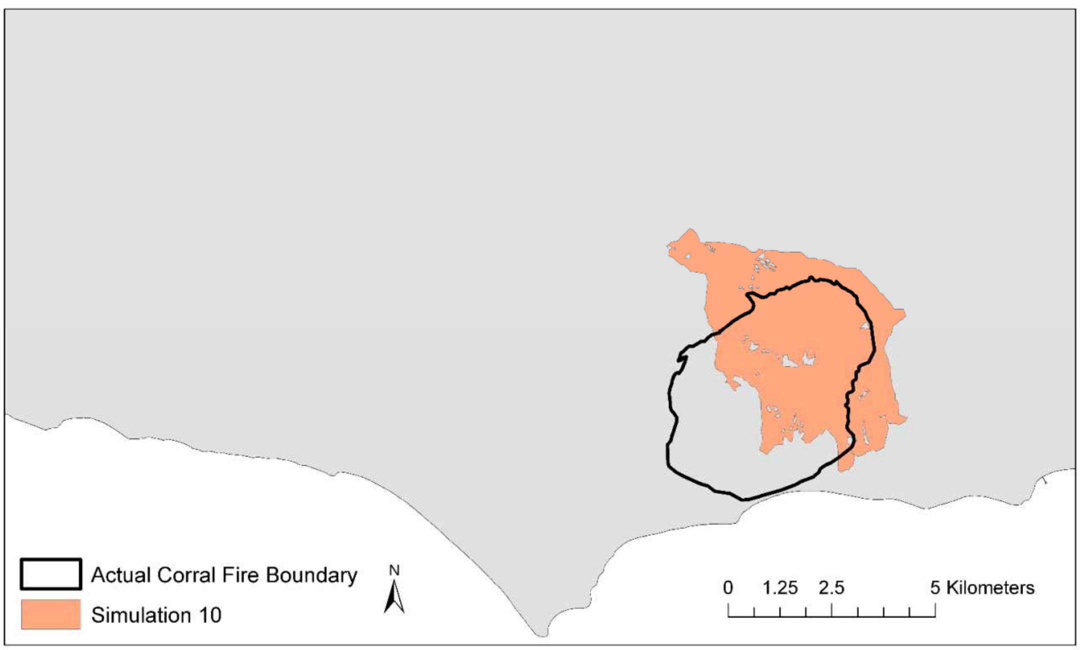

Appendix D11: Fire boundary from simulation C11

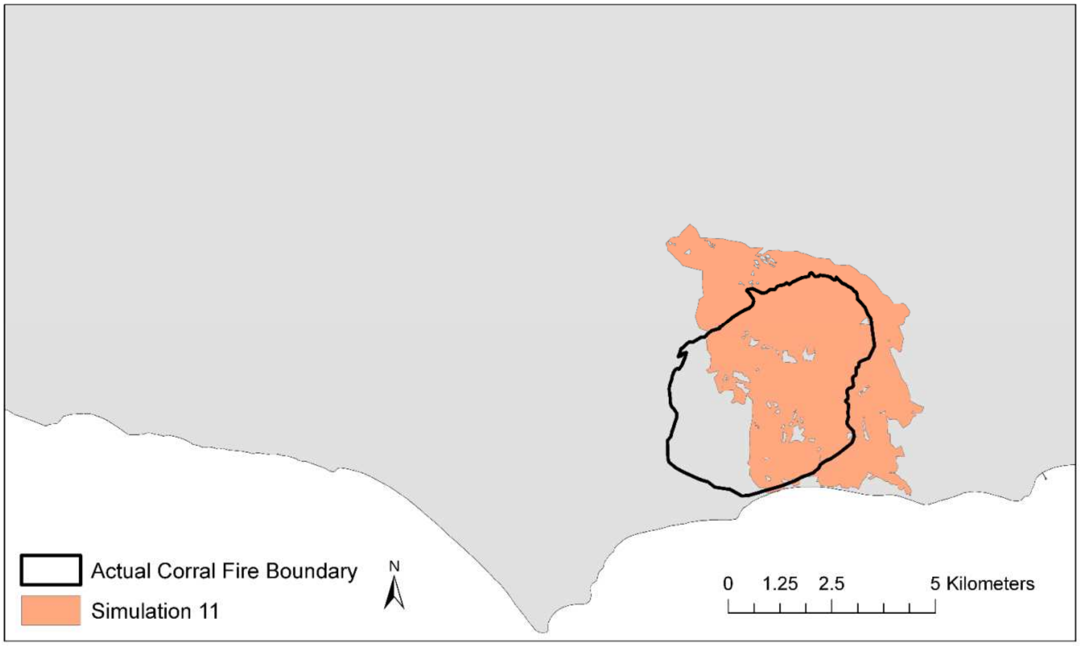

Appendix D12: Fire boundary from simulation C12

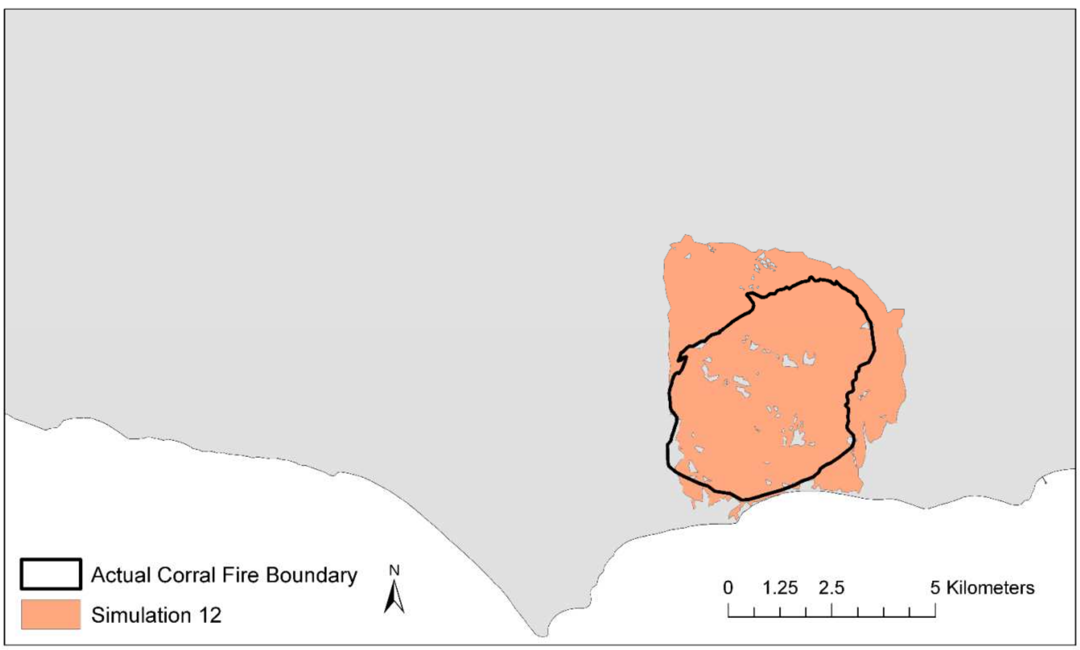

Appendix D13: Fire boundary from simulation C13

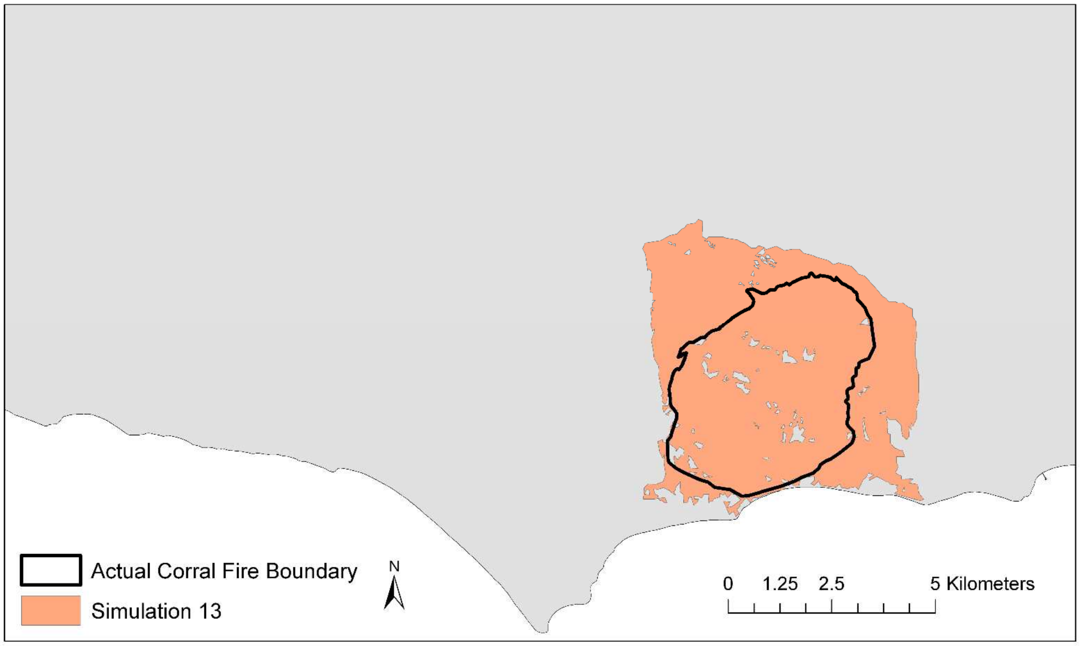

Appendix D14: Fire boundary from simulation C14

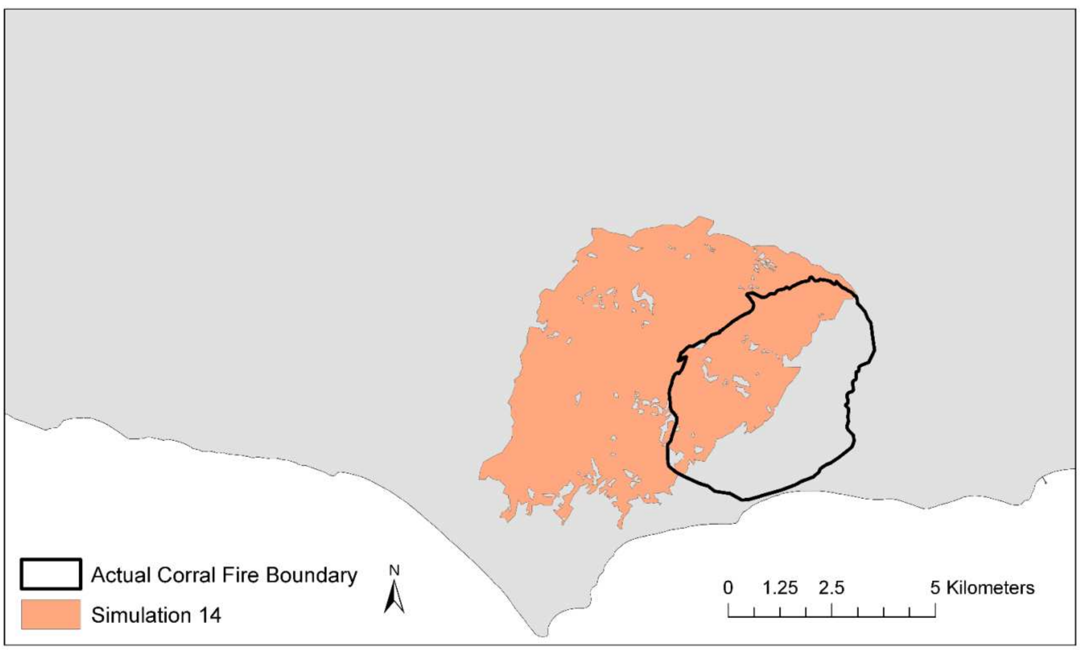

Appendix D15: Fire boundary from simulation C15

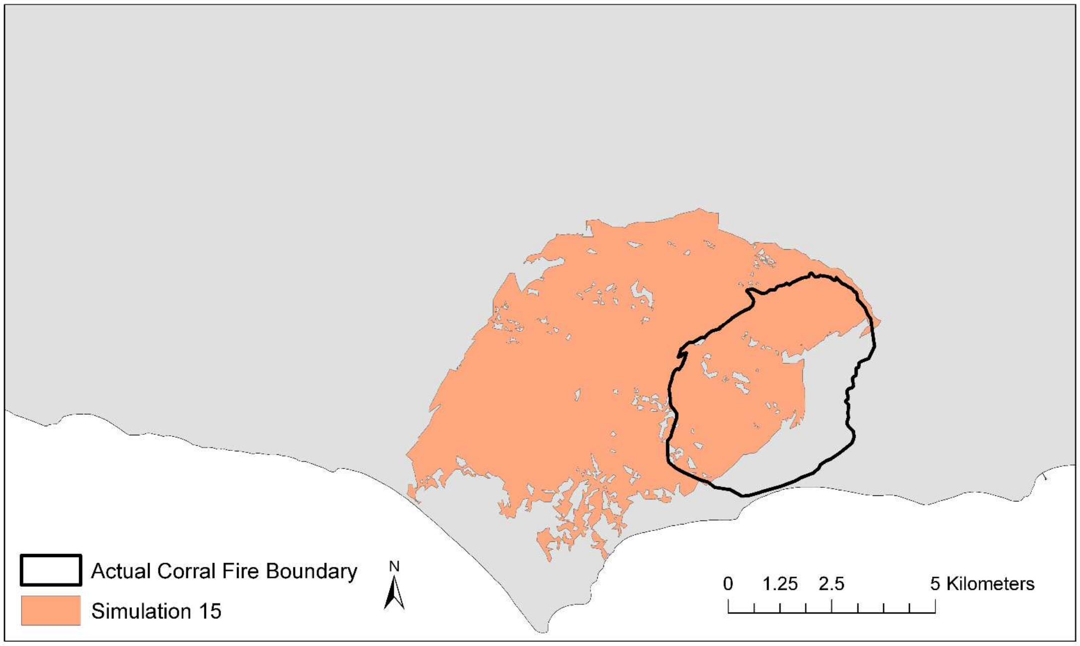

Appendix D16: Fire boundary from simulation C16

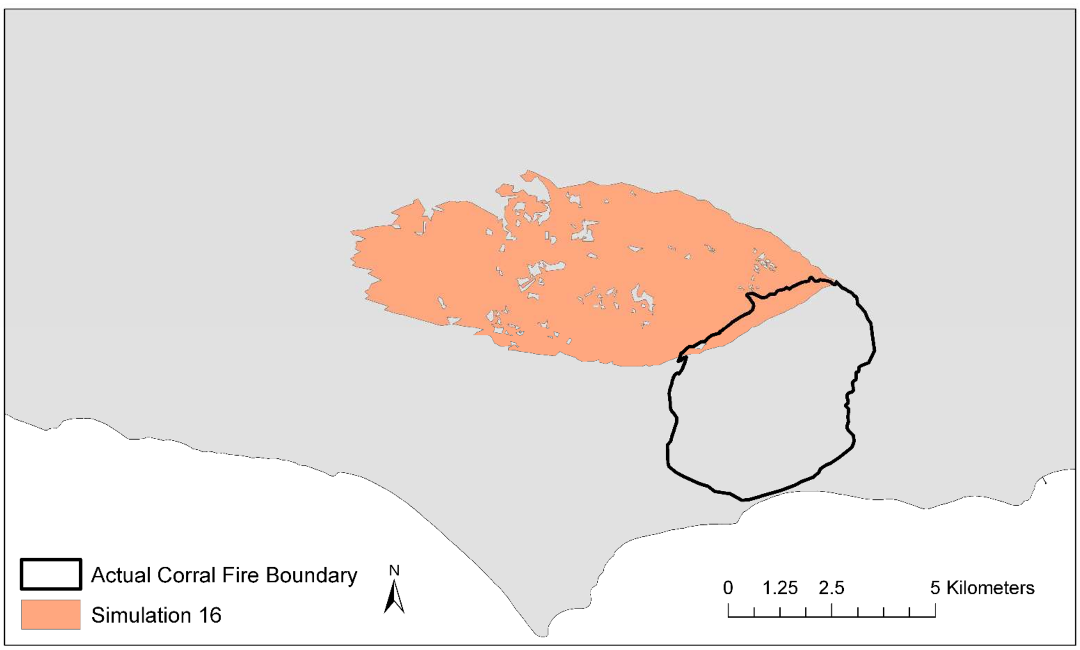

Appendix D17: Fire boundary from simulation C17

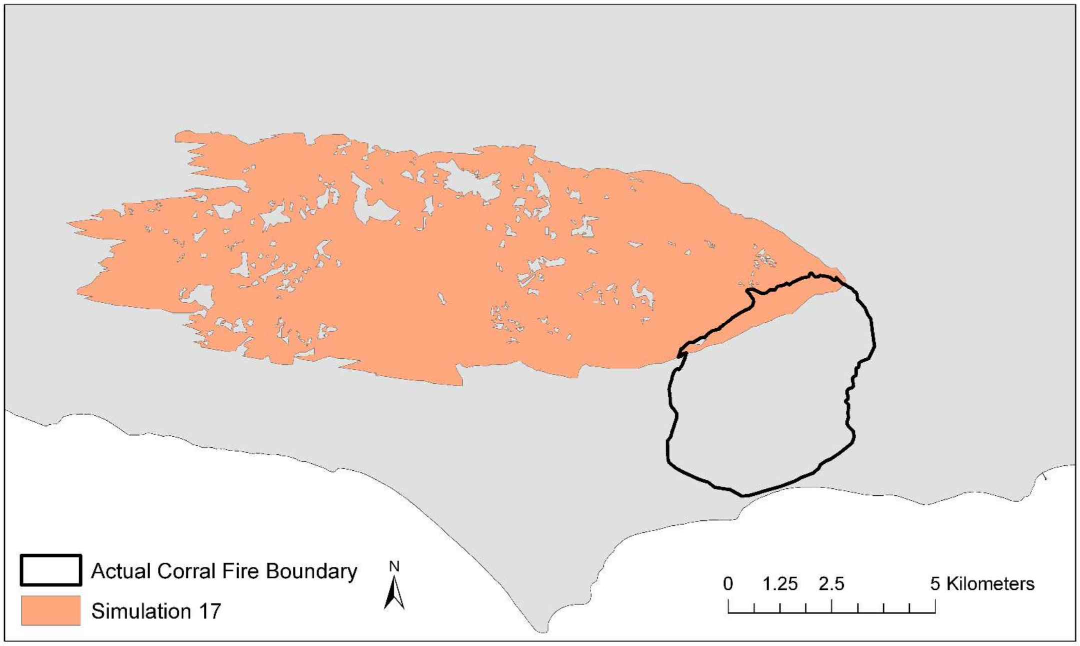

Appendix D18: Fire boundary from simulation C18

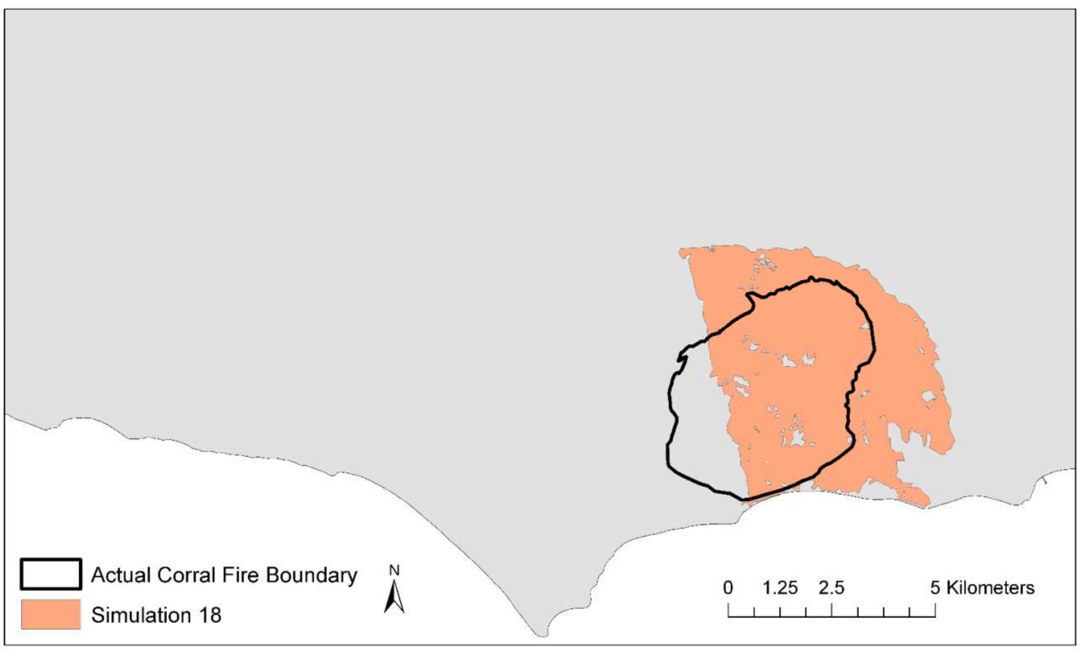

Appendix D19: Fire boundary from simulation C19

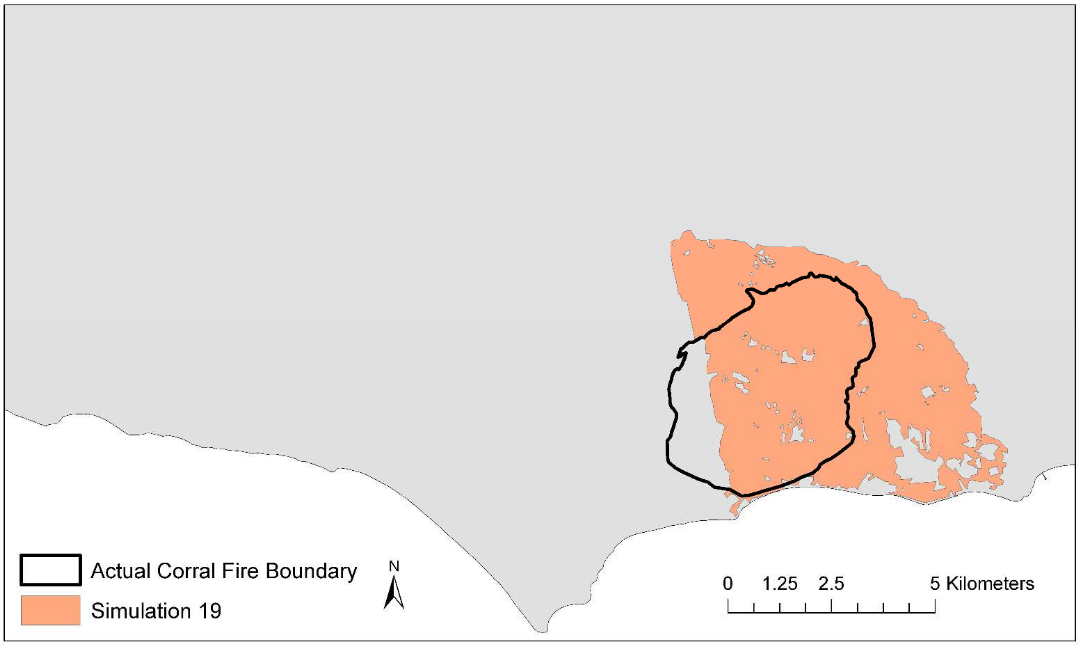

APPENDIX E – STUDY AREA-WIDE HISTORIC BURN FREQUENCY MAPS

Appendix E1: Simulation S1. 0°, 24 kph (15mph) wind grid

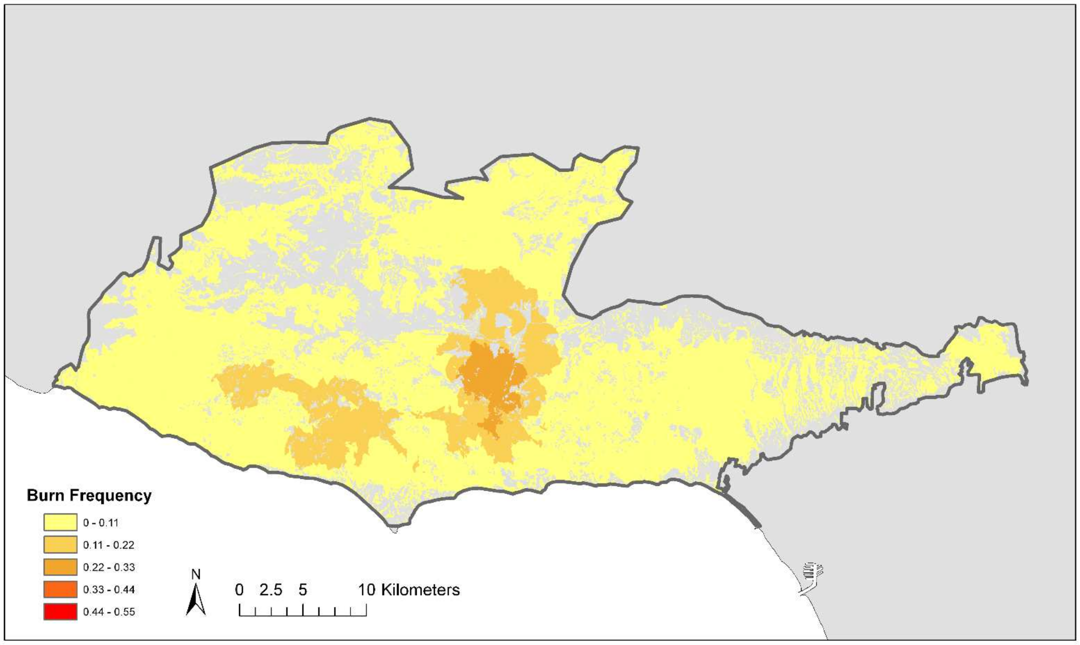

Appendix E2: Simulation S2. 90°, 24 kph (15mph) wind grid

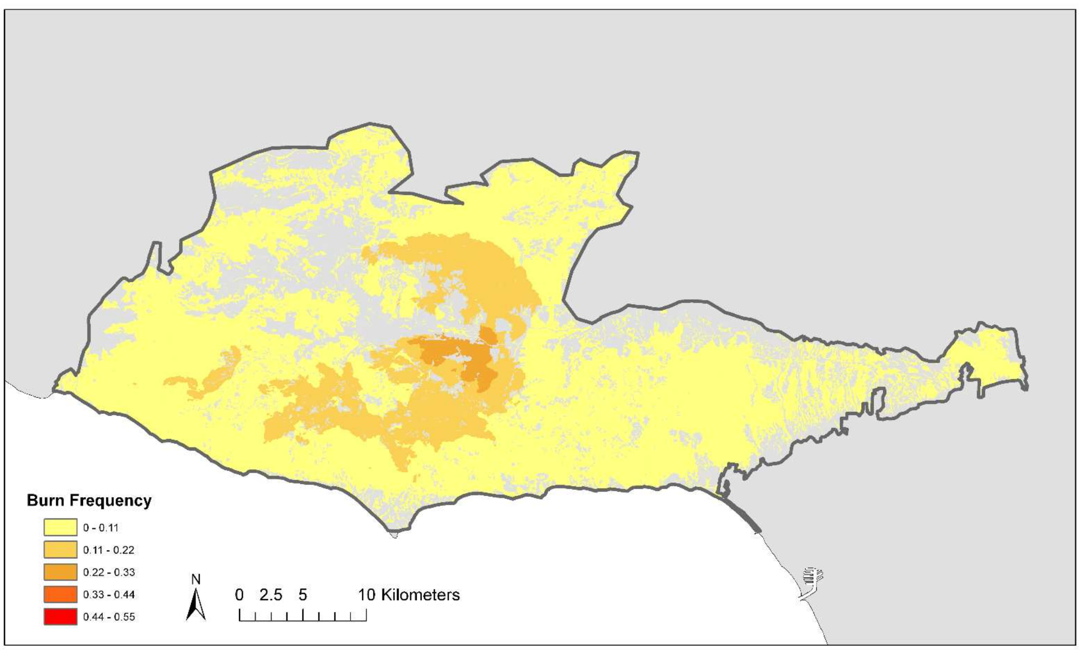

Appendix E3: Simulation S3. 45°, 24 kph (15mph) wind grid

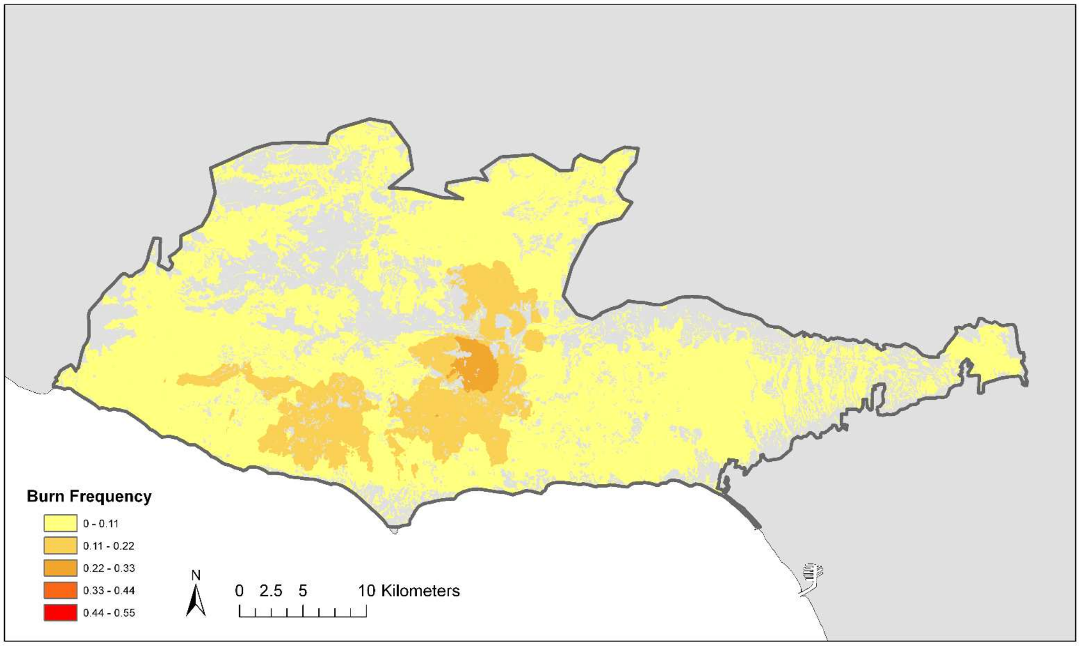

Appendix E4: Simulation S4. 337.5°, 24 kph (15mph) wind grid

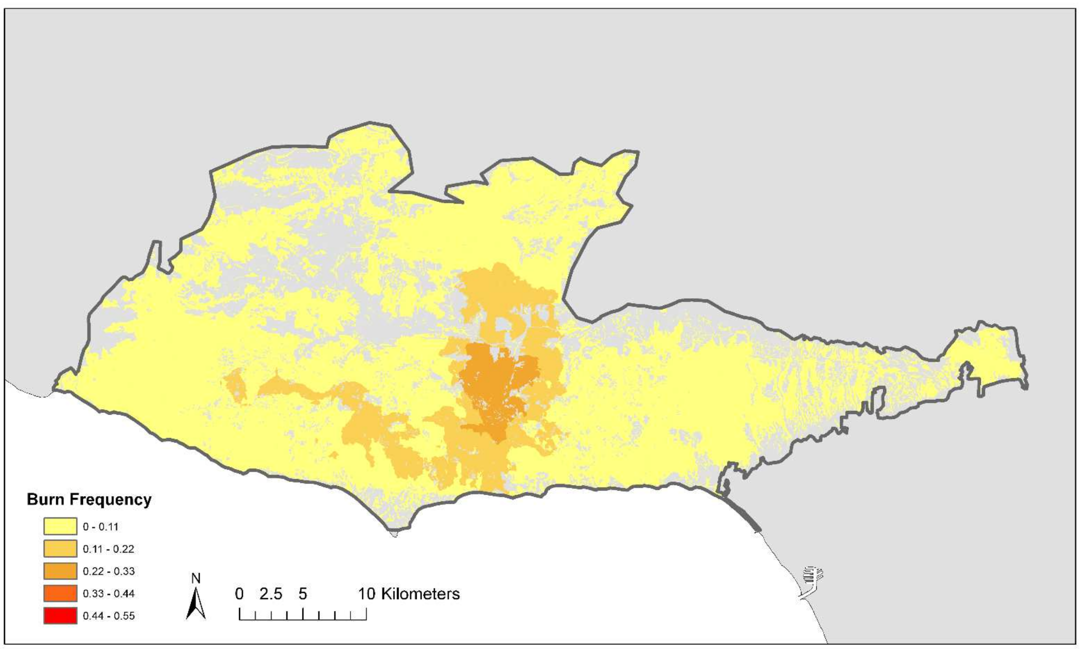

Appendix E5: Simulation S5. 90°, 40 kph (25mph) wind grid

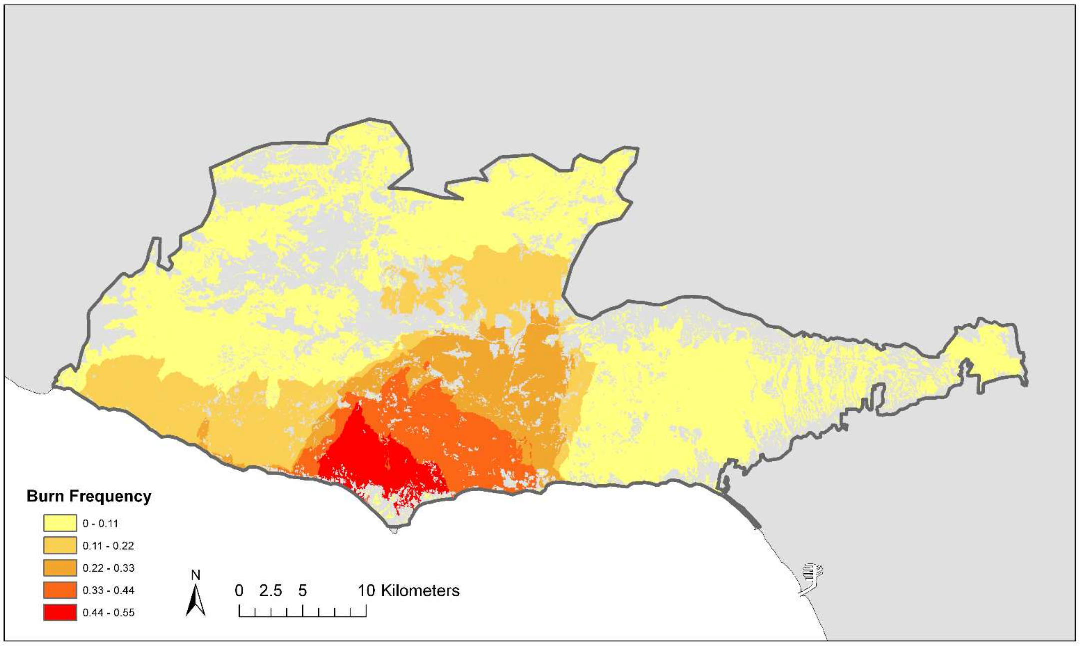

THIS PAGE INTENTIONALLY LEFT BLANK

APPENDIX F – STUDY AREA-WIDE HISTORIC BURN TIME MAPS

Appendix F1: Simulation S1. 0°, 24 kph (15mph) wind grid

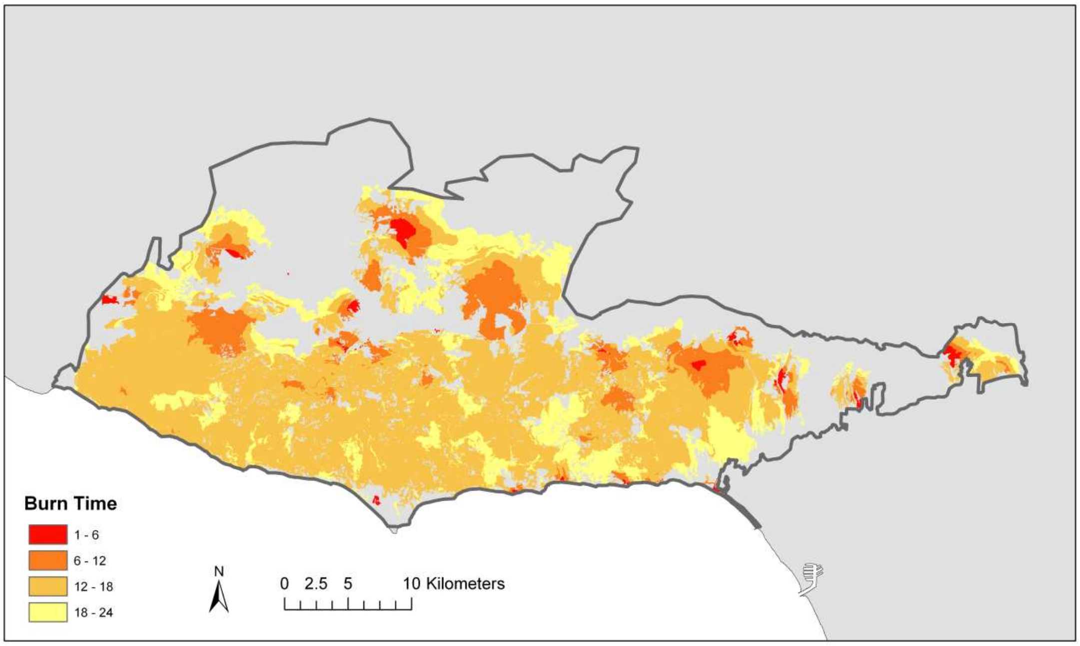

Appendix F2: Simulation S2. 90°, 24 kph (15mph) wind grid

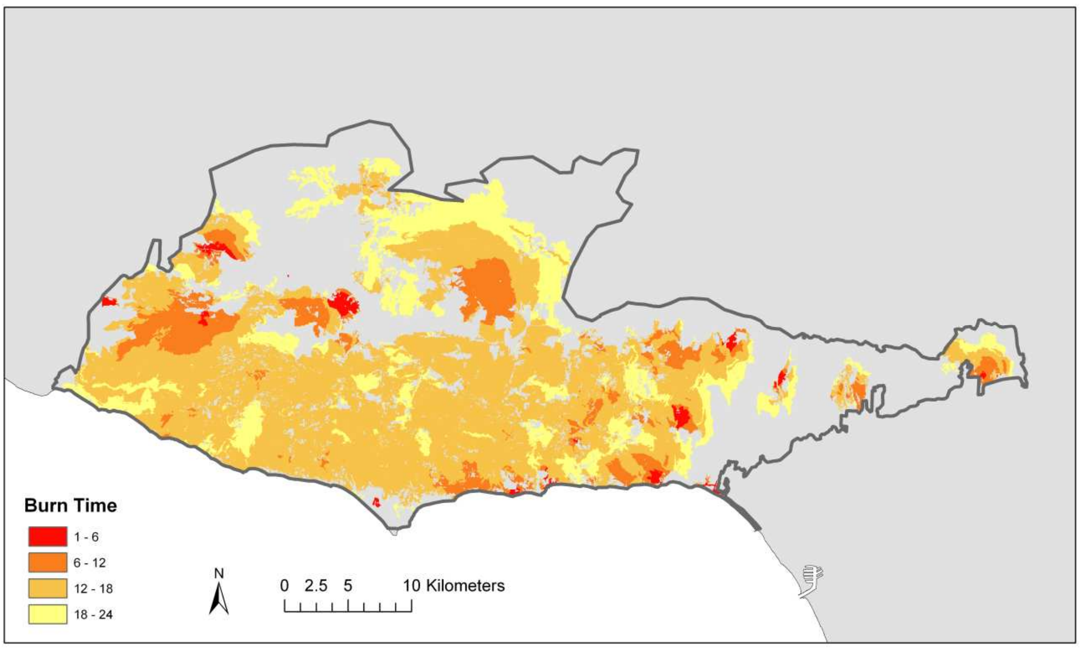

Appendix F3: Simulation S3. 45°, 24 kph (15mph) wind grid

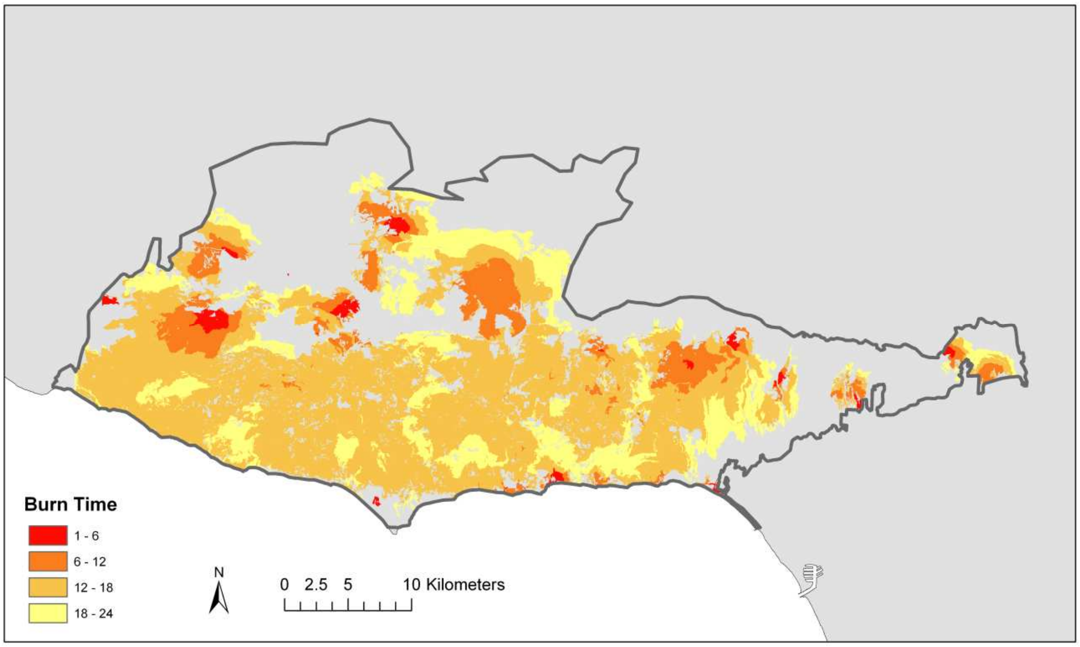

Appendix F4: Simulation S4. 337.5°, 24 kph (15mph) wind grid

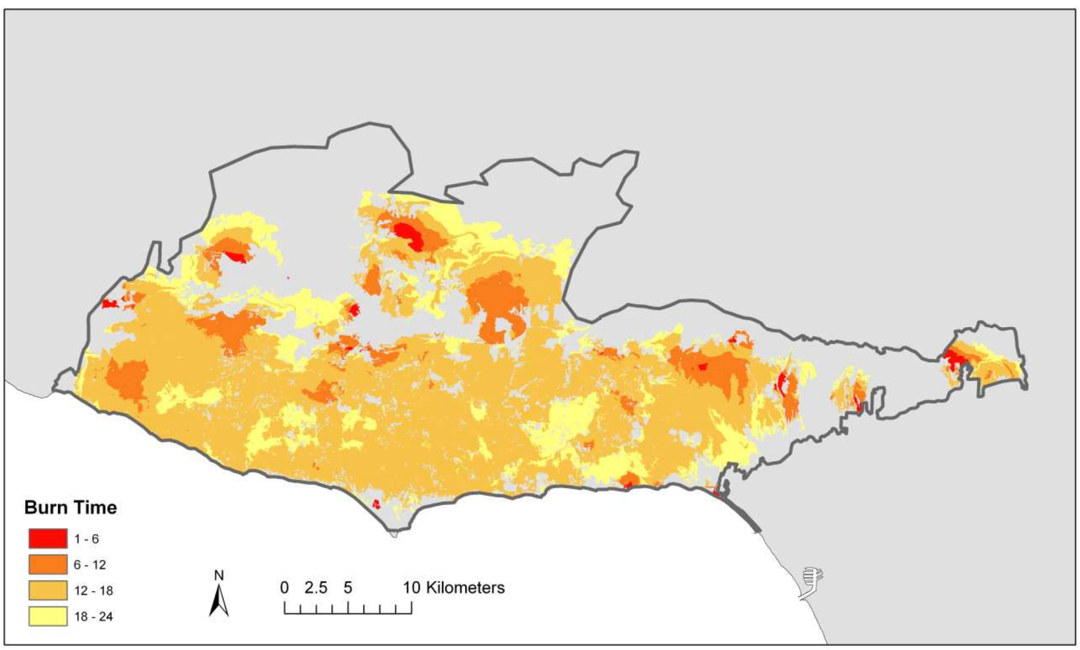

Appendix F5: Simulation S5. 90°, 40 kph (25mph) wind grid

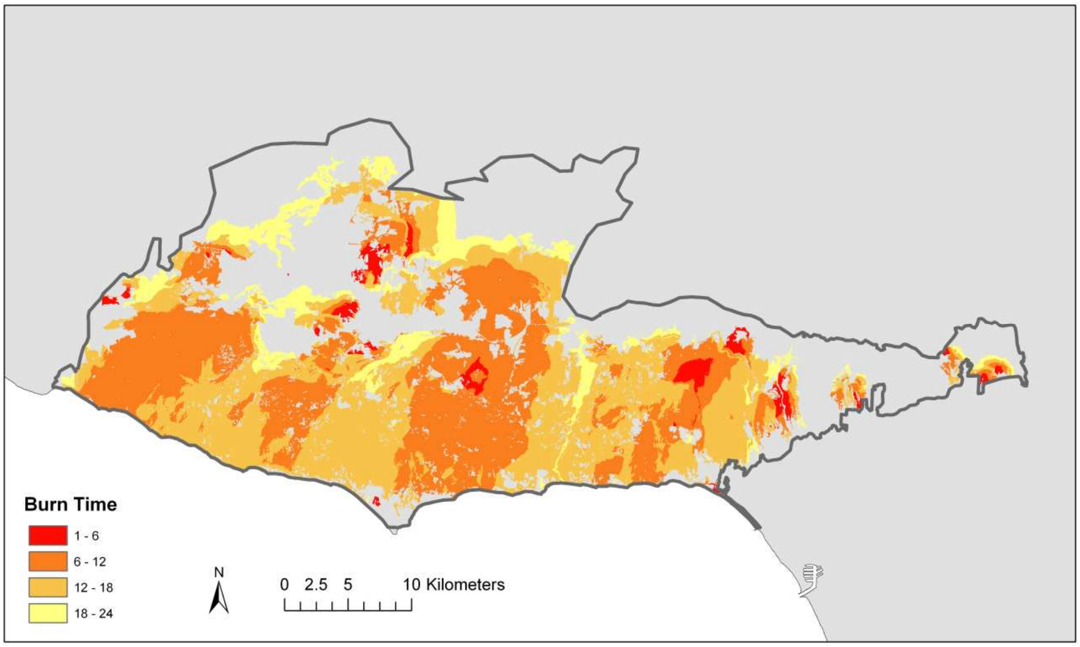

THIS PAGE INTENTIONALLY LEFT BLANK

APPENDIX G – STUDY AREA-WIDE HISTORIC HAZARD INDEX MAPS

Appendix G1: Simulation S1. 0°, 24 kph (15mph) wind grid

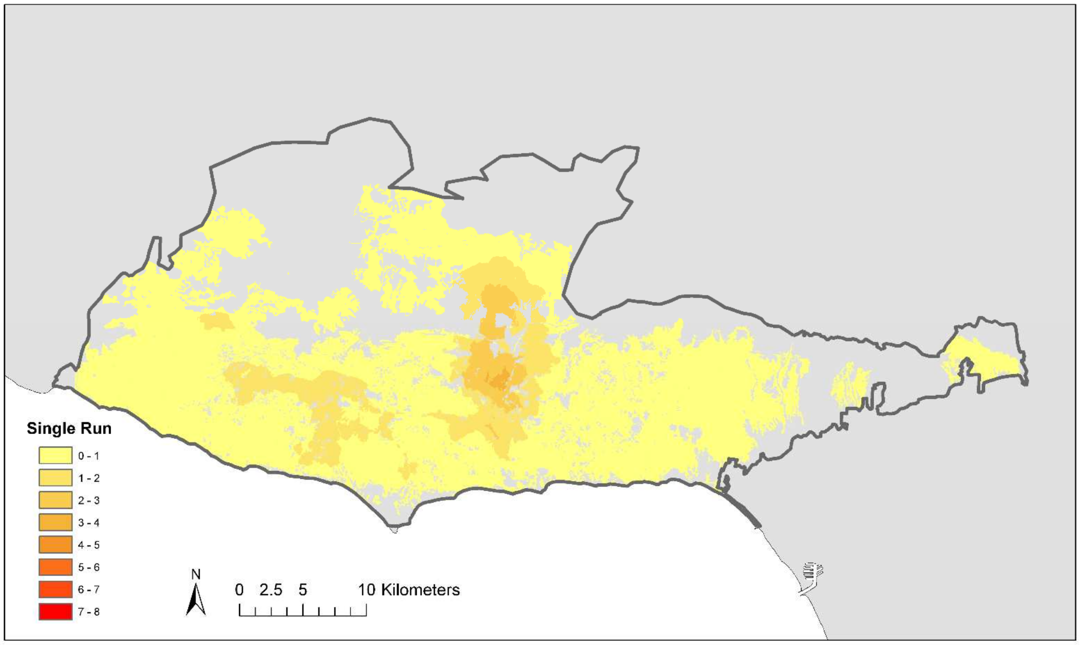

Appendix G2: Simulation S2. 90°, 24 kph (15mph) wind grid

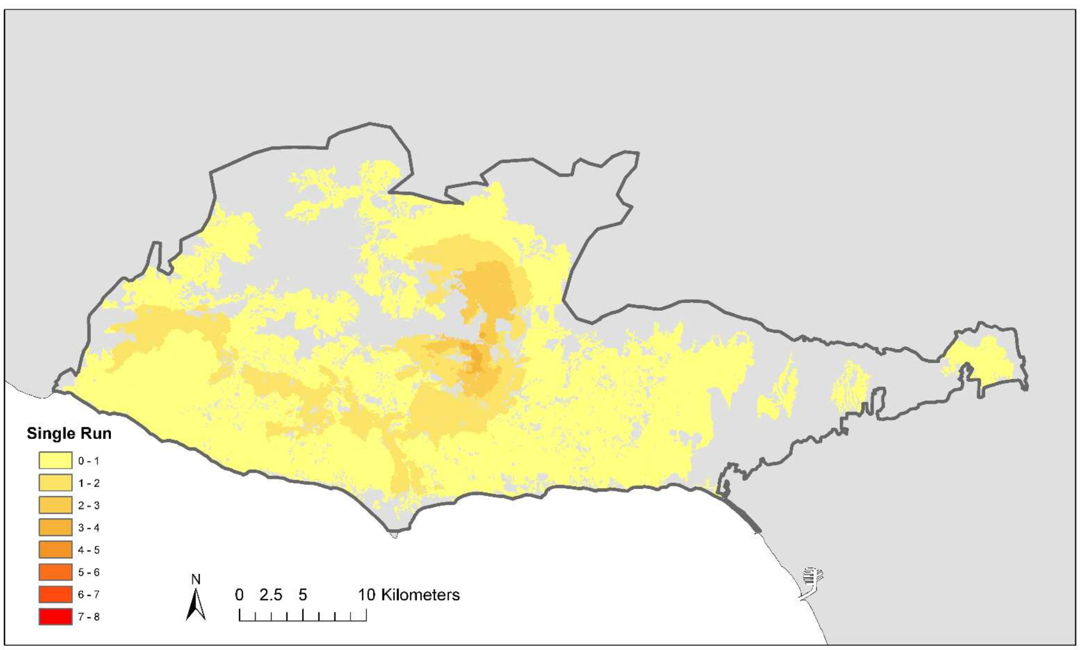

Appendix G3: Simulation S3. 45°, 24 kph (15mph) wind grid

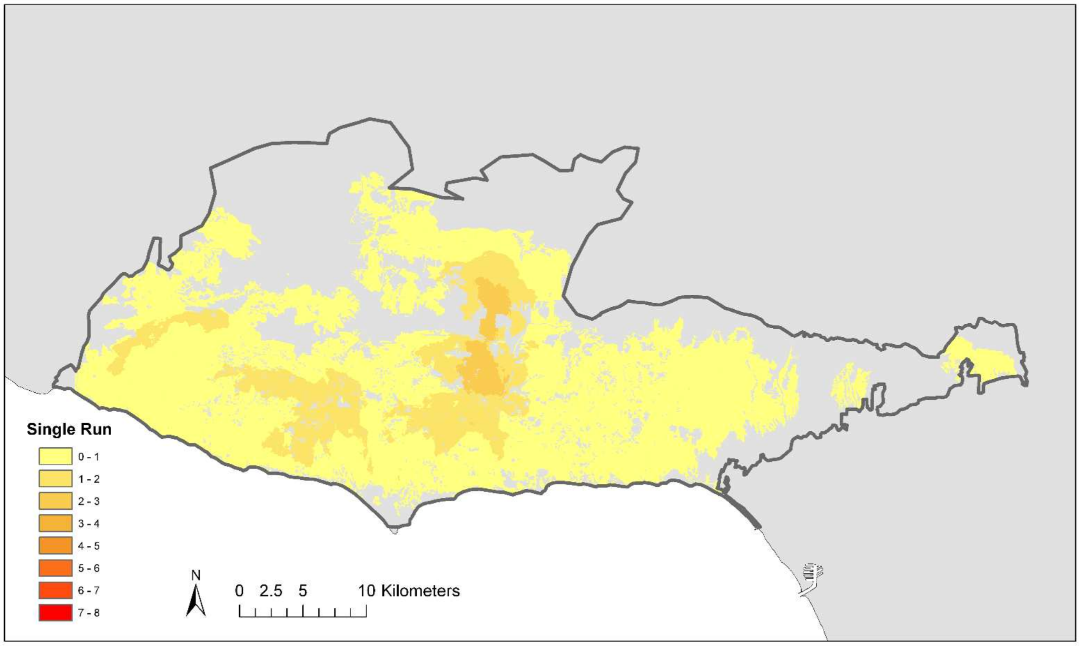

Appendix G4: Simulation S4. 337.5°, 24 kph (15mph) wind grid

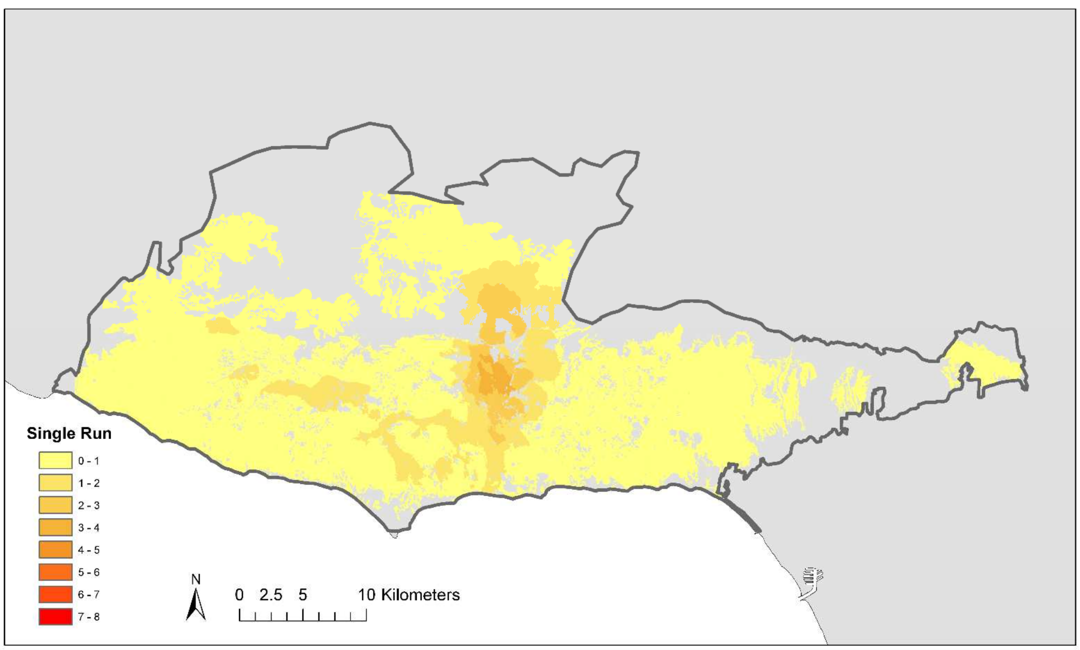

Appendix G5: Simulation S5. 90°, 40 kph (25mph) wind grid

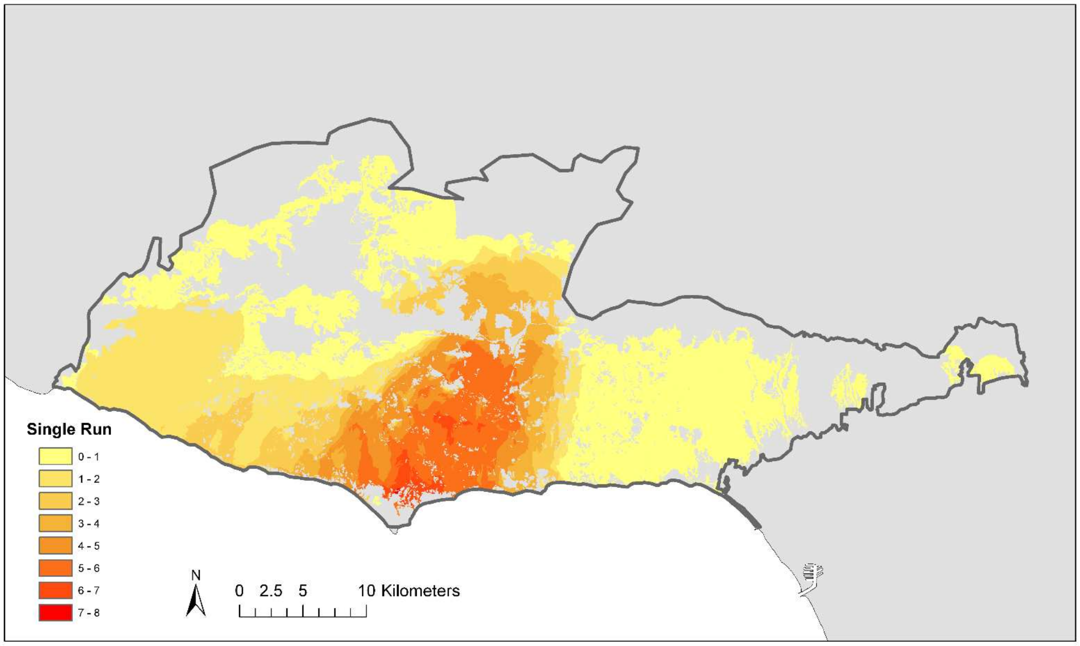

THIS PAGE INTENTIONALLY LEFT BLANK

APPENDIX H – OVERALL FIRE HAZARD INDEX MAPS

Appendix H1: Un-weighted hazard index map for historic ignitions

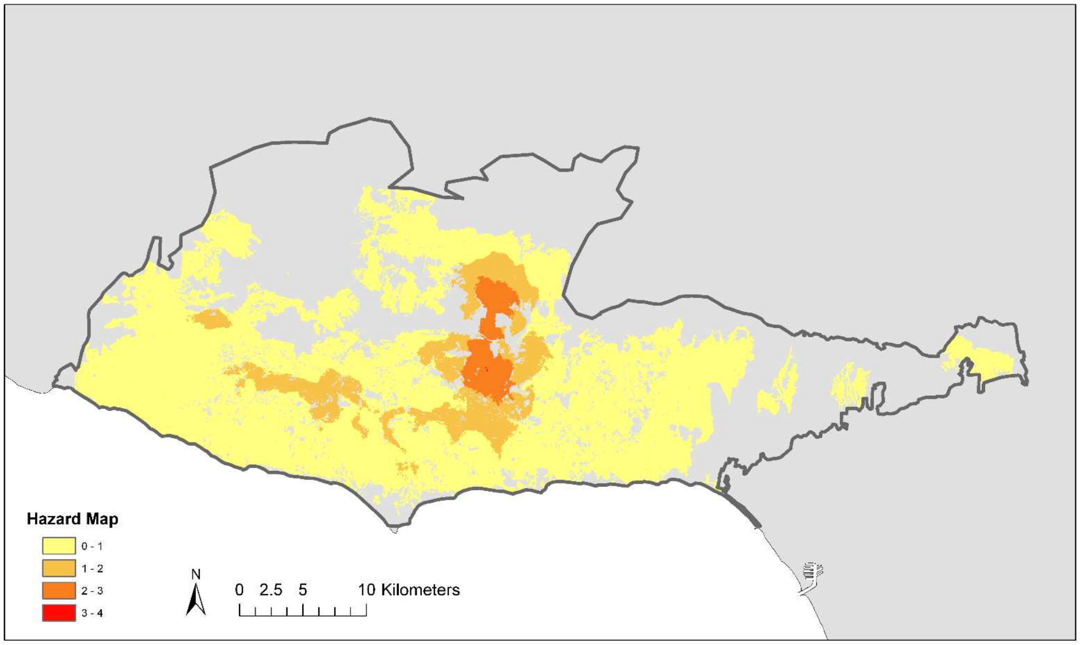

Appendix H2: Weighted hazard index map for historic ignitions

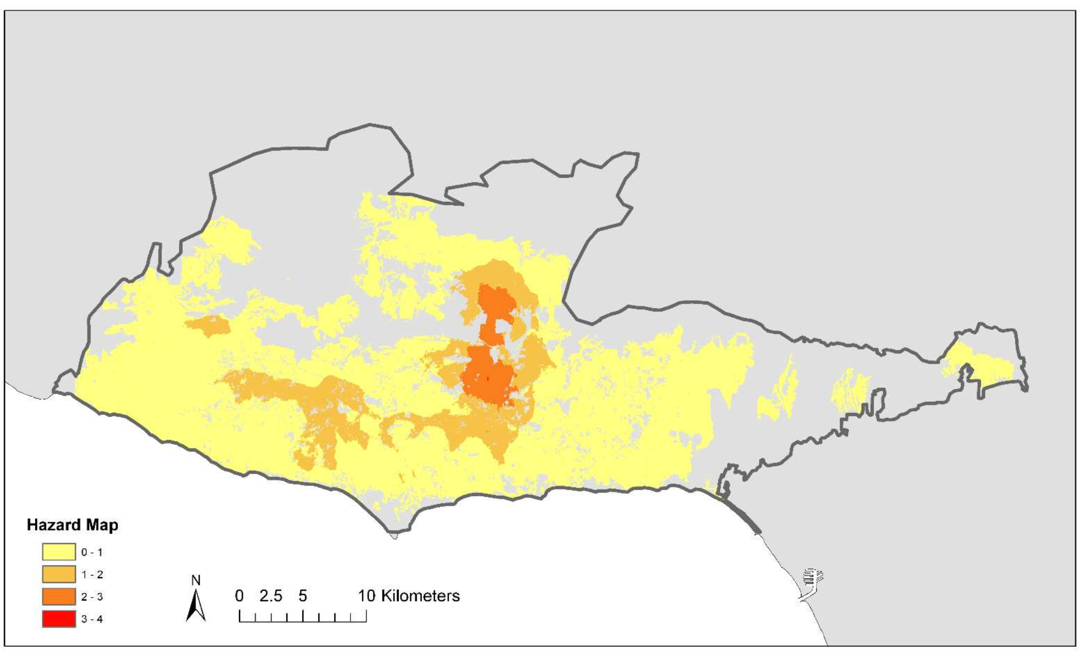

THIS PAGE INTENTIONALLY LEFT BLANK

APPENDIX I – CORRAL FIRE SIMULATION SUMMARY

Corral Fire Simulation Number	Total Simulated Fire Area		Area of Overlap with Corral Fire		Area Overburned		Area Underburned		Sørenson Metric
	ac	ha	ac	ha	ac	ha	ac	ha	
1	11,131.00	4,504.00	4,145.10	1,677.46	1,416.03	573.05	2,692.54	1,089.38	0.668631
2	17,906.00	7,245.00	4,304.00	1,742.00	13,602.00	5,503.00	347.93	140.32	0.381595
3	7,224.79	2,923.78	3,100.21	1,254.62	4,124.58	1,669.16	1,551.72	627.70	0.522065
4	3,375.42	1,365.99	1,959.39	792.94	1,416.03	573.05	2,692.54	1,089.38	0.488179
5	5,339.55	2,160.85	3,048.70	1,233.77	2,290.85	927.08	1,603.23	648.55	0.61026
6	3,565.43	1,442.89	963.35	389.85	2,602.09	1,053.04	3,688.58	1,492.46	0.234466
7	5,199.90	2,104.33	1,967.83	796.36	3,232.07	1,307.98	2,684.10	1,085.96	0.399486
8	2,496.19	1,010.17	60.67	24.55	2,435.52	985.62	4,591.26	1,857.76	0.016974
9	4,140.72	1,675.69	108.06	43.73	4,032.66	1,631.96	4,543.87	1,838.59	0.024579
10	4,477.57	1,812.01	2,553.40	1,033.33	1,924.17	778.68	2,098.52	848.99	0.559374
11	5,757.30	2,329.90	3,233.40	1,308.52	2,523.90	1,021.38	1,418.53	573.80	0.621257
12	7,200.00	2,913.00	4,412.00	1,785.00	2,788.00	1,128.00	239.93	97.32	0.74452
13	8,328.00	3,369.00	4,445.00	1,799.00	3,883.00	1,570.00	206.93	83.32	0.684904
14	9,213.00	3,727.00	2,247.00	909.00	6,966.00	2,818.00	2,404.93	973.32	0.324127
15	12,483.00	5,052.00	3,025.00	1,224.00	9,458.00	3,828.00	1,626.93	658.32	0.35308
16	8,292.75	3,354.00	359.53	145.00	7,933.23	3,209.00	4,292.40	1,737.32	0.055548
17	17,448.00	7,060.00	474.00	192.00	16,974.00	6,868.00	4,177.93	1,690.32	0.042896
18	6,671.00	2,700.00	3,402.00	1,377.00	3,269.00	1,323.00	1,249.93	505.32	0.600905
19	8,020.00	3,245.00	3,678.00	1,488.00	4,342.00	1,757.00	973.93	394.32	0.580496

**The Sørenson Metric is calculated as S = 2a/(2a+b+c), where a is the intersection of the area burned by the two fires, b is the area burned in fire 1 but not fire 2 and c is the area burned in fire 2 but not fire 1. A Sørenson metric value of zero indicates no agreement, while a value of 1 indicates perfect agreement.*

THIS PAGE INTENTIONALLY LEFT BLANK

Estimating Sample Size

We found that the minimum sample size to burn the whole Recreation Area is 120 fires.

THIS PAGE INTENTIONALLY LEFT BLANK

APPENDIX K – R SCRIPT

Appendix K1: R Script used for ANOVA F-test and multiple regression of overall weighted hazard index with input variables

```
# Read in the data
hazard1 = read.csv("SMMNRA_histhazard.csv")

# Set the fuel model to type
hazard1$fuel_mod = as.factor(hazard1$fuel_mod)

# Run the regression
hazard1.lm = lm(hweight_hazard~fuel_mod+elevation+slope+dist_fr_ignition, data=hazard1)

# Look at p-values
require(car)
Anova(hazard1.lm)

# Look at coefficients
summary(hazard1.lm)

# The coefficients for elevation, slope & distance are pretty similar
# but there's a much bigger range of values for distance
# Look at the coefficients on a scale of "per standard deviation"
coef(hazard1.lm)[12:14]*sd(hazard1[,4:6])

# Distance seems to be the most important, both with regards to the t statistic
# and the scaled slope.

# How well does a model with only distance do?
hazard1.dist.lm = lm(hweight_hazard~dist_fr_ignition, data=hazard1)
summary(hazard1.dist.lm)
# R^2 = 0.19: some predictive power, but imperfect.

plot(hweight_hazard~dist_fr_ignition, data=hazard1)
```

Appendix K2: R Script used for ANOVA F-test and multiple regression of 90°, 24 kph wind grid hazard index with input variables

```
# Read in the data
hazard1 = read.csv("s9015haz.edit.csv")

# Set the fuel model to type
hazard1$fuel.mod = as.factor(hazard1$fuel.mod)

# Run the regression
hazard1.lm = lm(s9015.hazard~elevation+fuel.mod+slope+dist.fr.ignition+asp.dir+kph, data=hazard1)

# Look at p-values
require(car)
```

```
Anova(hazard1.lm)

# Look at coefficients
summary(hazard1.lm)

# The coefficients for elevation, slope & distance are pretty similar
# but there's a much bigger range of values for distance
# Look at the coefficients on a scale of "per standard deviation"
# names(hazard1)to see names and columns of data, coef(hazard1.lm)for coefficients
coef(hazard1.lm)[15]*sd(hazard1[,12])
# distance from ignition still has the greatest coefficient of all the factors

# How well does a model with only distance do?
hazard1.dist.lm = lm(s9015.hazard~dist.fr.ignition, data=hazard1)
summary(hazard1.dist.lm)

#R^2=0.1518, F-statistic: 1.438e+05 on 1 and 803703 DF,  p-value: < 2.2e-16
```

Appendix L1: Reference Map of SMMNRA